Aramco
Journal of Technology

SUMMER 2020

Aramco
Journal
of Technology

The *Aramco Journal of Technology* is published quarterly by the Saudi Arabian Oil Company, Dhahran, Saudi Arabia, to provide the company's scientific and engineering communities a forum for the exchange of ideas through the presentation of technical information aimed at advancing knowledge in the hydrocarbon industry.

The *Aramco Journal of Technology* gratefully acknowledges the assistance, contribution and cooperation of numerous operating organizations throughout the company.

ISSN 1319-2388

Contents

A Real-Time Geomechanics Drilling Mud Window to Enhance Drilling Efficiency

Mohammed B. Alawami, Hussain I. AlBahrani, Salem H. Al-Gharbi, Mohammed M. Al-Rubaii, and Dr. Abdullah S. Al-Yami

Abstract / Enhancing the efficiency in drilling operations can lead to a significant reduction in the overall cost of a well's construction. Efficiency is generally achieved by maximizing the drilling rate of penetration (ROP) while minimizing nonproductive time (NPT), such as loss of circulation, well control, and stuck pipe incidents. Reducing the uncertainties associated with subsurface formations, especially formation stresses around the wellbore, is one key aspect to decreasing the frequency of NPT incidents.

Understanding wellbore stresses and the mechanical properties of subsurface formations is essential to optimize drilling surface parameters and drilling fluid properties to ultimately maximize the drilling ROP and minimize NPT. Determination of the geomechanical drilling mud window in real time allows drilling operations to proactively prevent fractures and/or formation instabilities. The availability of the geomechanical mud window in real time will enhance the rig reaction time to any abnormalities experienced while drilling, to maintain the bottom-hole pressure (BHP) consistently within the window.

The drilling mud window is constrained by a minimum and a maximum mud weight (MW) boundary. The lower limit represents the stability gradient and the upper limit represents the fracture gradient. Drilling with a MW below the lower limit may cause formation instabilities such as caving and swelling, which could lead to more severe consequences such as stuck pipes. Exceeding the upper limit of the MW may induce formation fractures that lead to loss of circulation, which then increases the risks of well control incidents.

The developed model automatically and continuously calculates formation mechanical properties such as Young's modulus and Poisson's ratio, using sonic logging-while-drilling data. Based on the formation's specific correlations, the model then determines the in situ stresses, induced stresses, and principle stresses. The fracture and stability gradients can be determined and converted to a MW for easier communication with the drilling crew. The minimum and maximum MWs are displayed as curves in real time, which allows immediate adjustments to drilling parameters and/or drilling fluid properties.

Geomechanics studies that contain the mud window are usually conducted pre-drilling, using offset well data, and these studies are often updated post-drilling only, which does not reduce the uncertainties associated with them. A real-time model maintains the mud window relevance and is up-to-date with the new data generated from the well.

Introduction

Drilling engineering is an integral step of the development of oil and gas wells. Drilling is a complex operation that constitutes numerous uncertainties that could lead to loss of time and money if not planned properly. Drilling engineers strive to deliver stable wells safely and in the shortest time. In other words, the ultimate goal is maximizing drilling efficiency. The two factors that play the biggest roles toward maximizing efficiency are the optimization of the drilling rate of penetration (ROP) and the reduction of nonproductive time (NPT) incidents.

The ROP can be described as the speed of subsurface rock removal and is commonly measured in feet or meters per hour. Increasing the ROP equates to less time spent on drilling a certain section or formation, and that eventually reduces the costs associated with the rig's daily rate and the tool's rental cost. The optimization of the ROP depends on numerous factors, including the bit type, drive system, lithology and mechanical properties of the drilled formation, drilling parameters, and hole cleaning conditions.

Although maximum ROP is generally desired, increasing the ROP in certain scenarios may be counterproductive as high drilling rates may lead to unintended consequences such as poor hole cleaning conditions, which could cause more severe incidents, such as stuck pipes. Therefore, the ROP must be delicately optimized to achieve maximum rates, which do not compromise the integrity and stability of the wellbore.

The reduction of NPT incidents can be even more critical than maximizing the ROP in terms of the impact on drilling efficiency. This can be mainly traced to the fact that NPT incidents can last for days without making any progress toward reaching the targeted depth. NPT incidents can be categorized into three major challenges: (1) stuck pipe incidents, (2) loss of circulation, and (3) well control.

Stuck pipe incidents are often the most lengthy and costly incidents as the drillstring, in some cases, cannot be successfully released. That may lead to abandoning entire drilled sections and sidetracking to continue drilling the reservoir. Stuck pipes can be classified as mechanical or differential stuck pipes. Mechanical stuck pipes can occur due to wellbore geometry, poor hole cleaning, or wellbore instability. The high differential pressure between the wellbore and the formation, on the other hand, causes differential sticking. An improper mud filter cake can also deteriorate the conditions and make the stuck drillstring even more challenging to release.

Loss of circulation events can occur when drilling through low-pressure areas, highly permeable formations, or naturally fractured formations. Losses can also be self-inflected if the pressure exerted on the bottom of the wellbore exceeds the fracture pressure of the formation while drilling. That can lead to induced fractures that open up a path for the drilling fluid to escape.

Drilling with mud losses can cause numerous complications such as environmental concerns and lack of a hydrostatic pressure barrier. The loss of the hydrostatic pressure is especially problematic as it can allow formation fluids to enter the wellbore. These fluid influxes can further decrease the bottom-hole pressure (BHP) and cause additional volumes to enter the wellbore. If not controlled properly, kicks can become uncontrollable and lead to well control scenarios.

Well control incidents can be a serious safety risk for the crew and can cause significant damage to rig equipment. Measures must be set in place to prevent fluid influxes from becoming uncontrollable. It is always a priority to maintain a healthy drilling fluid system as a primary barrier to any kind of fluid influx into the wellbore. Possible causes of well control incidents include a reduction in BHP, drilling through overpressured formations, or drilling with an incorrect mud weight (MW), or fluid properties.

It is extremely important to have proper measures in place to limit the impact and severity of NPT incidents when encountered. Subsequently, thorough preplanning and close monitoring of wellbore conditions to proactively mitigate these costly incidents is critical toward the success of drilling operations. One key aspect of drilling that must not be overlooked is the geomechanics of subsurface formations. An understanding of the geomechanics surrounding the wellbore is crucial to maintaining a stable wellbore.

Figure 1 shows different wellbore failures that could arise due to the geomechanics of the drilled formations[1].

Geomechanics in Drilling Operations

Geomechanics is a field of study that integrates rock mechanics with geoscience and reservoir engineering to understand the effects of various variables on subsurface rocks[2]. Geomechanical studies might be most important in the production phase, especially in hydraulic fracturing, as the operation's success is highly dependent on accurate estimations of the breakdown pressure. These studies can also play a major role in identifying potential drilling hazards related to wellbore stability, and how to minimize such risks. The elastic properties of subsurface rocks, for instance, give the drilling team an insight into the deformation behavior of the drilled formations[3]. It also allows for the selection of the most suitable casing and tubular

Fig. 1 *Different types of wellbore failures that may occur, and the caliper log signature associated with them[1].*

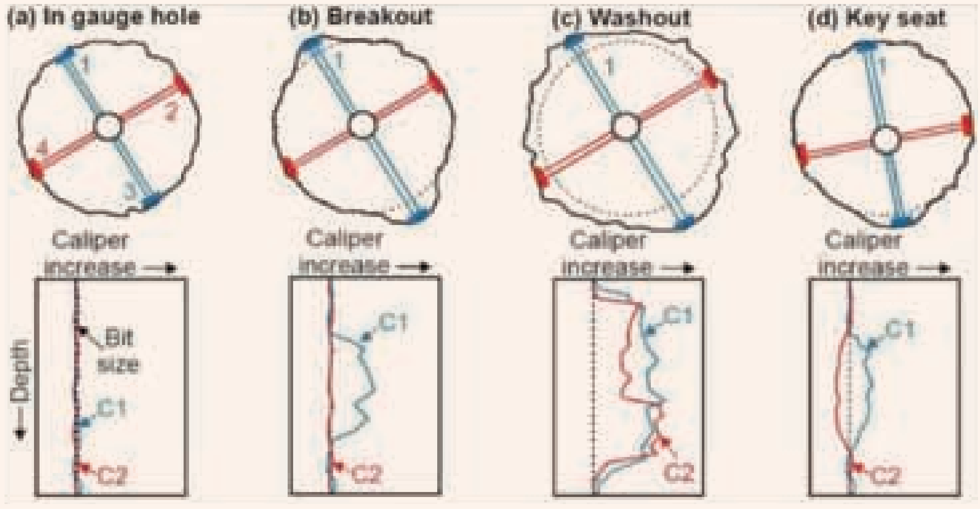

strength that can withstand the high pressures applied during fracturing operations.

Wellbore stability is influenced by numerous factors such as pore pressure, in situ stresses, and the strength of the drilled rocks. Drilling practices, and drilling fluid density and properties, can also have an impact on the stability of the wellbore. The removal of rocks during drilling operations disturbs the stresses around the wellbore, and it becomes concentrated near the wellbore. Wellbore failure occurs if the redistributed stress becomes greater than the rock's compressive or tensile strength[4]. The hydrostatic pressure of the drilling fluid becomes crucial to support the formation and prevent wellbore instabilities.

Drilling Mud Window

The drilling mud window is a range of drilling fluid densities that would deliver safe drilling operations and stable wellbore conditions. It is constrained by an upper and lower limit of MW values. MW is critical in drilling because it controls the hydrostatic pressure exerted at the bottom of the wellbore, and as the density increases, the BHP increases alongside it.

The goal is to continuously and consistently maintain the BHP within the window boundaries. The density of the drilling fluid, however, is not the sole contributor to BHP. The frictional pressure losses caused by the friction between the fluid particles and the wellbore wall during circulation of the fluid exerts additional pressure on the bottom of the well. The sum of the hydrostatic pressure and the frictional pressure losses equates to the BHP.

The BHP is commonly converted to a MW value denoted as the equivalent circulating density (ECD). The ECD takes the frictional pressure losses into account and paints a more accurate picture of the BHP. The MW must always be higher than the lower limit to avoid wellbore instabilities and kicks, and the ECD should always be lower than the upper limit to prevent induced fractures and loss of circulation.

The determination of the drilling mud window is most critical in wells where the margin between the minimum and maximum pressure values is extremely narrow. The narrow window wells are typically caused by a formation's abnormal pressure that increases the lower boundary, or by highly fractured formations or depleted areas that reduce the upper boundary and narrows it down[5]. In these wells, advanced drilling techniques, such as managed pressure drilling, can be employed to enable better control of the BHP. Such techniques, however, would not be effective without an accurate drilling mud window that serves as a guide to the BHP values.

The fracture and/or breakdown pressure of the weakest formation exposed to the wellbore determines the upper limit of the mud window. The breakdown pressure encountered while drilling is dependent on several factors, including:

- Azimuth and inclination of the wellbore.
- Mechanical properties of the formation rocks.
- In situ stress regime of the field.
- External influences that may occur while drilling, such as wellbore strengthening.

In narrow window wells, where it is not possible to drill with pressures below the maximum, due to well control risks, some techniques of wellbore strengthening can be applied to increase the breakdown pressure of the drilled formations. The estimation of the breakdown pressure in such cases is extremely valuable to assess the effectiveness of different wellbore strengthening techniques by comparing the breakdown pressure before and after applying the selected technique.

The lower limit of the window from a geomechanics' prospective is constrained by the stability pressure that maintains the rocks in stable condition. Drilling with pressures below the lower limit could lead to formation breakouts that disturb the stability of the wellbore. Wellbore instability issues increase the diameter of the wellbore, and create restrictions due to rock cavings, which thereby increase the risk of mechanical stuck pipes.

The pore pressure values of open formations should also be estimated to ensure that the hydrostatic pressure is higher to avoid well control incidents. The BHP must always be higher than both the stability and pore pressure, and the lower limit of the mud window must be adjusted accordingly in cases where the pore pressure gradient is higher than the stability gradient.

Drilling with enormous uncertainties in stability and fracture pressures can lead to avoidable wellbore instabilities, loss of circulation, and well control scenarios. The estimation of the drilling mud window reduces these uncertainties and provides a path toward maximizing drilling efficiency, especially in areas with narrow pressure windows.

If exceeding the boundaries is inevitable in certain wells, having the mud window available allows for proper planning of reactive measures that minimize the severity and duration of potential hazards.

Real-Time Modeling of the Mud Window

The drilling mud window is not a new concept. In fact, it is a standard practice for drilling engineers to estimate the mud window in the planning phase, even if the values are largely inaccurate. Geomechanical models are mostly used in the preplanning phase today, and new data from the current well is not utilized immediately to update the model. Estimating the mud window in real time provides enormous value in fields that encounter inconsistent wellbore stability issues from well to well.

Modeling the mud window in real time requires the calculation of numerous formation mechanical properties first. These properties are then used to estimate the stability and breakdown pressures, which in turn are used to determine the upper and lower limits of the safe window.

The model is based on the work published by Al-Bahrani and Noynaert (2016)[5], which depends on the

Fig. 2 *Summary of the process used to determine fracture pressure gradient[5].*

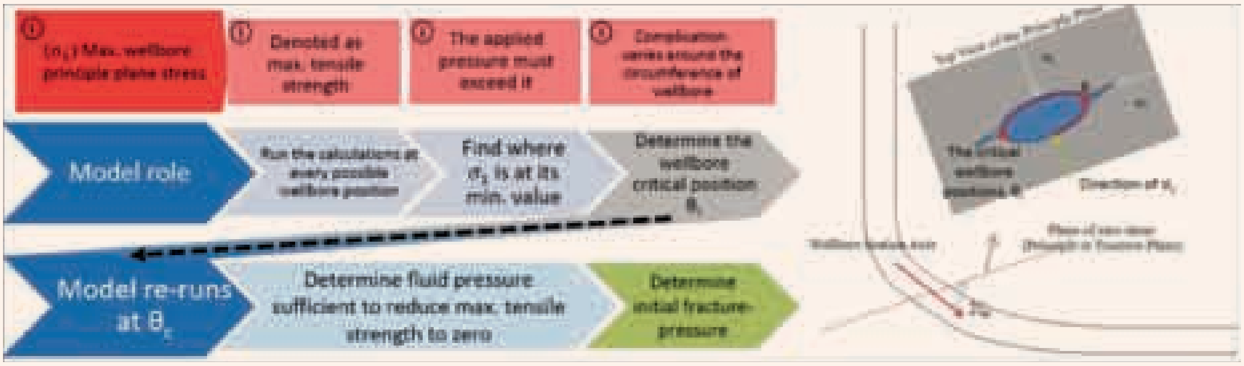

tangential stress concept introduced by Kirsch (1898)[6]. The concept is used to estimate the initial fracture pressure of the targeted formations in combination with the fracture propagation concept and several other well-established techniques in the literature. The tangential or hoop stress concept assumes that the fracture initiates when the hoop stress equates to zero. The additional factors that influence the fracture pressure are then studied to adjust the pressure values accordingly. In addition, the model uses Richardson's transformation[7] to transform the in situ stresses to be represented in relation to the wellbore coordinates. The subsequent step is the determination of the principal plane stress that the fractures would initiate within.

Figure 2 provides a summary of the process used to determine the fracture pressure gradient[5]. The model makes several assumptions throughout the calculations. These assumptions are linear elasticity and the poroelasticity theory, rounded wellbore, isothermal conditions, and impermeable wellbore wall. Some of these assumptions do not reflect the true conditions in drilling operations, and therefore, correction factors must be used to offset the error resulting from these assumptions.

Sonic logging tools are required to run the mud window model in real time. The model uses the shear and compressional waves as input to calculate critical formation mechanical properties. Two key parameters that allow us to estimate formation strength and stresses are Young's modulus and Poisson's ratio[8]. Both are determined using sonic logs. These parameters are then used to determine the required stresses, Fig. 3.

The estimation of the stability gradient in the model occurs through loops coded in the algorithm. The model uses the data from logging tools to calculate several formation mechanical properties such as Young's modulus and Poisson's ratio, as previously mentioned. These values are then used to estimate the unconfined compressive strength, friction angle, minimum and maximum stresses, and the Mohr-Coulomb parameter. The Mohr-Coulomb failure criteria is then calculated around the circumference of the wellbore and all of the corresponding variables are recalculated iteratively until the model reaches the wellbore pressure that causes rock failure. This pressure is then denoted as the stability pressure.

The results of the fracture and stability pressures are converted to equivalent MW values that are plotted vs. depth in real time. The purpose of this conversion is to provide a clear visualization to the rig crew that are likely more familiar with MWs than pressure values. This is especially beneficial when the mud window is paired with a real-time ECD plot that uses the window as a guide to maintain a stable wellbore.

The mud window model was run in two historical wells to validate the output and cross-reference the results with commercial software that are commonly used today as preplanning tools for geomechanical studies. The selected hole sections in the two validation wells were targeting two different lithologies and formation properties. The results from the model matched the commercial solutions, and that allows us

Fig. 3 *Representation of the workflow followed to determine the needed stresses in real time.*

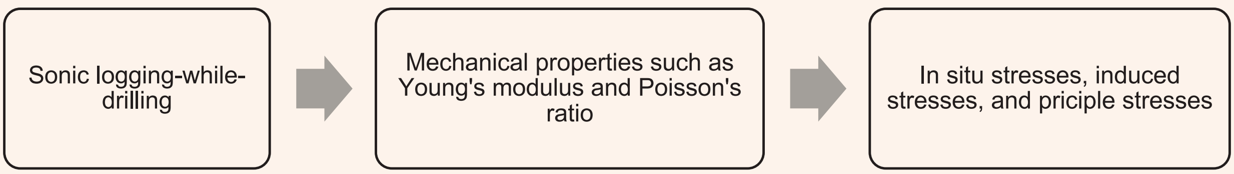

to take the next step of running the model in real time in a live well for final assessment, and to fine-tune the model if needed.

Conclusions

Cost optimization has become a priority for oil and gas companies, and drilling operations present a huge opportunity as it accounts for a large sum of well development costs. Increasing ROP and minimizing NPT incidents are key to enhance the drilling efficiency, and ultimately optimize drilling costs. Geomechanical studies can play a major role in both aspects. Understanding wellbore stresses and formation rocks' mechanical properties to identify the correct and optimum drilling fluid density from a geomechanical prospective is key. Such studies can improve the ROP as well as reduce wellbore failures encountered while drilling. These failures include induced fractures that could lead to loss of circulation and wellbore instability that can cause stuck pipe incidents.

Geomechanical studies are most beneficial when run in real time. Pre-drilling studies may still have enormous uncertainties associated with them as they are mostly based on offset well data. Taking advantage of the logging tools run while drilling to update geomechanical models is essential to maximizing efficiency. The real-time drilling mud window utilizes sonic logging-while-drilling data to calculate critical formation mechanical properties in real time and estimate the fracture and stability gradients instantly.

The results are displayed as curves of equivalent MW values presented to the drilling team for their assessment. This allows for a faster intervention from the rig crew in cases where the BHP is nearing the boundaries of the safe window. This is especially critical in wells where the margin between the fracture and stability gradients is extremely narrow. The model effectiveness can be enhanced even further by plotting an ECD curve alongside the mud window to immediately identify risky BHP conditions and make proper adjustments accordingly.

Acknowledgments

This article was prepared for presentation at the SPE Conference at the Oman Petroleum and Energy Show, Muscat, Oman, September 14-16, 2020.

References

1. Plumb, R.A. and Hickman, S.H.: "Stress-Induced Borehole Enlargement: A Comparison between the Four-Arm Dipmeter and the Borehole Televiewer in the Auburn Geothermal Wall," *Journal of Geophysical Research*, Vol. 90, Issue B7, June 1985, pp. 5513-5521.
2. Hamid, O.: "Integrated Reservoir Geomechanical Solutions Focus on Production Geomechanics," ARMA paper presented at the 53rd U.S. Rock Mechanics/Geomechanics Symposium, New York City, New York, June 23-26, 2019.
3. Heidari, B., Leong, S.T., Son, N.T. and Aznor, M.Z.: "Real Time Drilling Geomechanics Service, Case Study, Offshore Malaysia," SPE paper 172977, presented at the SPE Middle East Unconventional Resources Conference and Exhibition, Muscat, Oman, January 26-28, 2015.
4. Liz-Losada, R.J. and Alejano, L.R.: "New Safe Mud Weight Window Representations to Prevent Wellbore Instability," SPE paper 62800, presented at the IADC/SPE Asia Pacific Drilling Technology, Kuala Lumpur, Malaysia, September 11-13, 2000.
5. AlBahrani, H.I. and Noynaert, S.F.: "An Analyzing of Stress-Related Wellbore Strengthening Techniques," SPE paper 182959, presented at the Abu Dhabi International Petroleum Exhibition and Conference, Abu Dhabi, UAE, November 7-10, 2016.
6. Kirsch, E.G.: "Die Theorie der Elastizität und die Bedürfnisse der Festigkeitslehre," *Zeitschrift des Vereines deutscher Ingenieure*, Vol. 42, 1898, pp. 797-807.
7. Richardson, R.M.: "Hydraulic Fracture in Arbitrarily Oriented Boreholes: An Analytic Approach," in *Hydraulic Fracturing Stress Measurements,* Chapter 3, National Academy Press, Washington, D.C., 1983, pp. 167-175.
8. Chatterjee, C., Reyes, A., Lujan, V., Majumdar, C., et al.: "Geomechanics: A Solution to Drilling in Unconventional Reservoirs," SPWLA paper presented at the Society of Petrophysicists and Well Log Analysts 2nd Asia Pacific Technical Symposium, Bogor, Java, Indonesia, November 7-8, 2018.

About the Authors

Mohammed B. Alawami

B.S. in Petroleum Engineering, University of Oklahoma

Mohammed B. Alawami is a Petroleum Engineer with the Drilling Technology Team of Saudi Aramco's Exploration and Petroleum Engineering Center – Advanced Research Center (EXPEC ARC). He joined Saudi Aramco in 2014, and has since worked in several departments, including the Exploration and Oil Drilling Engineering Department, the Northern Area Drilling Operations Department, and the Drilling Real Time Operating Center (RTOC) to gain the knowledge and skills necessary to become a successful researcher.

Mohammed's research efforts are focused on drilling automation and optimization, particularly the development of drilling descriptive, diagnostic, predictive, and prescriptive real-time models. He has also explored the development of several local resources and worked on the development of drilling fluids and cement slurries.

Mohammed has published nine Society of Petroleum Engineers (SPE) technical papers, submitted three patent applications as a co-inventor, and contributed to nine technology deployments in the field. He is currently working on assignment with the Technology Deployment & Commercialization Team in EXPEC ARC.

In 2014, Mohammed received his B.S. degree in Petroleum Engineering from the University of Oklahoma, Norman, OK.

Hussain I. AlBahrani

M.S. in Petroleum Engineering, Texas A&M University

Hussain I. AlBahrani is a Petroleum Engineer with the Drilling Technology Team of Saudi Aramco's Exploration and Petroleum Engineering Center – Advanced Research Center (EXPEC ARC). He joined Saudi Aramco in 2011 where he worked in different positions, including as a Drilling Engineer in the Southern Area Oil Drilling Department, as a Reservoir Engineer in the Gas Reservoir Management Department, and as a Lab Scientist conducting research related to drilling engineering.

Hussain has received several awards, including the Texas A&M University Petroleum Engineering 1st place Award in the 2020 Ph.D. paper contest, the Society of Petroleum Engineers (SPE) 1st place Award in the 2020 Gulf Coast North America Regional Ph.D. paper contest, the 2016 Saudi Aramco CEO Excellence Award, the 2016 Saudi Aramco Board of Engineers Award, and he was a finalist for the 2018 ADIPEC Young Engineer of the Year.

Hussain published more than 15 papers and has 13 granted patents in areas that include geomechanics numerical and analytical modeling, and drilling fluids additives lab design.

He received his B.S. degree in Petroleum Engineering from King Fahd University of Petroleum and Minerals (KFUPM), Dhahran, Saudi Arabia, and his M.S. degree in Petroleum Engineering from Texas A&M University, College Station, TX. Hussain is currently working on his Ph.D. in Petroleum Engineering from Texas A&M University.

Salem H. Al-Gharbi

M.S. in Petroleum Engineering, Heriot-Watt University

Salem H. Al-Gharbi is Drilling Data Scientist with Saudi Aramco's Drilling Technology Team at the Exploration and Petroleum Engineering Center – Advanced Research Center (EXPEC ARC). He has over 15 years of experience in the domain of advance application development, targeting reservoir engineering, exploration, drilling engineering, operations and real-time challenges.

Salem was appointed as the technical leader for Saudi Aramco's Drilling Ahead of Bit smart initiative; he is also one of the founders of the Society of Petroleum Engineers (SPE) Drilling Uncertainty Prediction International Technical Section (DUPTS). Salem has participated in multiple local and international events as a committee member or key speaker in the domain of artificial intelligent and machine learning in the drilling domain. He also has authored several publications and holds several patents in this field.

Salem received his B.S. degree in Computer Science from King Fahd University of Petroleum and Minerals (KFUPM), Dhahran, Saudi Arabia, and his M.S. degree in Petroleum Engineering from Heriot-Watt University, Edinburgh, U.K.

Mohammed M. Al-Rubaii

M.S. in Petroleum Engineering, King Fahd University of Petroleum and Minerals

Mohammed M. Al-Rubaii is a Drilling Engineer with the Drilling Technology Division of Saudi Aramco's Exploration and Petroleum Engineering Center – Advanced Research Center (EXPEC ARC). He joined Saudi Aramco in 2012. Since that time, Mohammed has worked on several projects regarding hole cleaning automation, formation pressures automation, rheological properties of drilling fluid automation, bit hydraulics automation, and well drilling and operations performance automation.

He has developed several automated models and methods for drilling, which has contributed to increased optimization, time, and cost-effectiveness.

Mohammed is an active member of the Society of Petroleum Engineers (SPE) where he has served on several conferences. Mohammed has published 15 SPE papers, and initiated and co-chaired several SPE advanced technical workshop series in the region.

He is also an active member of the Dhahran Geoscience Society. Mohammed has filed 10 patent applications.

He is currently working on writing a chapter for a book entitled "Data Analytics for Drilling Process Improvement."

Mohammed received both his B.S. degree and M.S. degree in Petroleum Engineering from King Fahd University of Petroleum and Minerals (KFUPM), Dhahran, Saudi Arabia. He is currently studying for his Ph.D. degree in Petroleum Engineering at KFUPM.

Dr. Abdullah S. Al-Yami

Ph.D. in Petroleum Engineering, Texas A&M University

Dr. Abdullah S. Al-Yami is a Petroleum Engineer with the Drilling Technology Team of Saudi Aramco's Exploration and Petroleum Engineering Center – Advanced Research Center (EXPEC ARC). He has 18 years of experience with Saudi Aramco and previously worked in different positions, including as a Lab Scientist and Drilling Engineer, conducting research related to drilling engineering.

Abdullah has received several awards during his career, including Saudi Aramco's Research and Development Center (R&DC) Innovation Award and its Successful Field Application Award for his research work. He also received Saudi Aramco's EXPEC ARC Effective Publications Award. A member of the Society of Petroleum of Engineers (SPE), Abdullah was awarded the 2009 SPE Outstanding Technical Editor Award for his work on the SPE *Drilling and Completion Journal*. He also received the 2014 SPE Regional (Middle East, North Africa and South Asia) Drilling Engineering Award, and both the 2015 and 2016 CEO Saudi Aramco Excellence Award. In 2016, Abdullah received Oil & Gas Middle East Award "highly commended" recognition in the category of internal control valve (ICV) Strategy of the Year for his efforts in developing drilling products utilizing a local resources strategy. In 2017, he was awarded the Saudi Arabian Board of Engineering Award.

Abdullah is a coauthor of the textbook *Underbalanced Drilling: Limits and Extremes*; he has 16 granted U.S. patents and more than 80 filed patents; and has more than 80 publications to his credit, all in the area of drilling and completions.

Abdullah received his B.S. degree in Chemistry from Florida Institute of Technology, Melbourne, FL; his M.S. degree in Petroleum Engineering from King Fahd University of Petroleum and Minerals (KFUPM), Dhahran, Saudi Arabia; and his Ph.D. degree in Petroleum Engineering from Texas A&M University, College Station, TX.

A Novel Technique to Bring Killed Wells Back into Production

Christopher Wrighton, Dr. Jinjiang Xiao, Jamie Cochran, and Parijat Mukerji

Abstract / This article describes the development program for a new and innovative well intervention service for lifting naturally flowing wells back into production.

The well initiation service tool (WIST) is a highly efficient, slim hole pumping system that is conveyed and powered through a wireline power cable to the appropriate depth to lift high-density kill fluid; thereby lightening the fluid column to kickoff/initiate and allow the well to flow naturally to the surface.

A multiple resettable inflatable packer system has been developed to work with the permanent magnet motor pumping system, which allows the pump to be positioned and repositioned in the well as required. This design improves operational efficiency, enabling jobs to be conducted in a single run, rather than multiple runs, as would be the case with a conventional packer design.

The rigorous test program looked at each element of the WIST individually, and then as a system in both horizontal and vertical flow loops to verify performance. The novel multiple resettable inflatable hydraulic logic circuit worked perfectly, exceeding design and performance expectations. Planning is now in progress for three field trials to validate the performance of the WIST. This article will describe the development activities, results, and future plans.

This lightweight cable deployed pump system is an alternative to coiled tubing (CT) and nitrogen kickoff jobs, which can often be expensive and logistically challenging, requiring a large amount of equipment and personnel at the wellsite to perform the operation.

Introduction

The Problem

The oil and gas industry drills numerous new wells, and works over many additional wells annually. Wells are typically completed and overbalanced by using heavy kill fluid to prevent natural flow. Wells may also be killed to perform certain rigless operations safely. The circulation of the kill fluid typically removes overbalance pressure by nitrogen lifting, using coiled tubing (CT).

The Solution

An alternative and less expensive solution to starting wells was proposed, using a cable conveyed through a tubing pumping system, called a well initiation service tool (WIST).

While theoretical transient computer modeling was used in the past to show the approach should produce the desired result — to kickoff a "killed" well — this had never been demonstrated in practice. Given the complexity and potential inaccuracy of multiphase flow simulations, it was decided that the WIST theory of operation should be experimentally tested and validated under realistic conditions through a program to field-test three well deployments.

Statement of Theory and Definitions

WIST Theory of Operation

Wells that have stopped flowing can be split into two categories. First, wells that have the potential to flow naturally, but are currently overbalanced, and second, wells that will never flow naturally due to reservoir depletion, and require some form of artificial lift to induce production. The WIST is intended to be used on the first category of wells with the potential to flow naturally, but that requires a kill fluid or dead fluid to be removed prior to steady-state unassisted production.

Nitrogen lift jobs circulate a less dense fluid (a gas) into the wellbore with the intent to temporarily reduce the hydrostatic pressure exerted by the fluid column on the producing reservoir. This enables reservoir fluid to flow into the wellbore and displace the kill fluid and nitrogen out of the wellhead. A CT intervention is usually used to perform this technique, and eventually, the well should reach a pressure equilibrium point at which flow occurs unassisted.

An alternative method to start wells was proposed with the potential to require less surface equipment, personnel, and cost. By using a cable deployed submersible pump system, heavy kill fluid could be pushed upward and out of the wellbore from a temporary setting point in the production tubing. As heavy kill fluid is pushed out of the wellbore, lighter production fluid enters the wellbore from the reservoir to replace the displaced volume.

Over time, fluid in the wellbore will be swapped to a lighter fluid, which exerts less hydrostatic pressure on the reservoir, thereby reaching an equilibrium point after which the well will flow naturally. At this equilibrium point, the hydraulic work done by the submersible pump is reduced to zero, at which point the pump is no longer required and can be retrieved from the tubing under live well conditions.

Figure 1 shows four theoretical simplified plots of wellbore hydrostatic pressure at different times during the operation of a WIST, depicting the higher density kill fluid being gradually displaced with lighter reservoir fluid to initiate natural flow.

A typical pump differential pressure (head) over time plot would have a bell curve profile. With pressure (and pump work) increasing at the start of the operation as fluid is pushed up the wellbore by the pump, and as more lighter density fluid is pushed up the well past the pump, the head starts to reduce to zero, at which point the well flows naturally. As the differential pressure across the pump nears zero, the bypass valve opens and the flow bypasses the pump assembly.

It is anticipated that some wells may require flowing naturally at this higher flow rate with the WIST assembly in place for a period of time prior to retrieving the

Fig. 1 Four theoretical simplified wellbore hydrostatic pressure gradients at different times during the operation of a WIST.

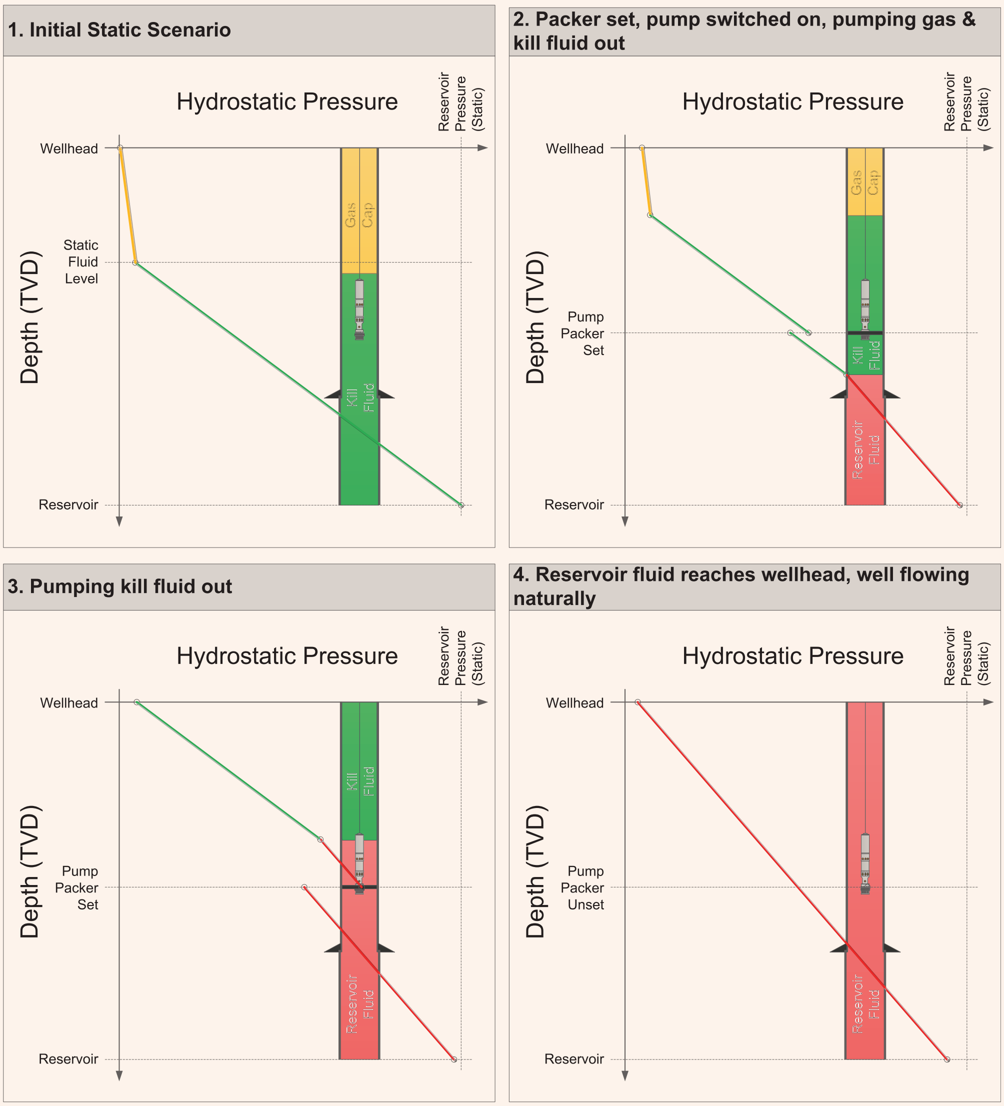

equipment to clean the well further and displace all traces of the kill fluid. This simplified theory described and depicted does not account for fluid interface mixing.

Method of Project Execution

A joint development program was established with the objective of proving whether or not the concept of using a temporary pump to liven wells rather than a nitrogen lift job is feasible. Table 1 lists the four program phases to develop and test the technology. This article discusses phases 1 and 3.

A three-party collaboration was established to achieve the project objectives with the wireline service provider, the well production operator, and the pumping technology provider. Weekly and monthly update meetings were held with all parties to keep track of the progress on actions and issues that required resolution.

Functional Requirements and Specification

The cable deployed the WIST system for unloading and livening new, worked over, killed, or low wellhead pressure wells consisting of: a pump, motor, resettable pack off, monitoring system, necessary valves (bypass, unloading, and check valve), cable, and necessary surface systems to deliver power and two-way communication to the downhole system.

The WIST is intended to be retrieved from the well once the well is flowing naturally. The system was designed to install within a 4½" 11.6# and a 4½" 12.6# production tubing. The system specification was agreed to, using a combination of currently available items and equipment, which required engineering development.

Table 2 lists the functional specifications of the WIST system prior to the program commencement.

Engineering Development of New System Components

WIST Technical Challenges

At the start of the project, the WIST concept was new and unproven, and several challenges were identified:

The requirement to run a pumping system through a completion — most commercial electric submersible pump (ESP) systems do not fit the tubing drift. A slim (3.00" outside diameter) electric submersible progressive cavity pump system, using a permanent magnet motor and magnetic gear technology, had already been developed for cable deployed artificial lift applications. Upon commencement of the project, this equipment had already been proven reliable and robust through extensive field-testing over a seven year period. This technology platform was selected to be used to test and prove the WIST concept in this program.

Transmitting sufficient power to the pumping system through a conveyance cable. For the deployment of the conveyance cable, the challenge is that it needs to be small enough to be used as a wireline-type conveyance cable under live well conditions with pressure control and winch equipment, while also transmitting sufficient electrical power downhole to drive the submersible pump. As such, the cable size has been optimized mechanically and electrically to efficiently meet deployment and operating requirements.

Isolating the intake and the discharge of the pumping system within the wellbore. A pump isolation pack off (packer) is required to isolate the pump intake from the pump discharge to enable the pump to do useful work within the production tubing. A standard packer system had been used prior to the development program, which consisted of a packer deployed and set in the wellbore, and a sealbore latch deployed on the pump intake in a separate run.

Preventing the pumping assembly from being pushed uphole upon well kickoff. As a well begins to flow naturally, the flow rate in the wellbore can easily exceed the pump rate of the WIST pumping system. In this scenario, the pump could become a flow choke. The development of a bypass valve was therefore required to prevent reverse differential pressure from building up with higher pressure below the pump than above it. This valve also has to function as a check valve to prevent backflow of fluid through the pump in the case of an equipment shut down event.

Interfacing the WIST system with existing live well intervention equipment. A key driver of the project is to exploit the value proposition of the reduced well workover cost. The WIST is conveyed

Table 1 The four joint development program phases of the WIST.

Phase	Name	Objective
1	Equipment Procurement and Verification Test	Phase 1: The procurement and verification testing of the necessary components for three of the onshore field trials of the WIST system.
2	Pilot Field Trial with Single Set Packer System	Phase 2: Perform one oil field trial onshore within Saudi Arabia in selected well candidates as proof of concept of the WIST application.
3	Development and Qualification Test of Multiple Resettable Packer System	Phase 3: Develop and qualify testing of a multiple resettable packer system to improve the efficiency of the WIST operation.
4	Further Field Trials with Multiple Resettable Packer System	Phase 4: Perform two oil field trials onshore within Saudi Arabia in selected well candidates as proof of the WIST multiple resettable packer system.

Table 2 *Functional requirements of the WIST system prior to the program commencement.*

Parameter	Functional Specifications
Machine Purpose Statement	A device for artificially lifting fluids from a well using electrical power for the purpose of initiating natural hydrocarbon flow from the well.
Principle of Operation	A submersible pump system for through tubing electric line deployment into live wells.
System Reuse Requirements	The WIST drive train components (motor, torque converter, and seal section protector) is capable for a minimum of three operations (well installations) with a maximum duration of five days each without any service, which cannot be achieved under field conditions (tear down, etc.).
	The WIST string components (packer, unloading valve, etc.) are capable for a minimum three operations (well installations) with a maximum duration of five days each without any service, which cannot be achieved under field conditions. The progressive cavity pump may be changed out between operations dependent on damage/duty, but is capable of 500 bbl total flow without redress under normal operating conditions.
Downhole Configuration	Cable — connector — monitoring sub — star point — motor — torque converter(s) — seal section protector — pump discharge sub — pump — bypass flow valve — rupture disc — unloading valve — anchor packer.
Time to Displace Fluid in Well	Target less than 24 hours for 200 bbl.
Pump Performance	Maximum 1,500 psi differential pressure rating across the pump.
	Minimum target flow rate at 1,500-psi differential pressure across pump at 75 bpd.
	Target flow rate at zero head, minimum 250 bpd.
Max Free Flowing Well Rate	10,000 bpd through packer system and bypass.
Deployment Speed	System is capable of deployment at normal e-line speeds of 50 ft/min.
Bullhead of Fluids	For contingency operations, fluid is capable of being bullheaded past or through the WIST through a rupture disk. Following bullheading operations, it is not expected for the WIST to be operated prior to retrieval.

using wireline equipment rather than CT equipment. Commercial success and technology adoption is contingent on the WIST being faster, cheaper, and more reliable than existing methods, e.g., the CT nitrogen lift technique.

It is therefore important that conveyance of the WIST is achieved with universally available oil field equipment, such as wireline logging units and pressure control equipment. Surface pressure control equipment was selected to meet the specifications and pass required testing based upon existing wireline well control requirements.

To increase the chances of successful field-testing, the unproven elements of the system were qualified by lab testing. The results of the lab testing were used to rapidly make iterative improvements to components to deliver a working system within the project time frame. Figure 2 shows the general arrangement in a schematic, detailing elements of the WIST configuration, which are proven, and those requiring engineering and testing to meet requirements.

Development of a WIST Bypass Check Valve

The technical program included a requirement to develop a solution for a flow bypass. The main design challenge was packaging multiple flow conduits and valves within a small envelope that did not create a high flow rate choke point. Balls and seats were selected as they are more compact and robust than flapper valves, providing a greater flow area.

Figure 3 is a diagram of the WIST bypass tool, which performs several functions as previously described. When the pump is operated in a forward direction, the ball lifts off the seat to allow flow to move through the packer bore toward the pump inlet. When subjected to differential pressure from above, this flow path closes and seals as the ball lands on the seat.

Should the well be sufficiently pressured to create a differential pressure from below the pump, the alternative flow paths will open as the balls lift off the seat to create a large flow path for the well fluids to bypass the pump.

Development of a Multiple Resettable Packer

The technical program included a requirement to develop a solution for a new multiple resettable anchor packer to increase the operational efficiency of the service tool. Landing and latching in a preset packer bore poses several operational problems, which are desirable to eliminate.

Fig. 2 The schematic with technology development and qualification status of the WIST.

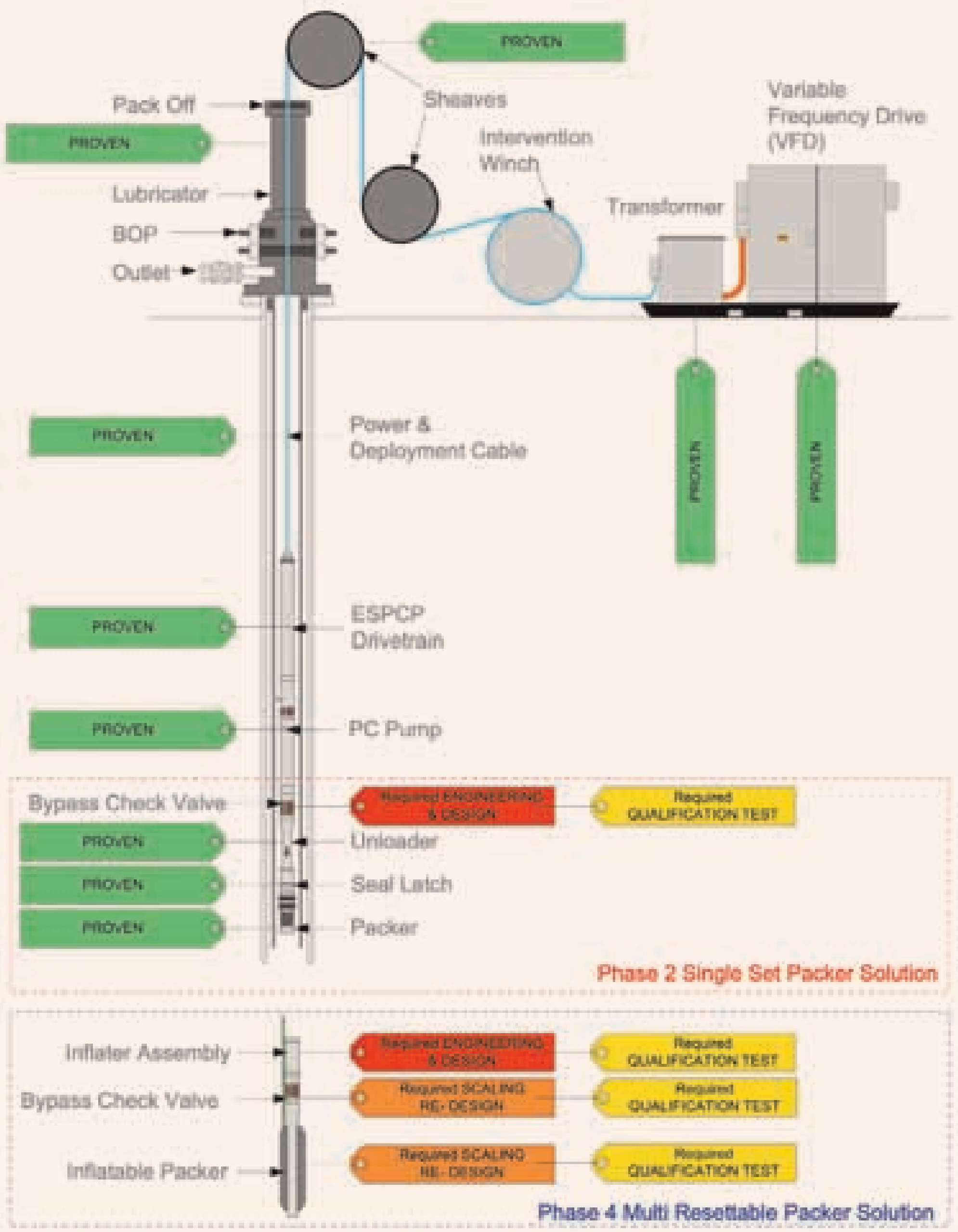

Fig. 3 The WIST bypass tool.

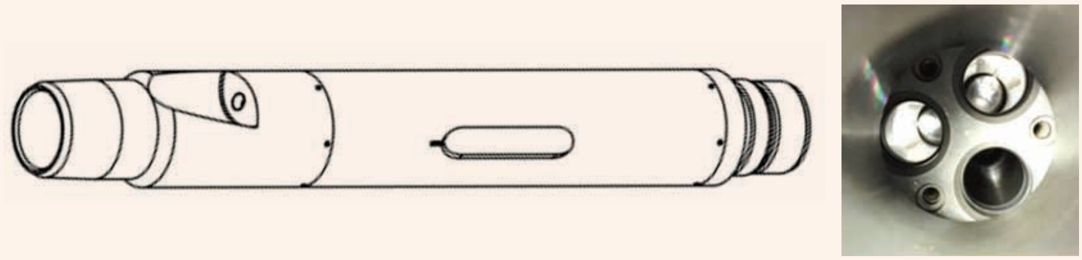

These problems are:

- Multiple intervention runs, increasing the job time, exposure, and cost.
- The increased requirement for additional surface equipment at the wellsite (slick line and wireline equipment).
- The increased chance of the well stopping flow during the packer retrieval (rephrase).

Setting and unsetting a packer, which is integrated into a cable deployed submersible pump assembly, is not straightforward, as traditional methods of setting are unavailable. For example, setting tools that rely on either explosive charges or hydrostatic differential pressure cannot be used. Further, rotational movement of the tool cannot be used. Any set or unset method, which uses shear stock, is also unsuitable.

After a period of engineering investigation, it was decided to use an inflatable packer system to create a temporary isolation seal between the intake and discharge of the pumping system. An inflatable packer was chosen as it can be inflated and deflated multiple times without redress, and the technology can also provide high expansion ratios to enable setting the WIST through tight completion restrictions. Inflatable packers do not require high setting forces, as do conventional slip and element style packers. Downhole tools, which require high setting forces, generally require redress of shear stock after each application (or run), and therefore, were deemed unsuitable for this multiuse application.

Inflatable packers are often inflated with a liquid pumped downhole, and given that the WIST already had a downhole electric pump system, it was logical to attempt to inflate the packer using the submersible pump. To direct the flow of fluid from the submersible pump system to the inflatable packer elastomer bag, an inflator assembly was required. The inflator assembly served the function of diverting flow to the elastomer bag until inflated, and then redirected the pump flow into the flow annulus for the main pumping operation. Once the pumping operation is complete, the inflator assembly is required to control the deflation of the elastomer bag so that it returns to near original drift size for repositioning elsewhere in the wellbore.

Initially, it was chosen to activate the inflator assembly through a combination of pump operation and cable manipulation. Designs for inflator assembly prototypes, mark 1 (Mk1) through Mk4, were developed using this principle. A spring loaded slotted mechanism was designed to cycle sliding sleeve ports between an open

Table 3 *Verification plan to field-test the equipment.*

Test	Process
Progressive cavity pump Flow Loop Tests (Phase 1)	1a. Standard progressive cavity pump flow test sequence repeated with 10 rotor/stator combinations up to 1,500 psi
	1b. Total volume endurance test 200 bpd and 500 bpd total
Dyno Tests (Phase 1)	2a. Factory Acceptance Test (FAT) — Static torque bench test
	2b. Standard Torque Drive 300 (3” diameter) FAT dyno automated sequence
	2c. Dyno endurance test
Bypass/Check/Burst Function Tests (Phase 1)	3a. Bypass function flow test
	4a. Basic packer set/unset repeat function testing
	4b. Inflatable packer outside diameter drift test
	4c. Inflatable packer endurance test
	4d. Inflated packer axial load test
	4e. Multiple packer set/unset cycle test with progressive cavity pump
Inflatable Packer Testing (Phase 2)	4f. Unloader sub-validation test
	4g. Burst disc sub-validation test
	4h. Torque resistance test
	5a. Load Test 3D printed manifold
	5b. Measure and 3.688” drift assembly post-test
	5c. Horizontal system integration test using flow loop
	5d. Vertical system integration test using flow loop in test well

Fig. 4 The dynamometer test bed apparatus.

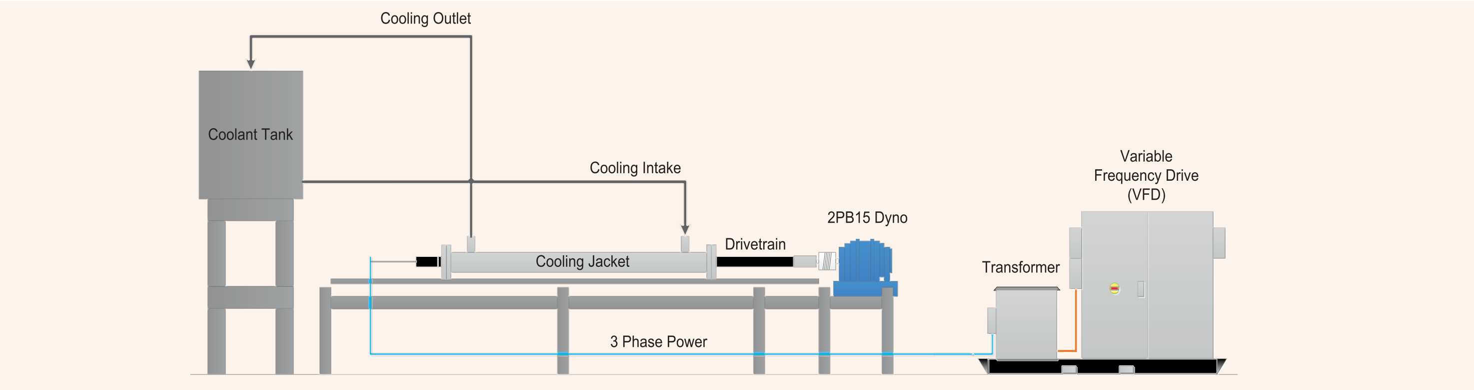

Fig. 5 The progressive cavity pump flow loop test apparatus.

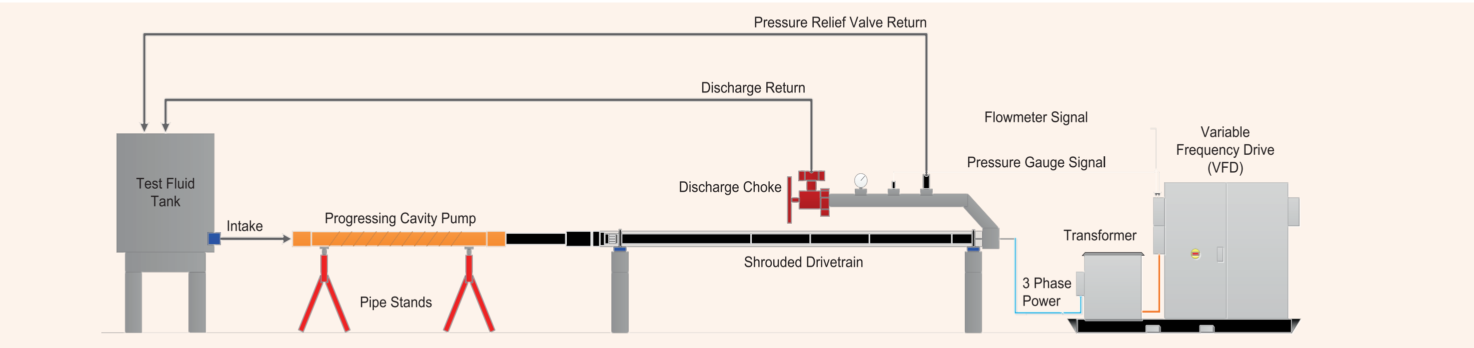

Fig. 6 The bypass valve test apparatus.

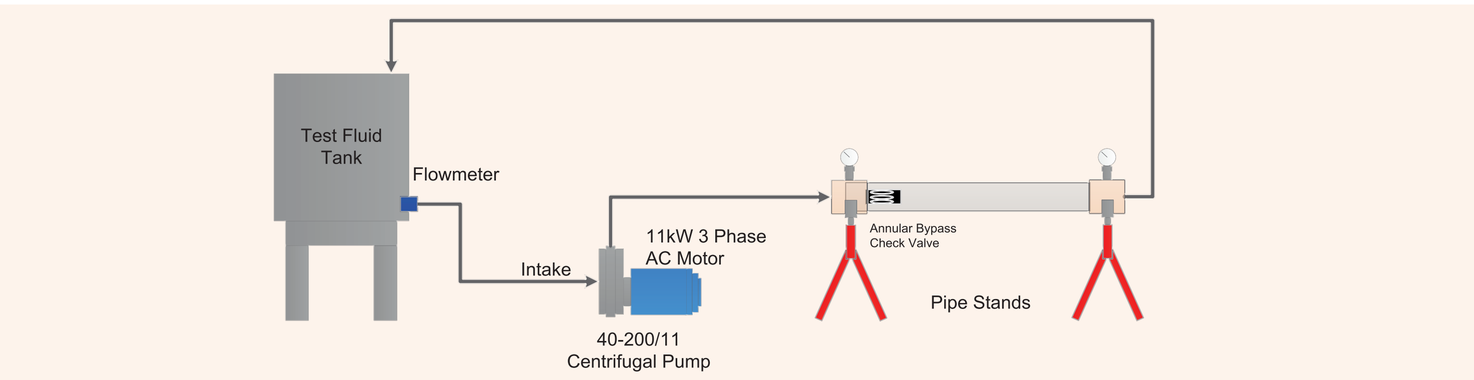

position and a closed position, while simultaneously diverting pressure and flow to the inflatable packer elastomer bag cavity and trapping/releasing pressure inside it.

This mechanism used cable manipulation to create an open/close motion, while the motor controller was used to regulate the pressure and flow generated from the pump. Unfortunately, following extensive testing, it was discovered that a combination of mechanism friction, which could not be overcome by gravity, and an imbalance of hydraulic piston areas, prevented this design concept from working.

A completely new type of inflator assembly mechanism was required. Instead of moving the cable and

Fig. 7 The horizontal flow loop test layout of the Mk1 to Mk4 prototype inflator.

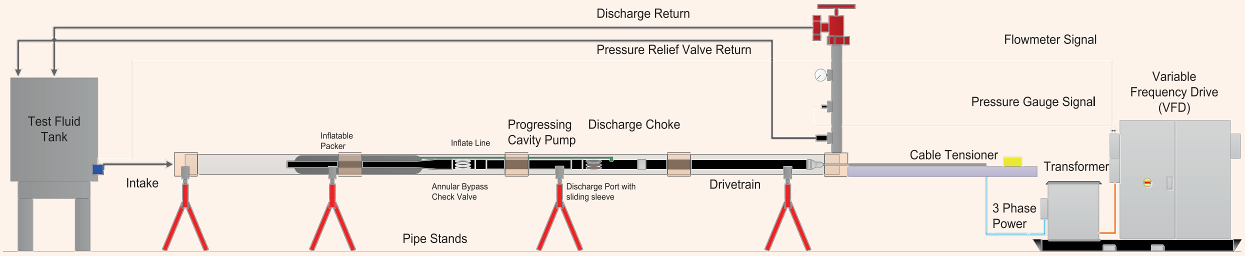

Fig. 8 The horizontal flow loop test layout of the Mk5 prototype inflator.

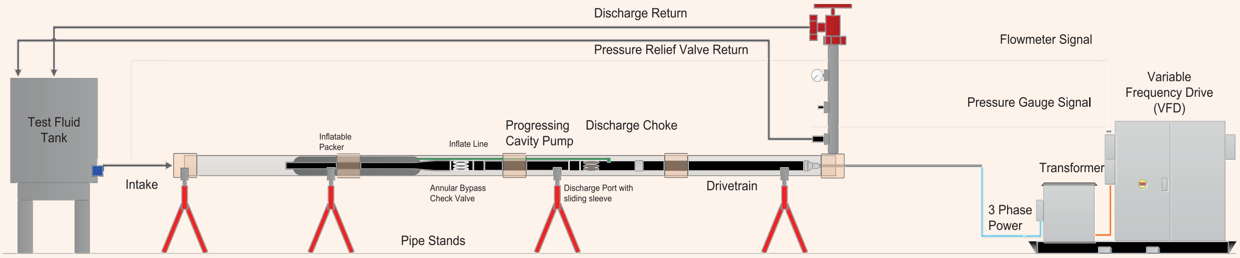

Fig. 9 The flow test layout of the Mk5 prototype inflator.

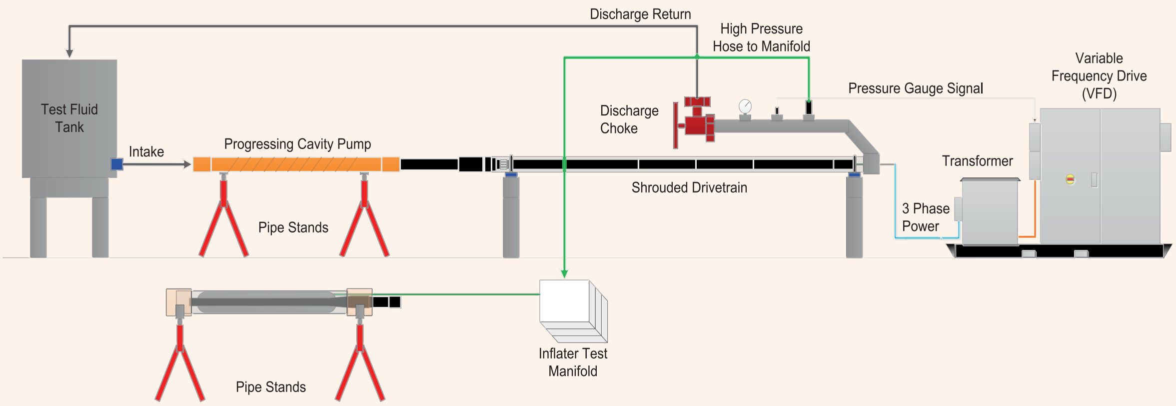

applying tension to manipulate a sliding sleeve across the pump discharge, the functionality of running the pump in reverse was utilized for control. By combining a hydraulic sequence control logic circuit, a check valve, and a pump (such as a progressive cavity pump), which can flow in two directions, it was possible to invent a system, which could selectively inflate and deflate an elastomer bag multiple times at different locations in a wellbore. Activation of the packer setting mechanism is independently controlled through the downhole pump motor direction and speed, operated through a control system at the surface in the wireline cab.

A novel hydraulic logic circuit was developed, which uses a counter intuitive concept. To deflate the packer, a higher pressure is used than the predetermined inflation pressure, thereby providing the user the ability to control when the packer inflates and deflates by: (a) operating the pump in reverse, and (b) dead head running at a speed that corresponds to either the inflation pressure or deflation pressure.

A summary of the evolutions of the prototype inflatable packer concepts, which were built and tested, are listed:

• Mk1: The initial design — cable manipulation

***Fig. 10** Photos of the SIT: The horizontal flow loop (left), and the test well deployment (middle and right).*

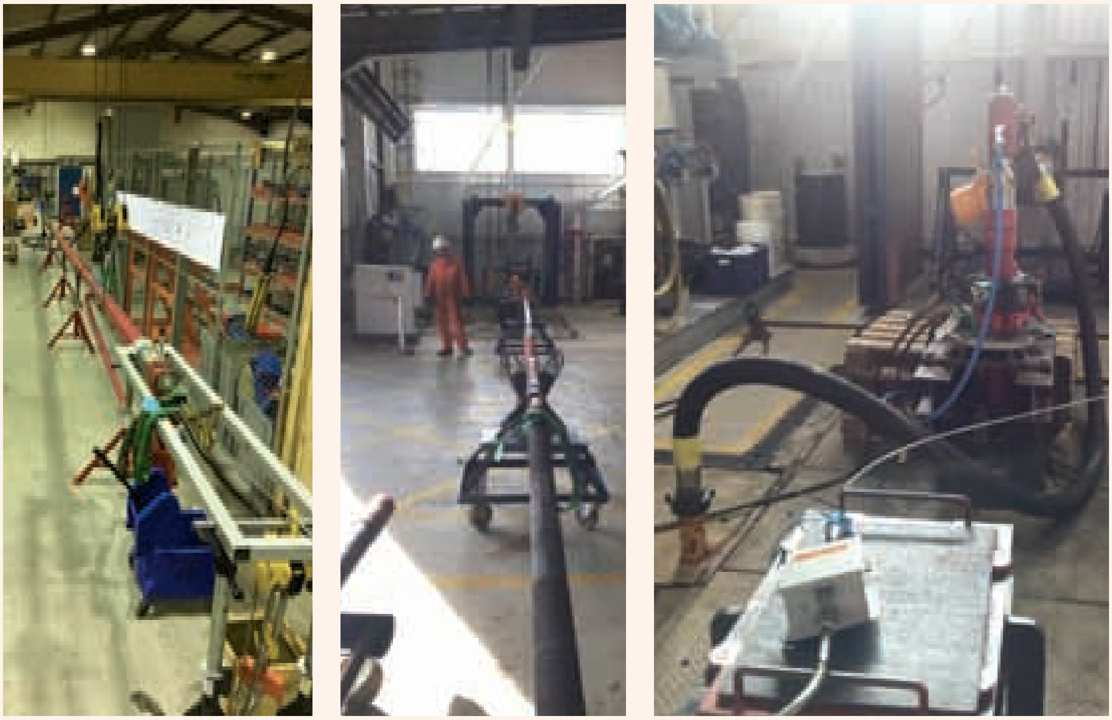

concept; unsuccessful.

- Mk2: Cable manipulation concept with modification to the piston areas for balance; unsuccessful.
- Mk3: Cable manipulation concept with further modifications to the hydraulic piston areas; unsuccessful.
- Mk4: Cable manipulation concept with the addition of multiuse shear pins to overcome and resist the piston force; unsuccessful.
- Mk5: Major change of function to inflate using a sequence control valve rather than cable manipulation; successful design promoted to the field-test stage.

It was possible to rapidly iterate the design, do prototyping and testing of the concepts through modification and reuse of parts, aided by close collaboration with manufacturing partners. The use of flexible and reconfigurable testing setups, and through the use of additive manufacturing — 3D metal printing — for parts was a significant advantage.

Verification, Qualification, and Field-Testing

Phase 1: Equipment Verification Testing

To ensure that the field-test equipment performed as expected, the following test plan was agreed to, Table 3. The test criteria were agreed by cross-referencing the requirements in the project specification document.

Dynamometer testing of the motor's drivetrain of the submersible pump system was conducted in line with standard factory acceptance test (FAT) quality procedures. The test apparatus consisted of a fluid tank (with cooling capability), a cooling shroud, a powder brake dynamometer, temperature, and power analyzer instrumentation tied back to the data acquisition system in the electric submersible progressive cavity pump variable frequency drive (VFD) package. Figure 4 shows the test configuration.

Flow loop testing was used to benchmark test the multiple progressive cavity pump combinations of the rotor and stator. This test was conducted so that the pump performance characteristics were well understood when used under field-test conditions. The test apparatus consisted of a fluid tank, a flow shroud, and a discharge manifold with manual choke, flow, pressure, and temperature sensor instrumentation tied back to the data acquisition system in the electric submersible progressive cavity pump VFD package. Figure 5 shows the test configuration.

Flow testing of the bypass valve was conducted to qualify the component for pilot field-test use. The test apparatus consisted of a fluid tank, a pup joint of 4½" tubing (with the same inside diameter (ID) as the test well tubing), a high rate centrifugal pump, flow, and pressure and temperature sensor instrumentation. Figure 6 shows the test configuration.

Phase 2: Equipment Qualification Testing

A horizontal flow loop was constructed using tubing pup joints of a similar ID to the project specification.

Fig. 11 The SIT layout for the vertical test well.

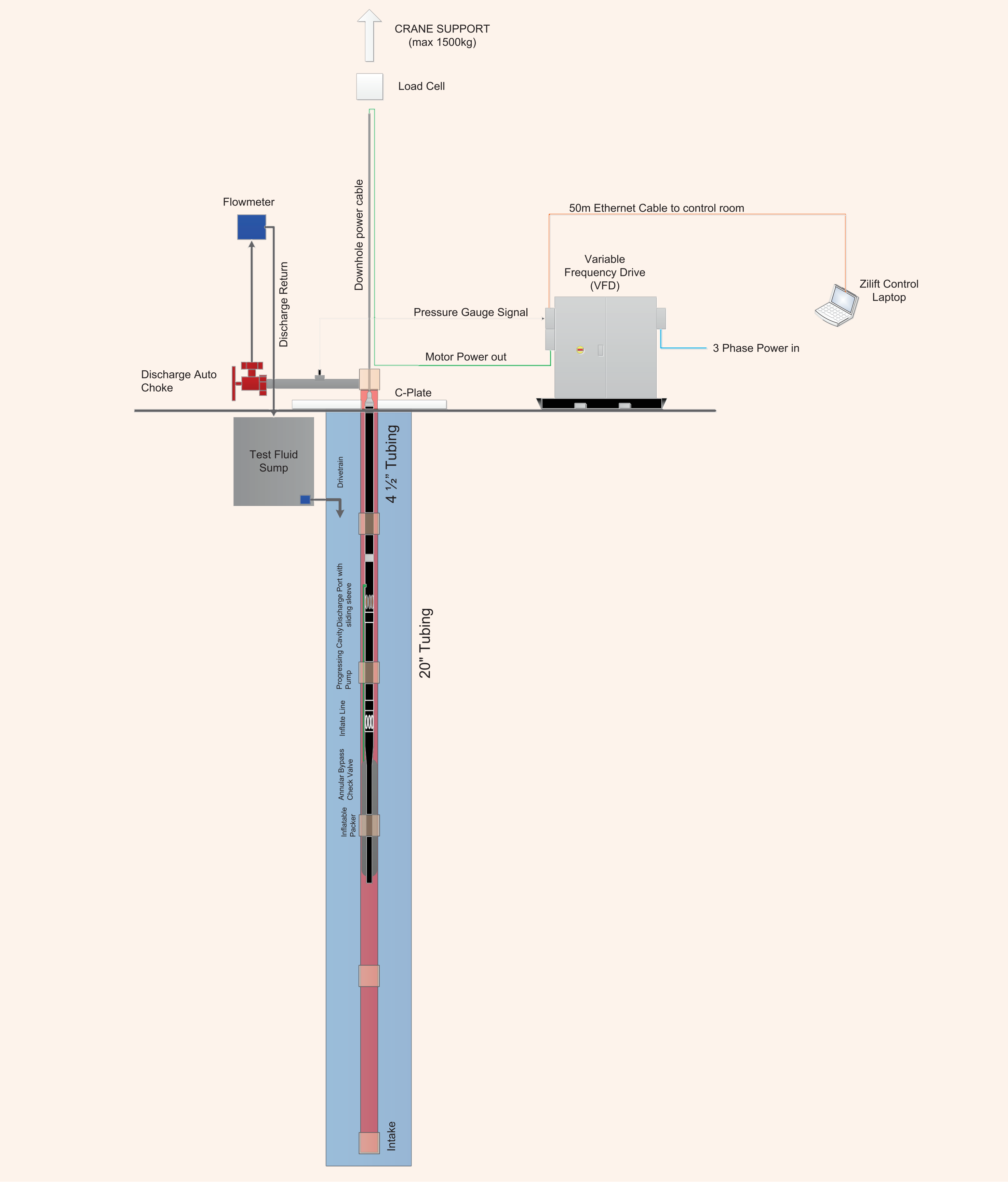

A cable tensioner system was fabricated to enable the cable to be pulled and manipulated during testing. Figure 7 is a schematic of the horizontal flow loop test layout of the Mk1 to Mk 4 prototype inflator. A similar setup was also used to test the Mk5 inflator, without using the cable tensioner functionality, Fig. 8.

The flow test setup was also used to inflate and deflate the packer with the Mk5 inflator manifold, Fig. 9. A high-pressure hose was routed from the discharge manifold of the progressive cavity pump to the hydraulic sequence control module connected to the packer.

To establish that the inflator mechanism functioned as intended in horizontal and vertical conditions, a system integration test (SIT) was conducted with the full bottom-hole assembly (BHA) in a horizontal flow loop, and then the flow loop was lowered into a test well to perform the same operations.

Figure 10 are photos of the layout of the horizontal flow loop apparatus as used in the horizontal SIT.

Figure 11 shows the layout of the vertical test well apparatus as used in the vertical SIT.

Figure 12 is a photo of the WIST BHA with an inflatable packer — Mk1 prototype.

Figure 13 shows iterations of the WIST BHA Mk1 prototype, the Mk5 (final), with the location of the hydraulic sequence control valve assembly.

Presentation of Data and Results

Tables 4 through 8 summarize the final testing results. The pass criteria were matched closely to the project specifications, and all tests achieved a pass against the requirements.

Evaluation of Results

Tests 1a through 2c confirmed that the cable deployed BHA, consisting of the motor torque converter and pump system, were suitable for the anticipated duty and service for a WIST. It also validated that the specific equipment sent to the field location was of suitable performance and build quality to perform during field trials. These tests were conducted as a routine matter and no specific issues were encountered as these elements of the total system were already field proven and semi-commercialized. Testing also gave a useful set of performance benchmarks for a selection of different progressive cavity pump rotors and stators under different temperature conditions.

Fig. 12 *Photo of the WIST BHA with an inflatable packer — Mk1 prototype.*

Fig. 13 *Photo of the WIST BHA with an inflatable packer — Mk5 prototype.*

Table 4 *Phase 1, Test 1 results summary.*

Test	Pass Criteria	Results	Pass/Fail
1a	Maximum 1,500 psi differential pressure rating across pump	Max pressure during test 1,560 psi at 500 rpm	Pass
1a	Minimum target flow rate at 1,500 psi differential pressure across pump 75 bpd	135 bpd at 1,500 psi at 500 rpm	Pass
1a	Target flow rate at zero head minimum 250 bpd	Max flow rate at zero head 343 bpd at 500 rpm	Pass
1b	Total flow greater than 200 bbl within a 24-hour period	Total flow during 24 hour period 206 bpd at 300 rpm	Pass
1b	Total flow greater than 500 bbl without redress	Total flow during endurance test 1,018 bpd at 300 rpm	Pass

Table 5 *Phase 1, Test 2 results summary.*

Test	Pass Criteria	Results	Pass/Fail
2a	Show a Torque Drive 300 drivetrain static pull out greater than 160 Nm	Field Trial Prototype (FTP) #6 187 Nm FTP #3 162 Nm	Pass
2b	500 rpm maximum speed, 10 min or greater	FTP #3 500 rpm run during dyno testing sequence for 150 min FTP #6 500 rpm run during dyno testing sequence for 150 min	Pass
2b	50 rpm minimum speed, 10 min or greater	FTP #3 50 rpm run during dyno testing sequence for 150 min FTP #6 50 rpm run during dyno testing sequence for 150 min	Pass
2b	Both systems pass the standard Torque Drive 300 FAT criteria	Full FAT sequence conducted for FTP #3 Full FAT sequence conducted for FTP #6	Pass
2c	Run dyno test continuously, 24 hours per day for duration of five days, each without any service	5 day non-stop endurance conducted for FTP #3 5 day non-stop endurance conducted for FTP #6	Pass

Table 6 *Phase 1, Test 3 results summary.*

Test	Pass Criteria	Results	Pass/Fail
3a	Show that bypass opens with differential pressure across the valve exceeds ~15 psi	Negligible differential pressure seen during test. Approximately 5 psi.	Pass
3a	Demonstrate minimal pressure drop while flowing/bypassing	Negligible differential pressure seen during test. Approximately 5 psi.	Pass
3a	Demonstrate valve functions to prevent flow in reverse flow direction	Flow witnessed in bypass direction, flow checked and prevented in opposite direction, with 100 psi.	Pass

Tests 3a through 3c were conducted without issue, and the results obtained were as expected.

Tests 4a through 4h were not so straightforward to complete, as they were initially conducted using the inflator mechanism versions (Mk1 through Mk4), which was subsequently found to be conceptually flawed. Once the inflator mechanism concept was changed, testing was conducted as planned, with most results within expected tolerances. All of the work for Test 4 was repeated once the prototype was changed to Mk5.

During part of Test 4, with inflatable packer pressure testing, it was noticed that the pressure held within the inflatable packer was not as steady as anticipated, with a higher than expected leakoff observed. This

Table 7 *Phase 2, Test 4 results summary.*

Test	Pass Criteria	Results	Pass/Fail
4a	5 × Set/Unset test with hand pump	5 × set and unset cycles performed with oil and hand pump. 5 × set and unset cycles performed with water and progressive cavity pump.	Pass
4b	Measure and 3.688" drift assembly post test	Drift assembly able to slide over deflated packer multiple times. Multiple Vernier caliper measurements also taken.	Pass
4c	Inflatable packer endurance test — 96-hour pressure drop limit	After hour 96, pressure in the packer had dropped from 800 psi to around 450 psi. Applied 8.5 MT load to packer mandrel — no slip.	Pass
4d	Inflated packer to withstand axial load equivalent to 1,500 psi difference	18,750 lbf/8.5 MT axial force applied using hydraulic piston. No packer movement observed. Tested twice, at 750 psi and 450 psi.	Pass
4e	Greater than 5 × set/unset test with the progressive cavity pump	30 set and unset cycles performed using progressive cavity pump.	Pass
4f	Demonstrate that unloader sub-shears at a predetermined load	Two tests performed using different shear rated stock, shear within expected range of force, unloader witnessed to open under load.	Pass
4g	Demonstrate that burst disc sub can be opened	One test performed, burst disc opened at expected pressure (1,000 psi) creating flow path.	Pass
4h	Apply ~400 Nm torque by hand to inflated packer	1,220 Nm applied during horizontal test.	Pass

Table 8 *Phase 2, Test 5 results summary.*

Test	Pass Criteria	Results	Pass/Fail
5a	Tensile load test sequence control manifold greater than cable strength	Load tested in hydraulic press to 3 MT (6,600 lbf).	Pass
5b	Pressure test sequence control manifold	Tested to 3,000 psi, pressure drop less than 80 psi in 10 minutes.	Pass
5c	Horizontal flow loop SIT 5 × set/ unset SIT Withstand 1,000 psi differential pressure across packer Assembly to pass drift after testing	Day 1: 5 × set and unset cycles performed in flow loop, 1,003 psi differential applied across packer with pump, assembly drifted to 3.688" at end. Day 2 (client witnessed): 5 × set and unset cycles performed in flow loop, 845 psi differential applied across packer with pump, assembly drifted to 3.688" at end. System operated remotely. System back flushed through bypass valve using high flow C-pump.	Pass
5d	Vertical test well SIT 5 × set/unset SIT Withstand 1,000 psi differential pressure across packer Assembly to pass drift after testing	Day 1: 5 × set and unset cycles performed in flow loop, 1,003 psi differential applied across packer with pump, assembly drifted to 3.688" at end.	Pass

phenomena was later attributed to a combination of contraction effects due to temperature and elastic hysteresis as the elastomer relaxed over time. To ensure that this effect would not cause any adverse operational effects, tests were repeated multiple times with different components (same effect observed), and a packer anchoring axial force test added to the test program. It was found that the pressure degradation effects can be managed operationally and mitigated by boosting packer pressure whenever it falls below a certain threshold.

Test 5 was the final and most important opportunity to qualify the multiple resettable packer system. Tests 5a through 5d were conducted without issue and the results obtained were as expected. Testing was performed multiple times, both in horizontal and vertical orientation to ensure that gravity effects did not influence the operation of the system. Several traits of the system were observed during testing, and a set of best practices for effective multiple resettable packer system operation were developed in preparation for use in the field.

Future Work

The full program included a set of three field tests — detailed in phases 2 and 4 in Table 1 — to demonstrate and further qualify the technology and technique under real well conditions. At the time of writing, it is anticipated that this scope of work is executed in the near future. In preparation, two sets of the WIST equipment have been exported to the Kingdom of Saudi Arabia, ready for deployment. A pilot field trial candidate well has been selected and the WIST technology will be demonstrated in the field trial.

Conclusions

This article has described the development for a new and innovative WIST for lifting naturally flowing wells back into production. This lightweight cable deployed pump system has been conceived as a cost-effective alternative to CT and nitrogen kickoff jobs.

Equipment matching the WIST specification was procured, developed as required and tested with a rigorous test program, verifying and qualifying each element of the WIST equipment as suitable to be released for a field-test.

As part of this project, a multiple resettable inflatable packer system was successfully developed to work in conjunction with the permanent magnet motor pumping system, which allows the pump to be positioned and then repositioned in the well with much improved operational efficiency. This capability was achieved after several attempts to perfect the setting mechanism, finally achieved using a novel hydraulic sequence control logic circuit invented specifically for this project.

Planning is now in progress for three field trials in the Kingdom of Saudi Arabia to validate the performance of the WIST.

Acknowledgments

This article was presented at the 2020 International Petroleum Technology Conference, Dhahran, Saudi Arabia, January 13-15, 2020.

About the Authors

Chris Wrighton

B.S. in Mechanical Engineering, The Open University

Chris Wrighton is a Research Consultant working at the Aberdeen Technology Office of Saudi Aramco's Exploration and Petroleum Engineering Center – Advanced Research Center (EXPEC ARC), where he provides artificial lift solutions.

Chris has more than 30 years of experience in the design, development, and application of rotor dynamic pumps and motors for major service companies and operators within the oil and gas industry.

He received his B.S. degree in Mechanical Engineering from The Open University, Milton Keynes, U.K.

Dr. Jinjiang Xiao

Ph.D. in Petroleum Engineering, University of Tulsa

Dr. Jinjiang Xiao is a Senior Petroleum Engineering Consultant working in Saudi Aramco's Exploration and Petroleum Engineering Center – Advanced Research Center (EXPEC ARC). His current focus is artificial lift research and development.

Prior to joining Saudi Aramco in 2003, Jinjiang spent 10 years with Amoco and later BP-Amoco, working on multiphase flow, flow assurance and deep-water production engineering.

He received both his M.S. and Ph.D. degrees in Petroleum Engineering from the University of Tulsa, Tulsa, OK.

Jamie Cochran

M.Eng. in Mechanical Engineering, University of Birmingham

Jamie Cochran is a Technology Manager working at Zilift Ltd. to innovate and integrate alternatively deployed artificial lift systems for novel well intervention applications.

He has 20 years of upstream oil and gas experience, gained from working in technical roles in well construction, well intervention, and production domains. In the last 10 years, Jamie has specialized in new product development at a variety of service companies, and has contributed to the invention of over 10 international patents. One recent patent concept features a novel method of setting and unsetting a packer for well intervention pumping applications.

In 2000, he received his M.Eng. degree in Mechanical Engineering from the University of Birmingham, Birmingham, U.K.

Parijat Mukerji

M.S. in Petroleum Engineering, Texas A&M University

Parijat Mukerji is the Technical Director for Production at Schlumberger Wireline HQ. He has been with Schlumberger for more than 28 years in various technical roles, working at various locations, including the Middle East, Africa, and Europe.

In his current global role, Parijat is responsible for the production logging and cased hole surveillance technology portfolio within the Wireline segment.

He began his career as a production engineer with the Oil & Natural Gas Corporation, India, where he worked at the Bombay High North offshore oil field for four years.

In 1984, Parijat received his B.S. degree in Chemical Engineering from Punjab University, Chandigarh, India. In 1991, he received his M.S. degree in Petroleum Engineering from Texas A&M University, College Station, TX.

High-Definition Modeling for Complex Multilateral Well with Smart Completions

Dr. Ghazi D. AlQahtani, Dr. Wisam Shaker, Menhal A. Al-Ismail, Dr. Tareq M. Al-Shaalan, Jibran Ayub, and Saud A. Al-Hoti

Abstract / Multilateral wells may vary in the number of laterals from two to more than 10 laterals. To control production on a lateral level, advance completion equipment, such as inflow control valves (ICVs) and dual ported permanent downhole monitoring systems — for real-time pressure measurements — are installed in the motherbore against each lateral to regulate reservoir fluids into the production tubing of the well, from an individual or a collective set of laterals. Multilateral wells equipped with advance completion tools become complex wells (hereinafter called the "complex wells") in reservoir engineering. Recently developed complex wells involve multiple designs and architecture for which the reservoir exposure for laterals can be thousands of meters.

A new generation of smart multilateral well completions are Manara-type wells where the laterals are divided into a number of segments or compartments using oil swell packers, and Manara stations are placed against each segment for quantifying the liquid rate, water cut, and real-time reservoir pressure measurements. Each station is equipped with an electrical control valve for controlling unwanted fluid production at a segment level. In this work, a new workflow is established to model and history match the Manara well with complex modeling features using the GigaPOWERS simulator and a compositional full field model. The established segment level history matching workflow includes four important milestones to achieve.

The first is an advance well completion design at which the physical well completion details are translated and converted into a grid-based completion detail with the help of preprocessing tools. The second step covers the generation of three complex well related input files for the GigaPOWERS simulator. The third step is the process of validating high frequency performance data, including flow rate, choke size, and pressure for the complex well stations. The last step involves conducting the history matching exercise on a segment level for every individual station to achieve the final history match model.

The conventional history match procedure generally includes three levels to match: field, group, and well. In this workflow, the station level match is done for the first time with a full field compositional model with a size of more than 61 million grid cells. The high-definition history match is achieved at a segment level for six stations that constitute a trilateral well with high frequency performance data. Complex well modeling in GigaPOWERS includes pressure drop calculations for several components. The pressure drops are related to friction, gravity, acceleration, and advanced tools, i.e., ICVs.

Modeling a complex well involves several pre- and post-simulation environment features at the segment level that should work in complete consistency. The achieved outcome enables a business impact evaluation for an accurate value proposition for complex well incremental rates, cash flow streams, and sensitivity prediction cases.

Introduction

Multilateral wells have been increasingly utilized in the last two decades in producing hydrocarbon reservoirs. One of the main advantages to using such wells against conventional and single bore wells comes from the additional access to reservoir rock by maximizing the reservoir contact area. Another advantage is the decreased number of wellheads required on the surface, and therefore, the reduced number of wells needed. Multilateral wells have evolved in the petroleum industry with more complex designs and architecture such as extended reach wells, maximum reservoir contact, and extreme reservoir contact wells[1].

Bouldin et al. (2017)[2] and Elfeel et al. (2018)[3] have presented one of the latest technology developments and adaptation where Saudi Aramco and Schlumberger jointly developed the new generation of well completion technology — where multiple inflow control valves (ICVs) were installed in each lateral in a single multilateral well. The laterals are divided into a number of segments through oil swell packers.

Integrated stations are placed in each compartment for downhole liquid metering, pressure, and water cut measurements. These stations are equipped with efficient electrical ICVs to optimize oil rate and control unwanted fluid production. Such technology may impact the long-term production optimization at the compartment level, and thereby will improve the overall sweep efficiencies, providing for more recovered oil.

Modeling multilateral wells equipped with advance completion tools, such as ICVs and inflow control devices (ICDs), requires advance simulation options. Features like grid segmentation, selective pressure drop computations due to frictional loss, acceleration, gravity, and ICVs and ICDs on well and field modeling levels, are critical to enable a more accurate representation of the physics related to fluid interaction with completion tools. Such modeling capability may have a significant impact on the field development decision making process.

Modeling complex wells have been addressed in the industry for more than 10 years. Al-Qahtani et al. (2009)[4] introduced a workflow for modeling complex wells from single to full field-scale simulation models.

In this article, segment level reservoir simulation history match is performed for a Manara-type well. Complex well modeling features were utilized to achieve dynamic calibration with performance data for the multilateral well on a field level. It is paramount to highlight that this work is unprecedented and resulted in a new workflow.

Complex Well Modeling Workflow

To model a Manara-type well that has performance data, a complete history match and dynamic calibration has to be established. Therefore, the scope can be identified as follows:

- Validate the performance data, including flow rate, chock size, and pressure for each station.
- Model the Manara well with the complex well format[5, 6] in GigaPOWERS™.
- History match the Manara well stations with actual performance.
- The field used in this study was for a full field compositional reservoir simulation model, which included more than 300 wells of different types and more than 20 years of history. The size of the model was more than 60 million cells with nine hydrocarbon components, in addition to water.

The Manara-type well under investigation is a trilateral well in which six ICVs were installed with two in each lateral, separated by packers, Fig. 1. The purpose of having this combination of ICVs and packers is to create stations at which pressure, temperature, and water cut measurements can take place. Figure 2 is a station level diagram illustrating the components involved. The packer's in-between stations are to create isolated-type compartments and to confer production through each station.

To model the Manara-type well, it is paramount to have the right simulator capability and environments to apprehend pressure changes occurring throughout the advent of ICVs in the completion system. The GigaPOWERS reservoir simulator with regular features cannot mimic accurately the fluid flow interactions with installed advance completions, and the related pressure losses on branch/station level details. Therefore, the GigaPOWERS complex well modeling features should be used to reflect fluid flow physics on the lateral/segment levels[5].

Before we go any further with the details of history matching workflow, we will first present important features to enable segmentation modeling for the Manara well. The following features are essential for complex well modeling:

a. Well Discretization (segmented well):
   - Zone isolation
   - Cross flow handling
   - Mechanical components handling
   - Horizontal, maximum reservoir contact, and

Fig. 1 The Manara trilateral well with six stations, in which ICVs are installed.

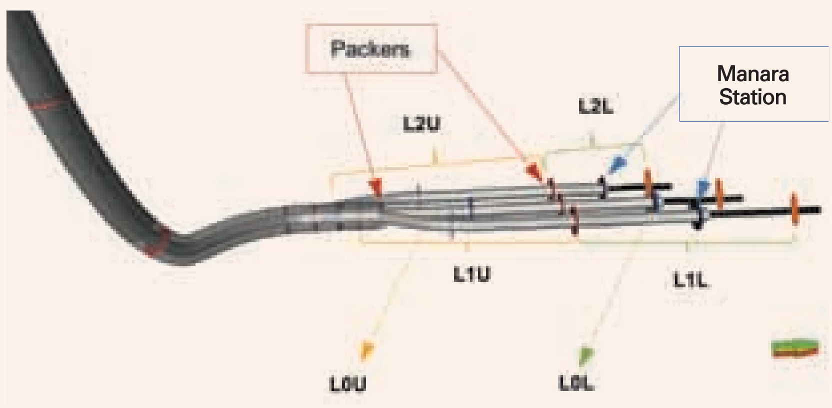

Fig. 2 *A diagram detailing the station measurement profile that takes place at each Manara station.*

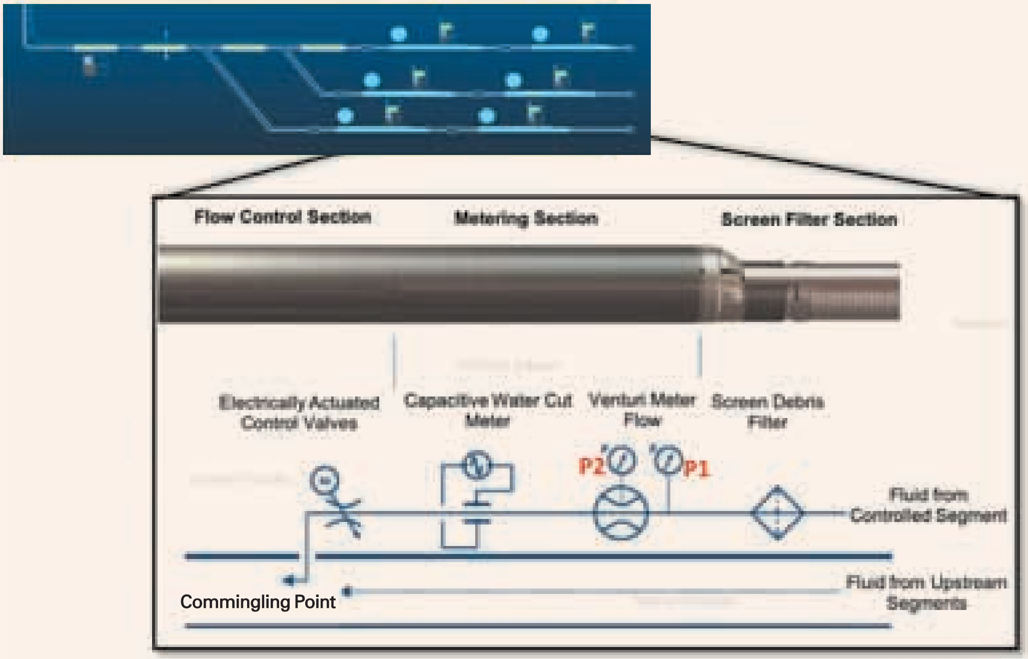

extreme reservoir contact well

b. Static and dynamic controlling

c. Fast convergence and robustness

d. No limitation to the number of branches or sub-branches (extreme reservoir contact)

e. Trajectory can be in IJK or XYZ (UTM coordinates)

f. Simulation from the sandface to the wellhead

g. Handling packer flow

The above-mentioned list of features represents the computational capability and performance improvements any simulator should have. GigaPOWERS has advance complex well modeling features in addition to the aforementioned basic ones. For the sake of the Manara well modeling, the important enabling features to focus on are a, b, c, and g. Feature g, in particular, is responsible for creating a compartment-type station to mimic the Manara design and performance.

Complex well modeling in GigaPOWERS includes pressure drop calculations for several components. The pressure drops are related to friction, acceleration, gravity, and advance tools (ICV and ICD). Figure 3 gives the important terms in each component contributing to pressure drop in the wellbore and completion of a general complex well.

The conventional history match procedure generally includes three levels to match, which are the field, group, and well levels. In this study, the station level match is done for the first time with a full field compositional model with a size more than 60 million cells. There are some prerequisites before the history match at this new level is attempted. For example, the frequency of the data to be matched for the Manara well is on a

Fig. 3 *Important terms in each component contributing to pressure drop in the wellbore and completion of a general complex well.*

The pressure drop within the complex well's wellbore for open hole completion is due to these components:

ΔP (Total) = ΔP (Gravity) + ΔP (Friction) + ΔP (Acceleration) **+** ΔP (tool)

Where,

$\Delta P\ (Gravity) = \rho g\, \Delta h$ (change in height)

$\Delta P\ (Friction) = 2 f \rho V^2$ (pipe roughness)

$\Delta P\ (Acceleration) = 2\rho V \frac{dV}{dL}$ (change in momentum) daily basis, covering about one year of performance. Moreover, the size of the full field model is huge, which causes a long simulation runtime, more than 8 hours. It was important to create a restart file that works well with the complex well option that takes into account daily time step computations at the segment level.

The established segment level history matching workflow includes four important milestones to achieve. The first is the advance well completion design at which the physical well completion details are translated and converted into grid-based completion details with the help of a preprocess tool. The second step covers the generation of related input files of the complex well for the GigaPOWERS simulator. The third step is the process of validating high frequency performance data for the Manara well's six stations, and applying corrections once needed. The last step covers conducting the history matching exercise on a segment level for every individual station, and achieving the final history match model. Figure 4 is a diagram summary for the established workflow.

Manara Complex Well Modeling

Well Completion Design and GigaPOWERS Input Files

As introduced in the previous section, the Manara well completion details were loaded into a preprocessor. The Manara well has three laterals and each has separate completion windows, Fig. 5. This example shows the

Fig. 4 *Complex well modeling workflow for historical wells.*

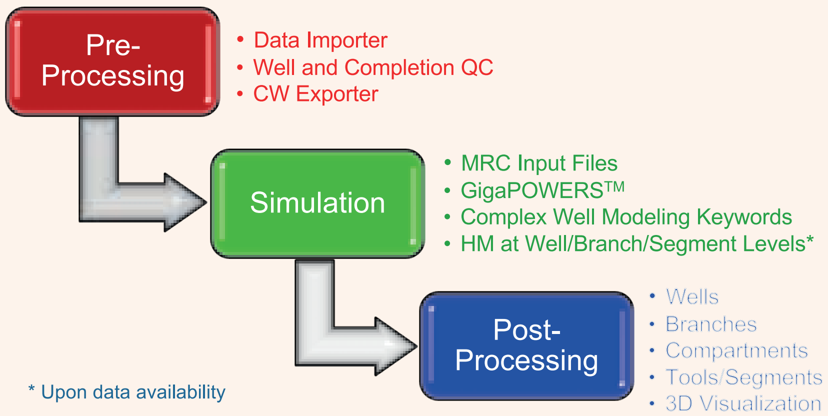

Fig. 5 *The Manara-type well completion specifications*[2].

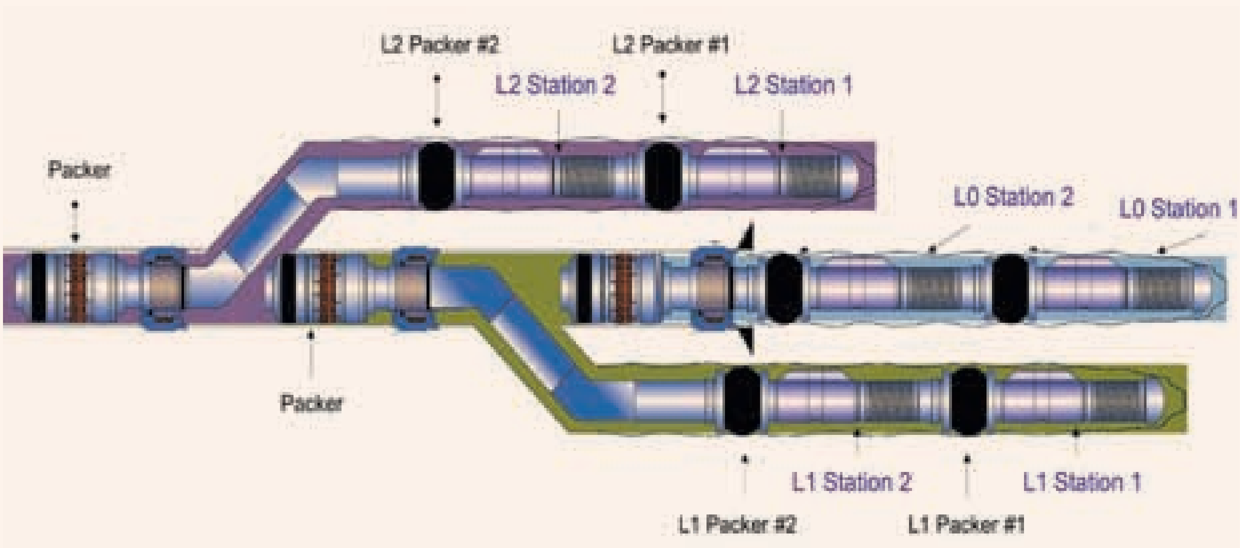

location of the packers, ICVs, and some completion equipment.

We give special attention to particular details related to the advance tools used in the Manara well. For instance, the ICV constriction area when the valve is in a fully open position is critical information — to be used as input data for the simulator — which impacts the accuracy of the pressure drop computations, due to advance tools. Figure 6 shows the ICV related information for the Manara well.

Once the completion details related to the packers, ICVs, the diameters of the completion equipment, and the advance tools' modeling parameters are captured, a completion diagram can be illustrated for the Manara well, Fig. 7. The length of each compartment is captured as well, which influences the productivity access for each station. Figure 8 summarizes in 3D generated Manara well completion details equipped with advance tools in the model.

Once complex wells are modeled and validated in the preprocessor, they are exported to the simulator. The simulator expects a certain input format to understand the details of the compartments, including locations, diameters, roughness, nozzle sizes, etc. The GigaPOWERS simulator provides a wide spectrum of features to support various types of advanced completions with different configurations. Therefore, customized preprocessing features were developed to bridge the complex wells modeling to GigaPOWERS.

These preprocessing features provide capabilities to export all the details captured by the engineers and incorporate them into the simulation model. These

Fig. 7 *Using Petrel (a pre-processor) to translate the physical Manara well completion details into a 3D simulation model. This shows the completion section with the location of the valves.*

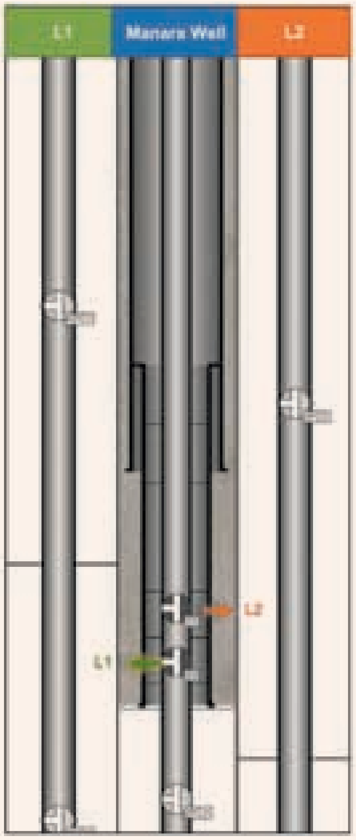

Fig. 6 *A detailed view of the valve in the fully open position, and also in the fully closed postion. This figure also shows the ICV when fully open, which is important for the complex well input file for GigaPOWERS.*

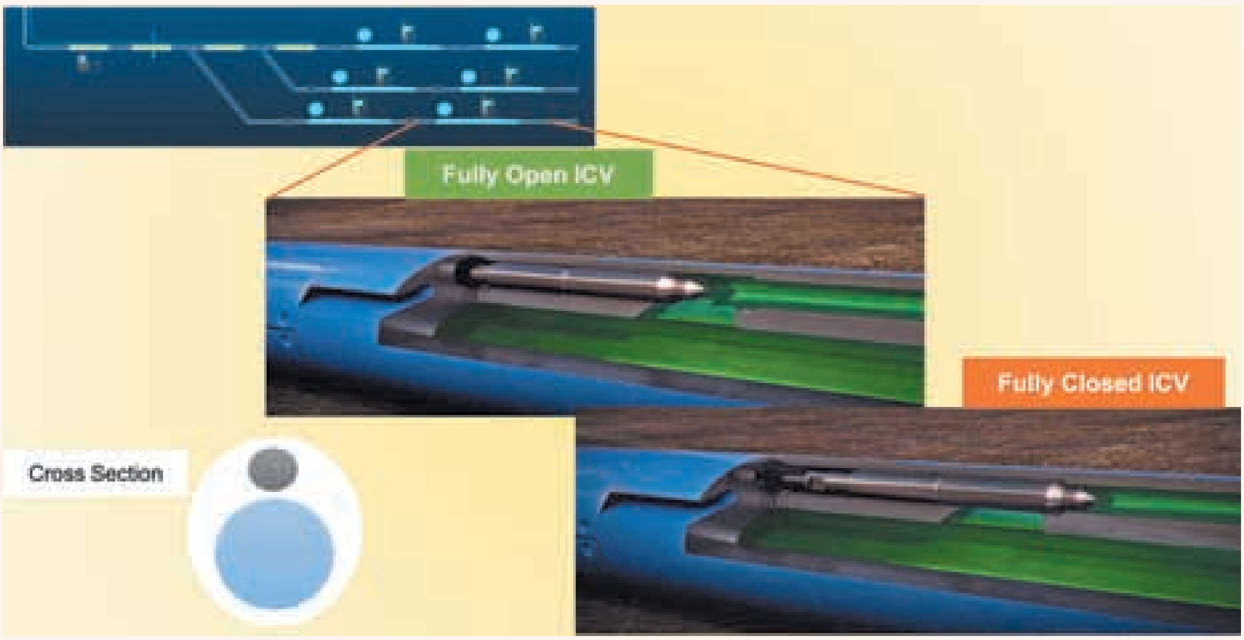

Fig. 8 A 3D view of the Manara well showing the details of the compartments and the location of the packers and ICVs for each station. The length for each station is also shown.

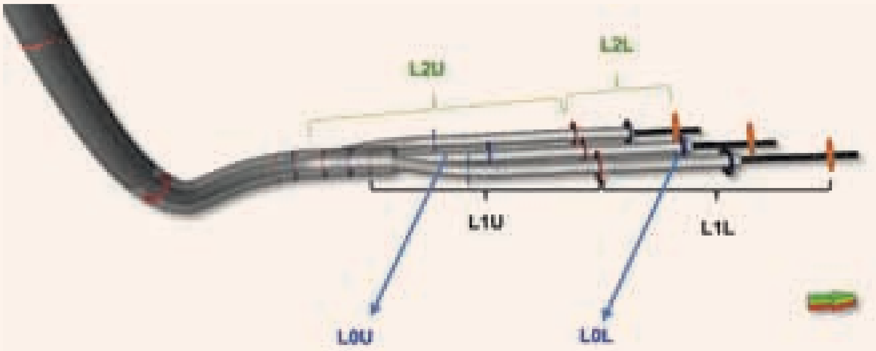

Fig. 9 The raw performance data for station L1U (Lateral 1 upper station). The gray line shows the P1 pressure measurement. The yellow line shows the P2 pressue measurement (normalized with the highest value). The blue line shows the calculated flow rate from the P1 and P2 values (normalized with the highest value).

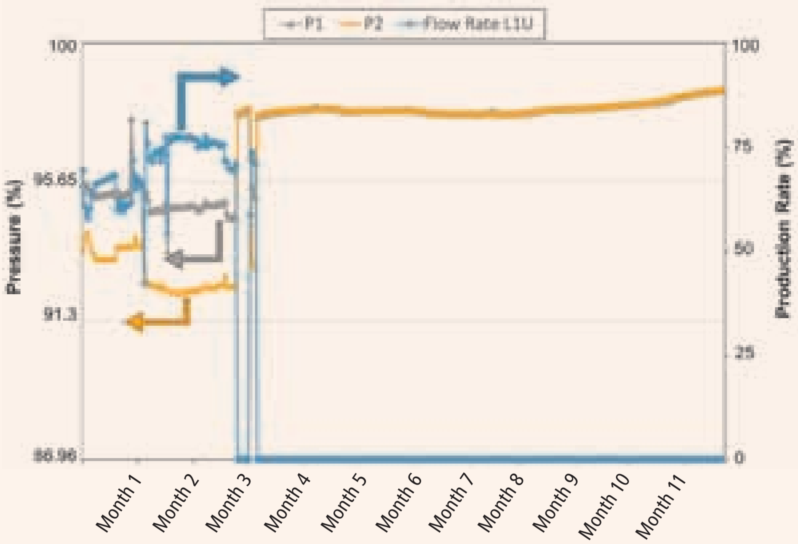

features are encapsulated into a plug in which was developed in-house on top of an existing preprocessor. The plug-in mainly generates three files for the simulator. The first file is the well's model file in which details of the well trajectories and advanced completions are specified. This file provides the simulator with the structure of the wells and the locations and type of each completion device. The second file is a catalog for the different types of devices. It specifies the specifications of each device such as nozzle size, roughness, coefficient values, etc. The third file provides the observed production rates.

Modeling complex wells is a challenging task, which involves multi-segmenting the well path to allow pressure drop calculations in each location. The challenge takes another dimension when the simulation model is huge, has fine resolution, and very thin grid cell

Table 1 The dimensions and description for the compositional full field model.

Number of Cells	> 60 MM
Cell Size	40 × 40 meters
No. of Layers	80
No. of Wells/Status	> 330
Type of Pressure-Volume-Temperature Model	EOS (Nine hydrocarbon components and water)
Water Aquifer Attached	Yes
HM Model Run Time	Average 7 hours on 2,000 cores

Fig. 10 *The flow rate history match normalized in percentage with respect to the highest value. The blue line is the model flow rate while the dark circles are the observed flow rate. The flow rate was input data for the simulator and the figure shows a perfect match between the model and the observed data.*

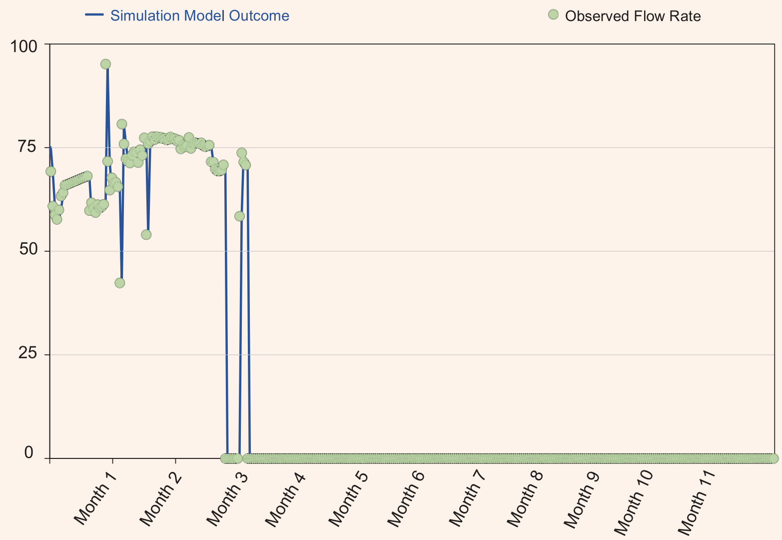

Fig. 11 *The BHP match at the beginning of the project using the original full field model before any modifications normalized in percentage form. The green line is the model output while the black circles are the observed data (averaged in days). It is evident that the BHP was not reproduced by the model since more than 10% is the difference, which needs further investigation.*

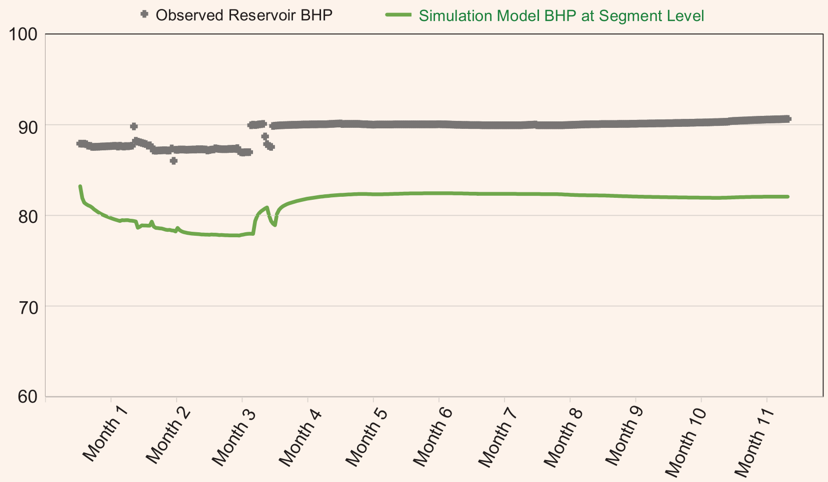

layers. Packers and devices are distributed within the wellbore, and their locations have to be preserved when exporting to the simulator. For that reason, each device is associated with one segment in which the simulator calculates various dynamic results to enable assessing the performance at segment level. The plug-in plays an important role to address and streamline these challenges by managing the multi-segmentation design to preserve well integrity.

A complex well modeling exporter is used to generate the complex wells' input files for the GigaPOWERS simulator. There are three types of complex well modeling files that can be generated using such a plug-in. These are data type files for the trajectory and perforation of the Manara well, rate file, and device file. On the devices file, Chen Corelations[7] was used as the correlation for calculating frictional loss since it was more suitable in handling the mixture of oil, gas, and water fluids, as in the case of the Manara well. In fact, the Venturi meter calculates the flow rate for single-phase flow, which mimics the condition of production from the Manara well. This correlation, using the Chen equation, reflects the homogenous mixture of the fluids' pressure drop calculation, which

Fig. 12 The saturation cross section showing the location of the Manara well with respect to the simulation modeling layers.

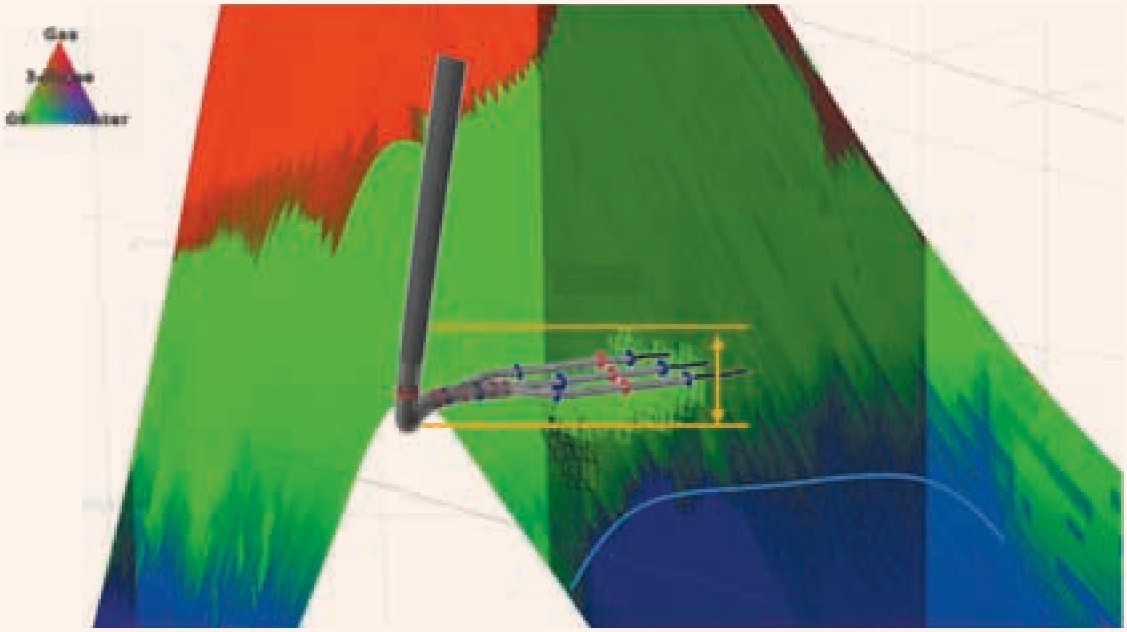

Fig. 13 The top view of the permeability in the X direction for the layers below the Manara well down to the OWC at layer 74. Note that the scale of permeability is one to three orders of magnitude. The blue color indicates one order of magnitude for the K values. The light blue indicates two orders of magnitude while the green color reflects more than two orders of magnitude for the K values. The top left red color shows the layer number while the dashed green colors show the projected well location.

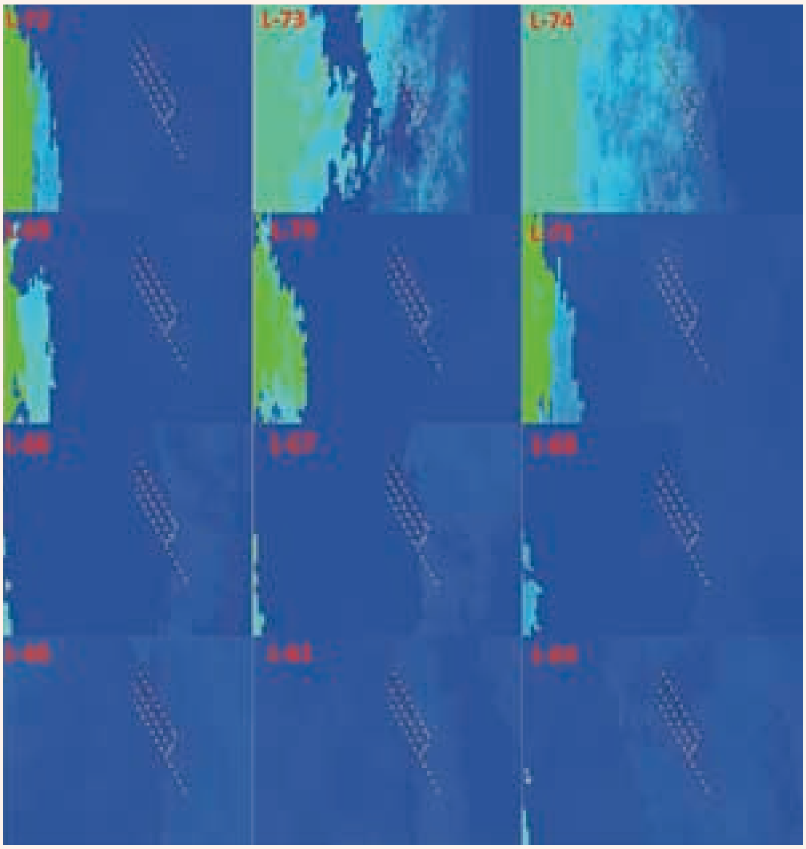

Fig. 14 *The permeability in the X direction for the layers of the Manara well placed in the simulation model. Note that the scale of permeability is one order of magnitude to three. The blue color indicates one order of magnitude for the K values. The light blue indicates two orders of magnitude, while the green color reflects more than two orders of magnitude for the K values. The top left red color shows the layer number while the dashed green colors show the well location.*

Fig. 15 *The permeability in the X direction for the layers above the Manara well from 56 to 37 in the simulation model. Note the scale of permeability is 1 md to 300 md. The blue color indicates one order of magnitude for the K values. The light blue indicates two orders of magnitude, while the green color reflects more than two orders of magnitude for the K values. The top left red color shows the layer number while the dashed green colors show the well location.*

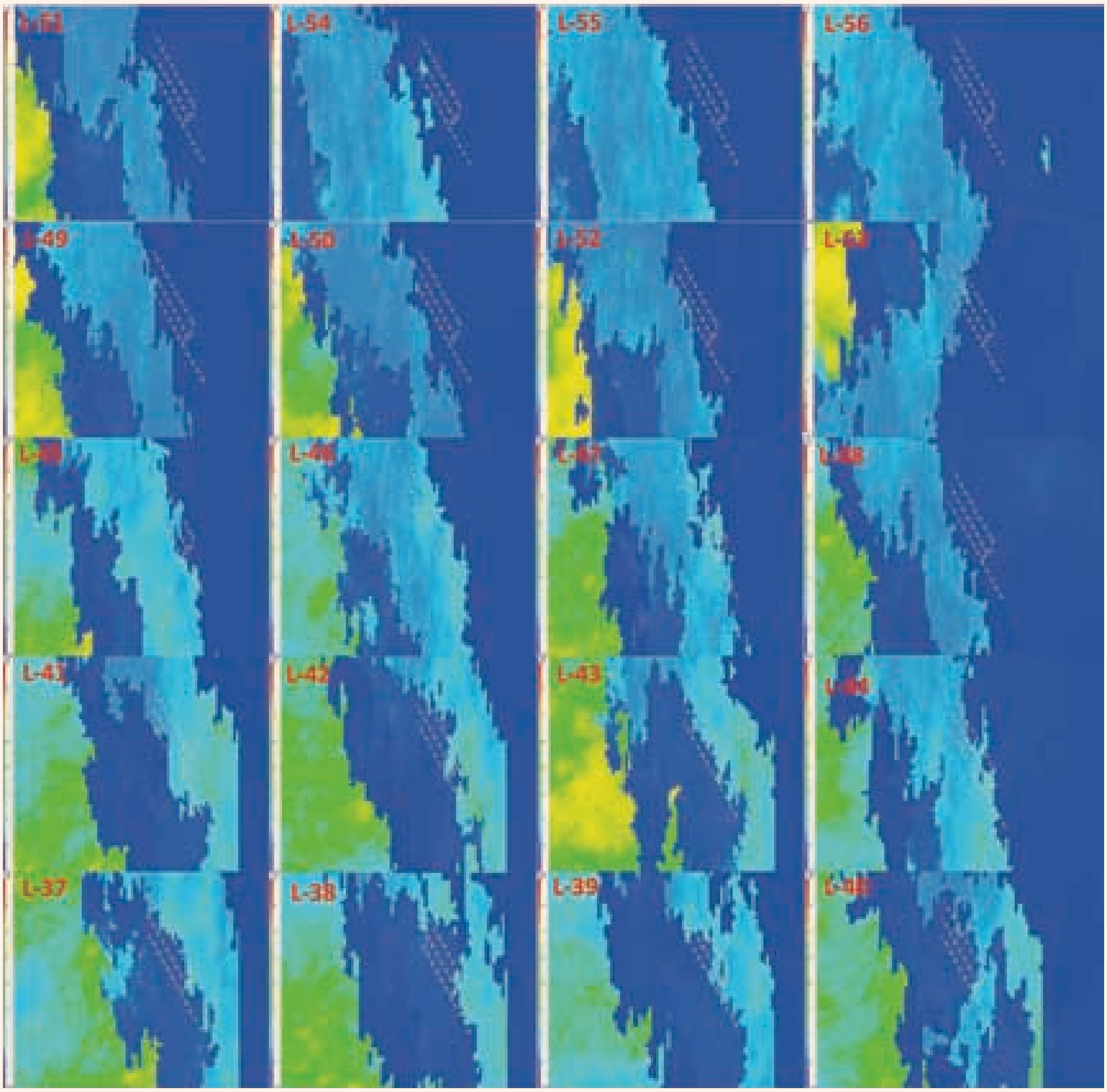

Fig. 16 *A summarizing figure for the permeability X in the I and J directions intersecting the Manara well. The figure shows the original model has very poor quality rock surrounding the Manara well.*

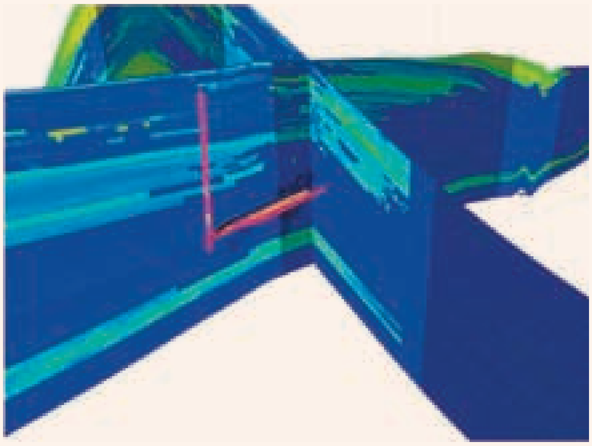

Fig. 17 *History matching simulation results compared with the observed data for BHP in percentage normalized by the highest value. The red color is a history matching simulation model where global and local modifications were applied to the full field model. The black circles are observed data (P1 values). The red line shows a very good history match for the L1U station.*

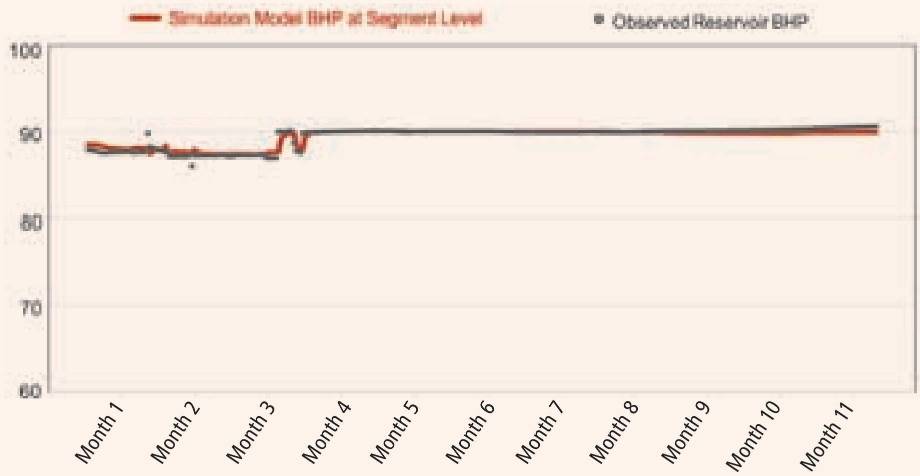

contradicts the Aziz mechanistic equation[8], which handles two phases, and has unstable performance with the full field model.

Complex well input data includes the three types of files previously mentioned, in addition to the regular simulation modeling files used in modeling conventional wells. The high frequency flow rate and pressure measurements for each station went through extensive validation and a quality control process, which will be explained in the next section of this article.

Performance Data Quality Control and Validation

High frequency performance data for the Manara well stations were obtained using a real-time monitoring platform. Figure 9 shows each station has an upstream pressure measurement, named P1 (just before the Venturi nozzle) and a downstream pressure measurement P2 (at the Venturi nozzle). From the two pressure measurements, the flow rate is calculated. The validation process should identify any anomalies in pressure or flow rate values, which should be corrected and modified properly prior to taking them into the reservoir simulator.

To illustrate, Fig. 9 shows the validated performance data for the Lateral 1 upper station (L1U). The gray line reflects the P1 measurement, which will be the bottom-hole pressure (BHP) to match, since it reflects reservoir performance, and the yellow line reflects the P2 pressure measurement while the blue line reflects the flow rate.

The Manara well was put on production and since then the comprising stations were on and off on regular pressure transient analysis (PTA) tests. Validating the performance data involves a quality check for the pressure measurements with the flow rate calculations and the choke size opening as a function of time. Hourly data were averaged into a daily basis for the duration of the intended history match period of about a year of performance.

The finalized set of data for every station is taken to the GigaPOWERS simulator as input data, which are the flow rate and choke size measurement, whereas the pressure, P1, will be the data to match for the Manara well full field simulation model. The next step in the workflow is to conduct the history matching process on the segment level of the six stations.

Flow Rate and BHP History Matching

Before we go into history matching details, it is immanent to provide basic information about the model used. Table 1 shows the dimensions and description for the compositional full field model.

In complex well modeling, it is important to explain the model related parameters that we will focus on during the course of matching the performance data for each station. Despite the fact that the post-processing environment for simulation is not 100% ready for the task we undertook, this project resulted in significant leverage for the pre- and post-simulation environment. Also, the workflow established to match the performance data and station level adds value to the history matching general process.

The parameters under focus were the flow rate and upstream BHP (P1). We were able to achieve excellent history match results for the Manara well stations. The flow rate were input values for the simulator, and the original model was able to reproduce the same amount of fluids on a daily rate frequency, Fig. 10. On the other hand, the initial history matched full field model was showing a difference of more than 10% with P1 values for every station, Fig. 11. Note that we are showing normalized values for the pressure and the flow rate for the L1U station in percentage form.

The BHP mismatch between performance data and the original model creates a need to dig deeper to find out the reasons. Each station had the detailed static, the dynamic related properties, and the surrounding environments looked at. Looking carefully into the model, it was clear that permeability tightness surrounding the Manara well's laterals were a major bottleneck that prevents enough pressure support, resulting in lower flowing and static grid block pressure values at the locations where the ICVs were placed.

Looking at a cross section of where the Manara well is landed at the model, Fig. 12, we note the following points. The three laterals for the Manara well are placed through three consecutive layers, 57 to 59 in the model, which is below the gas-oil contact (GOC) at layers 36 to 37, and above the oil-water contact (OWC) at layers 72 to 74. The permeability distribution in the X direction can be summarized through Fig. 13, which shows the top view for the region below the well from the OWC to the layer below the well.

Figure 13 also shows the permeability values below the Manara well, which is dictated by a tight rock region quality with an average permeability in one order of magnitude. Above this region, the Manara well is placed in the model in layers 57 to 59, Fig. 14, which also indicates that a tight quality rock region is still dominating the low permeability distribution surrounding the Manara well drainage area in the model.

Moving to the region above the well, Fig. 15, the permeability distribution continues with very low values just above the Manara well until almost 10 layers away, where better rock qualities with one order of magnitude increase, and start to show on and off in some of the layers until reaching GOC layer 37. From layer 56 to 48, better rock quality is noticed to the left side of the well; however, this was not enough to get the well's BHP at the segment level to match the performance data.

To summarize the permeability story in the Manara well area, we can say that the Manara well in the original full field model is placed in a tight quality rock with an average permeability in the range of one to two orders of magnitude. This can be seen clearly in Fig. 16, which shows the permeability X in a cross section of the I and J directions. The tight quality rock region is extended in the Manara well surrounding layers, and resulted in lower value grid block pressure computation at the location of the ICVs for each station.

The PTA obtained from the well transient tests for each station suggests a permeability and transmissibility modification that needs to be made to match the performance data. Moreover, the upper stations such as L0L, L1L, and L2L showed more than one order of magnitude increase in permeability. Such hard dynamic data are very critical to identify and reduce the paramount uncertainty factors, such as the permeability.

The history matching process continued with the above analysis to improve the BHP match for the flowing and static periods per station. There was a need to improve on global and local levels the permeability and transmissibility ranges to reflect and apprehend the observed and dynamic data for each station. On the area surrounding the Manara well, a range of permeability multipliers of six to 28 was implemented while the transmissibility of 1,000 was used. Note that an assisted history matching tool was utilized to scope the ranges of multipliers used. On the local side, a transmissibility multiplier was applied for stations L0L, L1L, and L2L with a reduction multiplier ranging from 0.1 to 0.07.

To achieve such a history match for every station, a new segment level option was used, which is a productivity index (PI) segment multiplier. This segment multiplier is applied at the complex well data file and it is functional at the perfs contributing to each station. The PTA provided invaluable information for each station, which is a major advantage of the Manara well

Fig. 18 The 3D cross section view for the permeability X. On the left, the original model before history matching while the right side shows the final model after history matching. The dark blue represents one order of magnitude of permeability, the light blue is two orders of magnitude, and the green represent three orders of magnitude, while the yellow and hot colors represent four orders of magnitude.

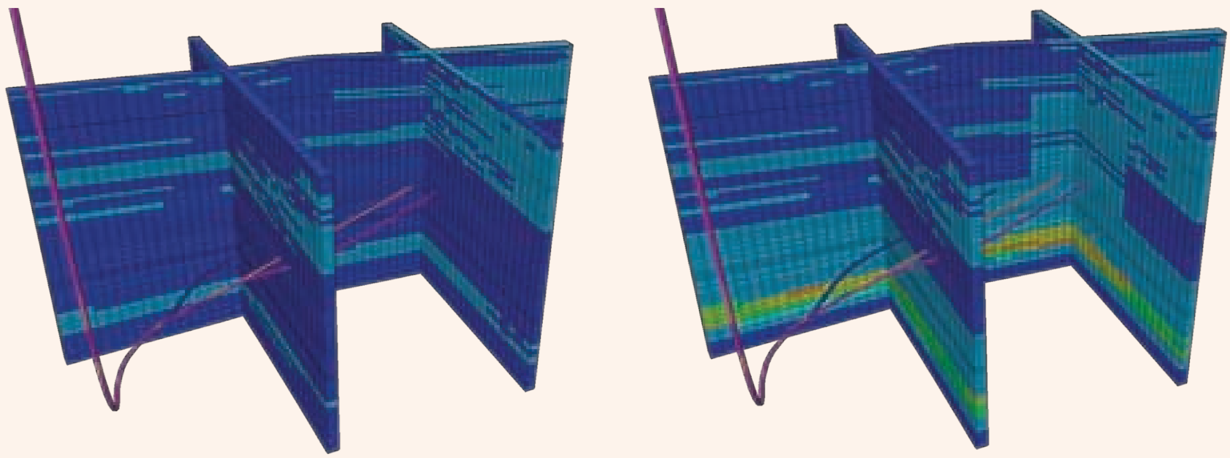

Fig. 19 The permeability distribution for two simulation models normalized to the highest value in logarithmic scale. The magenta color is for the original model before the history match, while the blue color shows the final history match model.

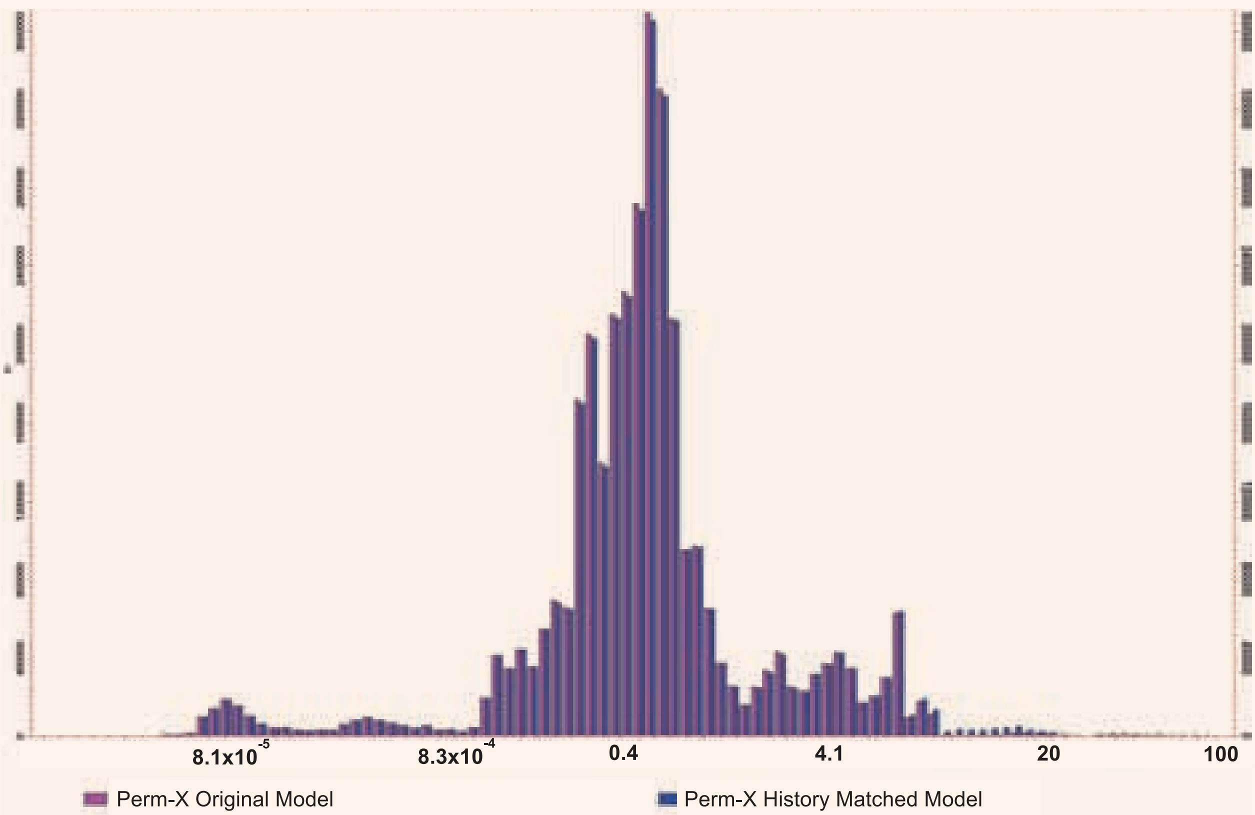

type. A range of 1.5 up to 3 PI multipliers were applied for each station, which resulted in better comparison to the PTA PI computed values. The history matched model shown in Fig. 17 in red color is the final match for the L1U station, accommodating the needed modification to achieve the performance data measured for each station in the Manara well. With less than 2% in pressure difference, every station was history matched at the segment level for the first time in Saudi Aramco and on an industry level. This high-definition history match is unprecedented for the flow rate and reservoir BHP for each station.

Figure 18 shows the permeability cross section for the before and after history match model results. The 3D cross section permeability model on the right side is the history matched model view while the left one is before the history match. Looking at the impact of the permeability modification made, Fig. 19 shows a histogram of a full field model horizontal permeability distribution before and after history matching, which is normalized in the logarithmic scale.

Conclusions

History matching of the Manara well is made for the first time on a high-definition scale, on a segment level for six stations using GigaPOWERS complex well modeling features with a compositional full field model. The combination of geological parameters and segment level advance completion attributes were significant factors to achieve station level history matching.

This project established a new workflow that introduced a station level history matching process. We believe that such an achievement is opening the floor for enabling real time modeling and history matching automation at a fine detailed completion level. Such studies entail modeling hundreds of complex wells on a large field-scale, which used to be a challenge, but is now a reality.

Acknowledgments

This article was presented at the 2020 International Petroleum Technology Conference, Dhahran, Saudi Arabia, January 13-15, 2020.

References

1. Saggaf, M.M.: "A Vision for Future Upstream Technologies," *Journal of Petroleum Technology*, Vol. 60, Issue 3, March 2008, pp. 54-98.

2. Bouldin, B., Turner, R., Bellaci, I., Abu Ahmad, Y., et al.: "Intelligent Completion in Laterals Becomes a Reality," SPE paper 183949, presented at the SPE Middle East Oil and Gas Show and Conference, Manama, Kingdom of Bahrain, March 6-9, 2017.

3. Elfeel, M.A., Tonkin, T., Watanabe, S., Abbas, H., et al.: "Employing Smart Flow Control Valves for Fast Closed-Loop Reservoir Management," SPE paper 192926, presented at the Abu Dhabi International Petroleum Exhibition and Conference, Abu Dhabi, UAE, November 12-15, 2018.

4. Al-Qahtani, G.D., Elrafie, E.A., Abbas, R.T., Ikuku, C.E., et al.: "Complex Well Modeling Workflow Enabling Full Field Optimization and Forward Decisions," SPE paper 120050, presented at the Latin American and Caribbean Petroleum Engineering Conference, Cartagena de Indias, Colombia, May 31-June 3, 2009.

5. Al-Shaalan, T.M., Dogru, A.H., Al-Youbi, A.H. and Ismail, H.: "Parallel Computation for Complex Wells Modeling in Full-Field Reservoir Simulation," SPE paper 182657, presented at the SPE Reservoir Simulation Conference, Montgomery, Texas, February 20-22, 2017.

6. Dogru, A.H., Fung, L.S.K., Middya, U., Al-Shaalan, T.M., et al.: "A Next-Generation Parallel Reservoir Simulator for Giant Reservoirs," SPE paper 119272, presented at the SPE Reservoir Simulation Symposium, The Woodlands, Texas, February 2-4, 2009.

7. Chen, N.H.: "An Explicit Equation for Friction Factor in Pipe," *Industrial & Engineering Chemistry Fundamentals*, Vol. 18, Issue 3, August 1979, pp. 296-297.

8. Petalas, N. and Aziz, K.: "A Mechanistic Model for Multiphase Flow in Pipes," *Journal of Canadian Petroleum Technology*, Vol. 39, Issue 6, June 2000, pp. 44-55.

About the Authors

Dr. Ghazi D. AlQahtani

Ph.D. in Petroleum Engineering, Texas Tech University

Dr. Ghazi D. AlQahtani is a Petroleum Engineering Specialist leading the Advance Simulation Modeling Group at Saudi Aramco's Reservoir Description & Simulation Department. Prior to this, he led several integrated reservoir study projects and supervised gas and oil reservoir management and simulation units under the Upstream business line. In 2018, Ghazi graduated from Saudi Aramco's Technical Development Program, as a Specialist in Complex Well Modeling and Optimization.

He initiated and co-developed "OPTIMA," a unique Saudi Aramco patented integrated simulation-based solution to assess reservoir productivity by nominating "sweet spots" for optimal oil field development. Ghazi also initiated and co-developed "WePO," an innovative well placement optimization algorithm to find the optimum locations and trajectories for hydrocarbon wells in large-scale reservoirs using transshipment network formulations and graph theory principles.

He has authored four U.S. patent applications, with two granted and two pending. Ghazi has also coauthored a book entitled "Fundamentals of Corrosion and Scaling for Petroleum and Environmental Engineers." He has contributed to more than 20 published journal and conference papers on areas covering reservoir simulation technologies, field development plans, well placement optimization in conventional/unconventional reservoirs, and accelerating the development of integrated professionals.

Ghazi served as a Ph.D. Committee member and participated in several geoscience and petroleum related conferences, workshops, and symposiums as Chairman, Keynote Speaker, Steering Committee Member and Presenter. He is a founding member of the Digital Technology Governance Association, and a member of the Society of Petroleum Engineers (SPE) and the Saudi Council of Engineers.

Ghazi received his B.S. degree in Petroleum Engineering from King Fahd University of Petroleum and Minerals (KFUPM), Dhahran, Saudi Arabia. He received his M.S. degree in Petroleum Engineering from the University of Southern California, Los Angeles, CA. Ghazi received his Ph.D. degree in Petroleum Engineering with a minor in Industrial Engineering at Texas Tech University, Lubbock, TX.

Dr. Wisam Shaker

Ph.D. in Petroleum Engineering, University of Calgary

Dr. Wisam Shaker is a Petroleum Engineer working in Saudi Aramco's Northern Area Reservoir Management Department. Currently, he is leading the qualification assessment team to assess the new generation of the well completions of smart multilaterals.

Wisam has extensive experience in the oil and gas industry. He has held several technical positions in the field of reservoir and production engineering in the Middle East, North Africa, North America, and Arabian Gulf. During this time, Wisam's achievements include sustaining daily hydrocarbon field production rates, participating in the field development process, leading technical studies, and evaluating the new technology to maximize hydrocarbon recovery factors.

As for his academic career, he developed and taught several courses for undergraduate studies in petroleum engineering. Also, Wisam supervised several engineering projects for final year students of petroleum engineering.

He has published numerous papers, reviews, and patents, including unique workflows to reduce reservoir uncertainties by incorporating a new surveillance plan, equalizing hydrocarbon reservoir pressure, and real-time production optimization for smart multilateral wells.

Since 2008, Wisam has been a registered member with the Association of Professional Engineers and Geoscientists (APEGA) as a Professional Engineer. For his engagement in supporting and monitoring inexperienced engineers, Wisam was awarded several certificates of appreciation.

In 1983, he received his B.S. degree in Petroleum Engineering from the University of Baghdad, Baghdad, Iraq, and in 1989, Wisam received his M.S. degree in Petroleum Engineering, also from the University of Baghdad. In 2015, he received his Ph.D. degree in Petroleum Engineering from the University of Calgary, Alberta, Canada.

Menhal A. Al-Ismael

M.S. in Petroleum Engineering, King Fahd University of Petroleum and Minerals

Menhal A. Al-Ismael is a Petroleum Engineering Systems Analyst working in the Simulation Systems Division of Saudi Aramco's Petroleum Engineering Applications Services Department, where he provides solutions and system support to reservoir simulation studies.

Menhal has more than 10 years of experience in petroleum engineering systems support, working on many projects in the area of field development planning and optimization.

He is a Society of Petroleum Engineers (SPE) Certified Petroleum Engineer.

Menhal received his B.S. degree in Information and Computer Science, and his M.S. degree in Petroleum Engineering, both from King Fahd University of Petroleum and Minerals (KFUPM), Dhahran, Saudi Arabia.

Dr. Tareq M. Al-Shaalan

Ph.D. in Mechanical Engineering, University of Wisconsin-Madison

Dr. Tareq M. Al-Shaalan is Petroleum Engineer Professional in Saudi Aramco's Strategic Modeling Technology of the Petroleum Engineering and Development Department. He is leading Saudi Aramco's massively parallel simulator GigaPOWERS. Tareq previously worked with the Lab Research and Development Department for two years.

He has published more than 15 technical papers in journals and at conferences, including *Combustion Science and Technology*, the National Association of Corrosion Engineers (NACE), the Society of Petroleum Engineers (SPE), and the International Petroleum Technical Conference (IPTC).

Tareq works in different areas of computational fluid dynamics such as direct numerical simulation, sandstone stimulation modeling, and reservoir simulation such as coupling reservoir simulators with a surface network simulator, dual porosity dual permeability modeling, corner point geometry, solver, nonlinear solver, and complex well modeling.

In 1989, he received his B.S. degree in Mechanical Engineering from King Fahd University of Petroleum and Minerals (KFUPM), Dhahran, Saudi Arabia. In 1992, Tareq received his M.S. degree in Mechanical Engineering, and in 1997, his Ph.D. degree, also in Mechanical Engineering, both from the University of Wisconsin-Madison, Madison, WI.

Jibran Ayub

M.S. in Petroleum Engineering, Aalborg University

Jibran Ayub is a Senior Reservoir Engineer in Saudi Aramco's Reservoir Simulation Department working at Shaybah field. He has more than 15 years of experience in conventional and advanced reservoir engineering and other petroleum related activities; with field experience in reservoir characterization and field development projects, complex wells, fracture/injectivity modeling, water quality monitoring, enhanced oil recovery, microbial reservoir souring, and reservoir simulation modeling.

Jibran is a Chartered Engineer with the U.K. Engineering Council, and a member of the Institution of Chemical Engineers.

He received his B.S. degree in Chemical Engineering from the University of Engineering and Technology, Lahore, Pakistan, and his M.S. degree in Petroleum Engineering with a major in Reservoir Engineering, from Aalborg University, Esbjerg, Denmark.

Saud A. Al-Hoti

M.S. in Petroleum Engineering, New South Wales University

Saud A. Al-Hoti is a Senior Petroleum Engineer currently working in the Gas Reserves Unit in Saudi Aramco's Reservoir Engineering in Upstream Development Strategy and Reserves Department (UDS&RD). Prior to that, he worked as a Simulation Engineer in the Reservoir Simulation Division of the Reservoir Description and Simulation Department.

Saud has more than 14 years of experience in reservoir simulation and reservoir management.

He received his B.S. degree in Petroleum Engineering from King Fahd University of Petroleum and Minerals (KFUPM), Dhahran, Saudi Arabia, and an M.S. degree in Petroleum Engineering from New South Wales University, Sydney, Australia.

A Novel Stimulation Design Approach Revives a Challenging Gas Field

Abdulrahman A. Al-Mulhim, Saad Hamid, Abdul Muqtadir Khan, and Chan C. Hoong

Abstract /

Multiple attempts to commercially produce from a horizontal well in a challenging sandstone formation completed with the plug-and-perf method were rendered unsuccessful. An innovative stimulation strategy was proposed for the next candidate in an attempt to improve post-fracturing productivity. Three different types of proppant fracturing treatments were performed as a first-time application, including hybrid slick water treatment, low guar cross-linked treatment, and carbon dioxide (CO_2) foam fracturing.

A hybrid design combining high-rate slick water at the beginning, and low guar loading cross-linked gel at the end of the treatment was pumped in two stages. This allowed minimizing the cross-linked fluid pumped while enhancing fracture half-length. Second, conventional low guar fracturing was implemented in four stages. Cross-linked gel loading was reduced by 25% compared to gel that was utilized in offset wells. Finally, a CO_2 foam fracturing design with a novel biopolymer linear fracturing fluid was implemented in the last stage. This reduced water consumption and improved the chance of increased gas production by yielding a higher conductivity fracture network.

Friction pressure for CO_2 foam was calibrated using bottom-hole gauge data that was obtained with downhole gauges run prior to the calibration testing. The new calibrated friction numbers were then used for the bottom-hole treating pressure calculation during the treatment. CO_2 foam fracturing was found to be a significant success for this well based on multiple evaluation criteria.

First, the use of foam helped conserve 1,000 bbl of freshwater compared to conventional stages. Second, the foam treatment allowed two times faster cleanup compared to other stages, based on cleanup time normalized over fluid volumes. Finally, production logging results showed that the foamed treatment achieved better production compared to other treatments in the well, considering the productivity index (PI) was normalized by the proppant mass, porosity, and zone mobility. The CO_2 stage normalized PI was significantly higher than the other stages in the well. After the well was cleaned up, a production log was conducted, and it was analyzed to corroborate the higher production: 70% of the production contribution was seen from the CO_2 treatment interval.

In most of the literature, estimates of the friction correlations for foams are based on empirical data. This article provides the calculations of friction pressure based on field data. The combination of measured bottom-hole data and post-cleanup production logging demonstrates the potential productivity improvements that can be achieved through novel design approaches. This type of data is rare in the industry and can help to improve the design of foamed fracturing treatments.

Introduction

Well-A, a gas well, was completed with a cemented lateral, and it was decided to complete with the plug-and-perf method for fracturing purposes so as to place the well on commercial production. There were three offset horizontal wells in the area, Wells B, C, and D, and they were studied before finalizing the plan for candidate Well-A. A quick-look summary of the offset wells in the area are shown in Fig. 1 and Table 1.

As can be observed in the summary in Table 1, Wells C and D are cemented laterals, which were not able to produce commercially. The candidate well, Well-A, was a similar cemented lateral in the area, and it needed a novel approach as far as design and overall strategy were concerned.

Well-A is a horizontal well in a dry gas reservoir with a low condensate gas ratio, which included a pilot hole to select the lateral landing point. Based on the analysis of the pilot hole data, lateral landing, reservoir quality, and completion quality indicators, it was decided to finalize eight stages of fracturing treatment in the lateral.

The fracturing technology planned for the candidate well was uniquely strategized. It was decided to treat the lateral with three different treatment designs: (1) hybrid slick water fracturing, (2) conventional fracturing with low polymer loading, and (3) carbon dioxide (CO_2) foamed fracturing. The reason for designing with these three different techniques was to target the potential problems and compare the effectiveness of these techniques.

Fig. 1 *Candidate and offset wells in a 3D grid.*

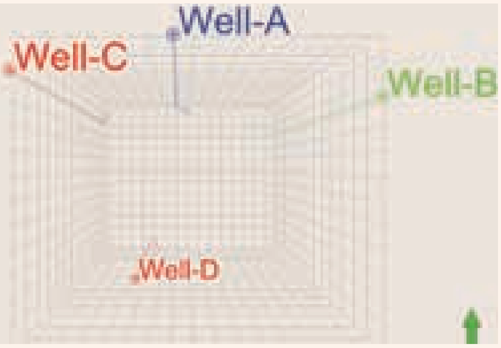

Candidate Well Background

Vertical Pilot Hole: Landing the Lateral

A vertical pilot hole was drilled for the candidate well, and open hole logs were analyzed to characterize the reservoir and net pay to correctly plan the lateral landing point, and plan the trajectory for the lateral, Fig. 2. In addition to porosity and permeability evaluation, a formation testing tool was deployed to take samples and evaluate the mobility at different depths along the vertical section. Based on a comprehensive study of the collected data, the lateral plan was finalized.

Figure 3 is a horizontal lateral log analysis for the pilot hole, where each vertical interval is equal to 100 ft. The total coverage of the log is ~700 ft.

Horizontal Lateral

The lateral was planned to cross 70 ft of reservoir vertical net pay zone to access ~2,700 ft of horizontal open hole section. The deviation across the horizontal was 87.3° to 88.8° at an azimuth of 23° to 32° away from the maximum horizontal stress direction — preferred fracture plane.

All of the data shown in Fig. 3 were used to guide the selection of the best fracturing design.

Overall Design Strategy

Stage Selection: Perforation Placement

Data across the full lateral was analyzed to finalize the stage intervals and perforation depth. A unique algorithm was used wherein the entire log data was fragmented twice based on the reservoir quality index (RQI) and the completion quality index (CQI), derived from petrophysical and geomechanical parameters. Porosity was used as the indicator for a good reservoir, and a low calculated stress gradient was used to indicate a good completion. The two discrete logs were then used to determine an aggregate composite log, Fig. 4. The best combinations were then selected to finalize the completion strategy. This strategy was described in detail by Cipolla et al. (2011)[1], which focused on tight gas and shale completions.

For the selection of the perforation clusters, some more criteria were employed and established, making the process complete, Table 2:

- Clusters were not spaced too close to minimize the stress shadow effect.
- Casing collars and centralizers were located, and cluster depths were moved away from those sections to prevent near wellbore admittance issues.
- Stress contrast between the clusters was low, to eliminate dominant fracture growth.
- Clusters for the same stage were placed in the same rock lithology.

Fracturing Treatment Design

The next critical step in the cycle of the completion workflow was to assign a treatment type to each stage. The fracturing techniques used in Wells C and D used cross-linked fluid with conservative polymer loading of 40 lb/Kgal. Several parameters, like the pumping rate achieved during the calibration, fluid leakoff with water, the benefit of energized treatment, etc., were chosen as criteria to finalize the design. The following design options were considered:

- Hybrid treatment with slick water
- Conventional treatment with low polymer loading
- CO_2 foamed fracturing treatment in the last stage

Hybrid treatment with slick water. Sharma et al. (2004)[2] detailed this technique in their work and showed that it yields longer propped fracture half-lengths compared with slick water or cross-linked treatments. The hybrid design was implemented in

Table 1 *Candidate offset well summary*

	Distance from Well-A (km)	Completion Method	Number of Stages	Well Azimuth	Date	Amount of Polymer (lbm)	Normalized Gas Rate	Normalized Flowing Wellhead Pressure
Well-B	8.6	Open Hole MSF	5	Shmin	Sep. 15	17,600	1.00	1.00
Well-C	6.6	Plug-and-Perf	5	Shmin	Dec. 17	38,400	0.18	0.19
Well-D	11.7	Plug-and-Perf	4	Shmin	Apr. 18	16,800	0.00	0.00

Fig. 2 *Vertical pilot hole log analysis (red color fill, gas; blue color fill, water).*

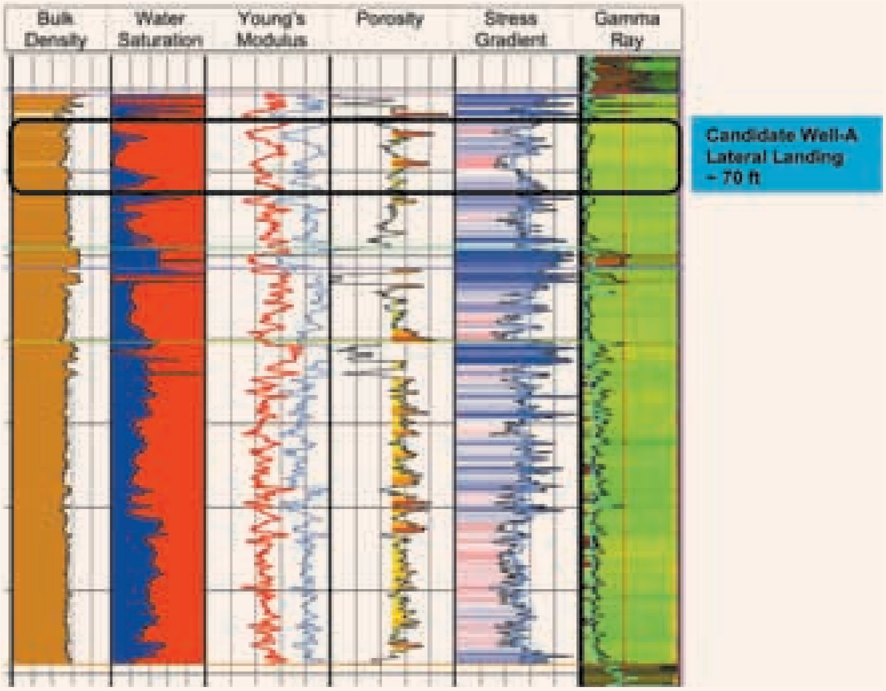

Fig. 3 *A horizontal lateral log analysis for the pilot hole (red color fill, gas; blue color fill, water).*

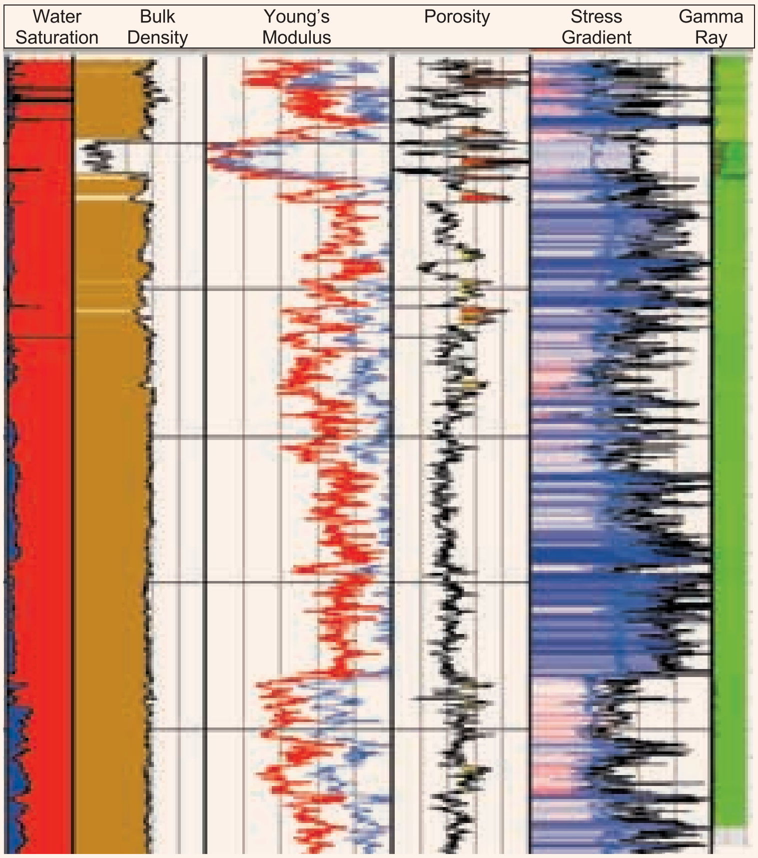

Fig. 4 Composite log based on the RQI and CQI. The first letter is for the RQI, and the second letter is for the CQI; G is for good, and B is for bad.

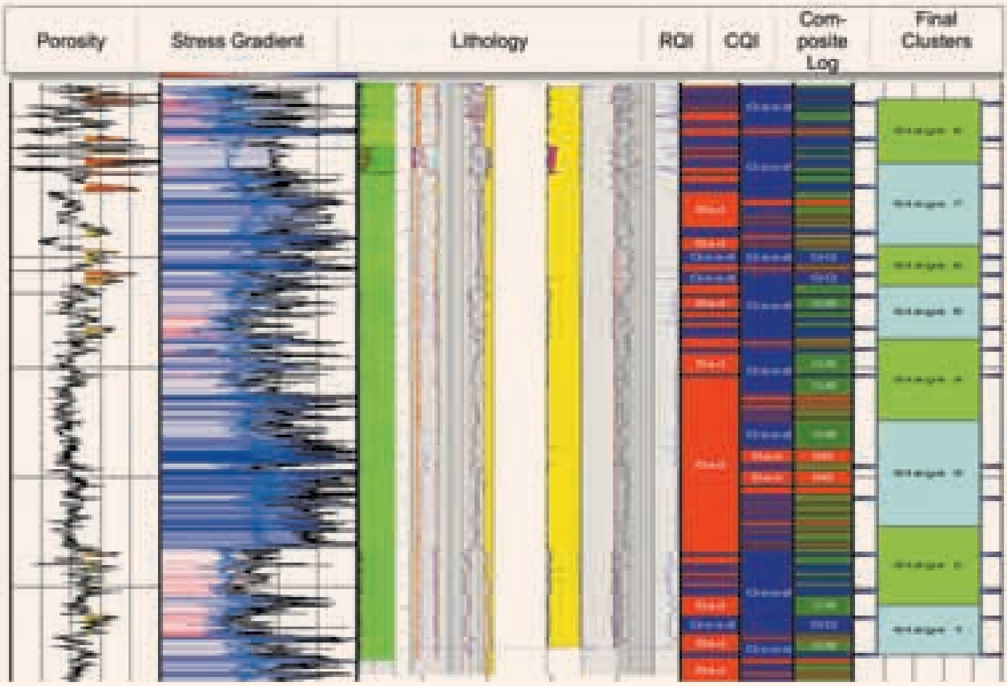

Table 2 Perforation cluster summary (porosity and stress gradient numbers are normalized; the maximum of all was assumed to be 1.00 for normalizing).

Stage Number	Perf Spacing (ft)	RQI (Porosity >X%)	CQI (Stress <Y psi/ft)	CQI	Normalized Stress Gradient	Normalized Porosity
8	160.5	Good	Good	GG	0.84	1.00
8	214.5	Good	Good	GG	0.83	0.89
7	205	Good	Good	GG	0.98	0.89
7	107.5	Good	Good	GG	1.00	0.67
6	78	Good	Good	GG	0.95	0.67
6	92	Good	Good	GG	0.95	0.89
5	144.5	Good	Good	GG	0.94	0.67
5	93.5	Good	Good	GG	0.92	0.78
4	114.5	Good	Good	GG	0.86	0.67
4	410.5	Good	Good	GG	0.87	0.67
3	143.5	Bad	Good	BG	0.98	0.67
3	253	Bad	Good	BG	0.99	0.67
2	164	Good	Good	GG	0.95	0.78
2	117.5	Good	Good	GG	0.94	0.78
1	165	Good	Good	GG	0.92	0.78
1	—	Good	Good	GG	0.93	0.67

stages 1 and 4, as based on the diagnostic injection test, these intervals achieved injection up to 50 bbl/min and demonstrated good efficiency of 35% to 40% with treated water. This approach combines high rate slick water treatment at the beginning and low guar loading cross-linked gel at the end of the treatment. This approach allows reducing the volume of cross-linked fluid pumped to place proppant, and then significantly increase the fracture half-length as a result of using less viscous slick water fluid with low proppant concentration ramps.

The latter part of the stage with cross-linked fluid can be used to gain fracture conductivity. Stage 1 finished with near wellbore screen out when larger proppant (20/40 high strength proppant) hit the perforation at the end of the treatment. The design for stage 4 was modified based on this result to use smaller size proppant and this stage was successfully placed.

Conventional Low Guar. This technique reduces polymer damage by reducing the amount of polymer used in the fluid. The gel loading in the fluid system was reduced by 30% to 40% compared to Wells B, C, and D. The fluid recipes were optimized to achieve the desired rheology at reservoir temperature. Figure 5 shows the optimized rheology with the 25 lb/Kgal system.

Conventional fracturing with reduced gel (guar-based) loading was implemented in stages 2, 3, 5, and 7. These stages were selected because the rate achieved was not very high and with lower efficiency of 15% to 20% with water making them unsuitable for slick water hybrid treatments.

CO_2 Foamed Fracturing. The foamed proppant fracturing treatment, pumped in the last stage, was the critical change that was brought forward to maximize production and achieve the economical limit that was not done with Wells C and D; therefore, this treatment will be the focus for this case study.

CO_2 Foamed Fracturing Treatment

Design and Methodology

Since the first application of CO_2 for stimulation in the early 1950s, foams have been used as hydraulic fracturing fluids. Many authors have shown the benefits of using energized fluids[3]. Foams are generally classified as a special kind of colloidal dispersion in which a gas phase is dispersed in the continuous liquid phase. Foam quality (FQ) is defined as the ratio of gas volume to the total volume (gas + liquid). In addition to good proppant carrying capacity and viscosity, foamed fluids have three main advantages over conventional non-foamed fracturing fluids:

1. The gas phase can provide cleanup energy for an underpressured reservoir.
2. Decreased water content per unit volume of fracturing fluid helps to minimize water injected into the formation.
3. Better fluid loss control enables effective extended fracture half-lengths.

Liquid CO_2 acts as a superior surfactant, and the liquid phase enables creating a high quality foam, and consequently, adds two significant benefits, which are that it adds energy to the low-pressure reservoir to initiate flow back, and it reduces interfacial tension between reservoir fluids and the fracturing fluids. Better fracture cleanup can be achieved with supercritical CO_2 being used as a fracturing fluid, which also helps to remove or prevent water blocks.

The low pH environment that the CO_2 imparts aids in minimizing clay swelling, thereby reducing formation damage. This technique was used for carbonates in the area with outstanding production performance and reduced cleanup time. Rahim et al. (2018)[4] showed the results of the CO_2 foamed treatments in carbonate reservoirs, which prompted the initiation of this technique in the clastic rocks in the area.

Fig. 5 Rheology profile for optimized 25 lb/Kgal polymer loading fluid system.

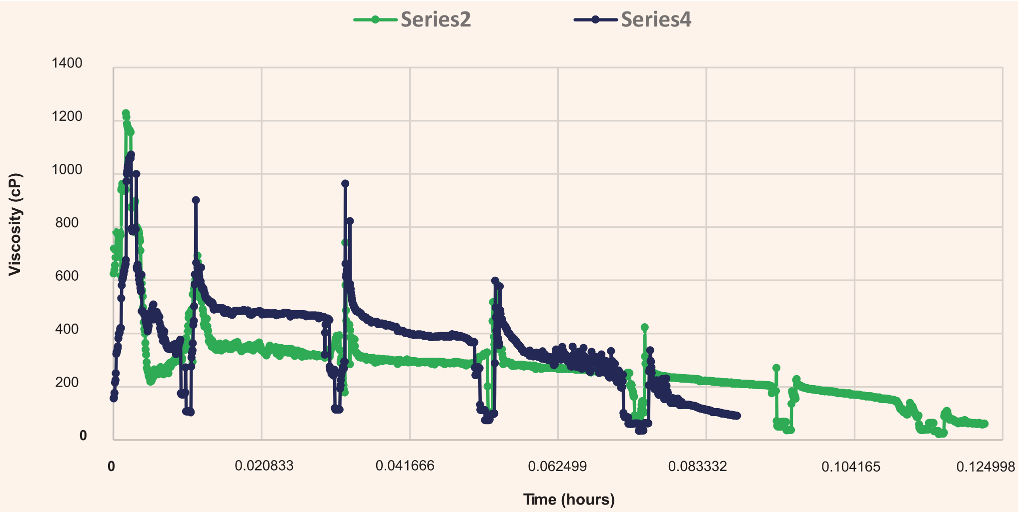

The case study detailed in this article has utilized a novel biopolymer-based slurry gel designed for a low pH system at high temperatures for improved performance over conventional guar-based gel systems. The differentiating chemical structure, Fig. 6, enables it to render more viscous foams, achieving enhanced proppant transport in high temperature CO_2 environments while retaining high retained conductivity in the proppant pack upon breaking.

This fast hydrating viscosifying linear gel system uses the CO_2 fraction in the fluid as a primary mechanism to develop stable rheology for fracturing and proppant carrying purposes. A complimentary, competent foaming agent along with the stabilizer was used to maintain stable foam rheologies at high temperatures, Fig. 7[4]. This fluid mix was tested to be equivalent or superior to the current carboxy methyl hydroxypropyl guar foam fluid systems, and causes significantly less proppant pack conductivity damage because of reduced gel loadings and no crosslinker, Fig. 8. The test was done at 200 °F, wherein the retained conductivity of novel biopolymer was tested after being contacted with CO_2. Test conditions were replicated using 20/40 proppant at a constant closure stress of 4,000 psi and a concentration factor of 10.

Fig. 6 *Representation of conventional guar cross-linked polymer (left) and novel biopolymer-based system (right) on a semi-molecular level.*

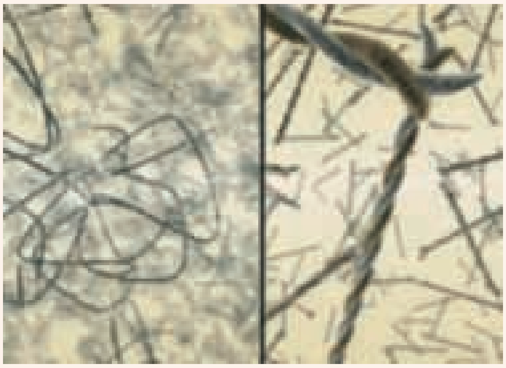

The fluid system used was the least damaging to the formation, which is in line with the previous two techniques finalized for the rest of the stages, striving to reduce the polymer damage. The critical part of this operation was to realize the fact that the liquid phase does not have adequate viscosity to be an effective fracturing fluid on its own. Therefore, it was critical for this treatment that CO_2 rates are maintained during the proppant stages of the treatment.

The job was designed with 40 lbm/1,000 gal polymer to gain enough fracture width for proppant placement. The amount of proppant planned was 185,000 lbm with a maximum bottom-hole proppant concentration up to 3.5 PPA. A total of 300 tons of CO_2 at a bottom-hole foam quality of 58% was planned for this treatment.

Treatment Execution: CO_2 Foam Friction Calibration

A downhole memory gauge was installed during the calibration injection treatment to calibrate the friction pressure for the foamed fluids. The gauge was limited to a maximum pressure of 16,000 psi and a temperature of 350 °F for operations. The following procedure was implemented in steps to acquire sufficient data for correct friction pressure calculations.

1. The full wellbore column was displaced with 58FQ CO_2 + base fluid. (The initial wellbore fluid was slick water.)
2. The total injection rate was varied in three steps to generate points to characterize the friction pressure. Four points on the slurry rate were obtained, i.e., 25 bbl/min, 29 bbl/min, 35 bbl/min, and 40 bbl/min. Drastic rate changes were avoided to ensure the efficiency evaluated from the decline data was

Fig. 7 *Rheology development of the CO_2 foams with different base fluids[9].*

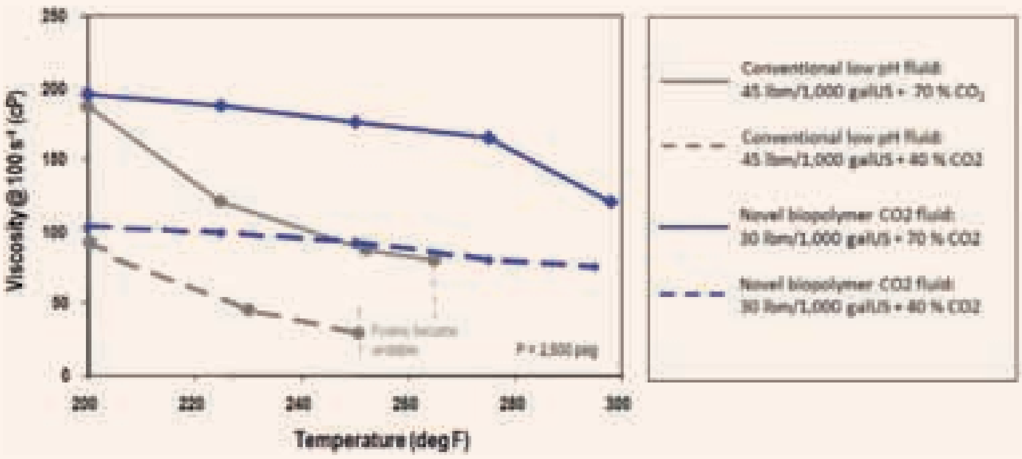

representative for the proppant fracturing redesign.

3. There was a short shutdown of 20 seconds with 58FQ in the tubing column, enough to capture the instantaneous shut-in pressure and evaluate the correct hydrostatic pressure. This step is vital to assess the specific gravity of the foamed fluid with the cool-down.

4. The gauges were retrieved after the closure pressure was achieved from the calibration decline. The bottom-hole pressure (BHP) and temperature data from the gauge were merged with the other job parameters.

Fig. 8 The retained conductivity test results compared at 200 °F.

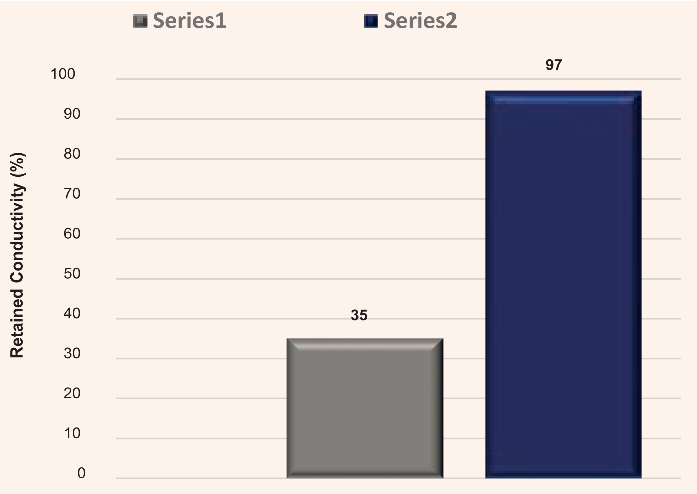

5. The measured bottom-hole treating pressure was then used to analyze the decline and evaluate the efficiency, and the end of job net pressure.

The friction pressures were calculated at each rate and used as a starting point for the pressure match for the full data. The BHP match was done with the newly calibrated friction pressures, Fig. 9.

It can be observed here that the estimated friction pressure can be offset by a significant magnitude in the absence of such real data, and consequently, cause erroneous BHP calculations. Figure 10 shows the difference between the default and calibrated frictions. At the design injection rate for the fracturing treatment, calculated based on the data in Fig. 9, the BHP calculated would have been overestimated by 1,700 psi.

Treatment Execution: CO_2 Foamed Proppant Fracturing Treatment

CO_2 assisted foam was efficient in controlling leakoff. The fluid efficiency analyzed for the CO_2 foam fluid was 35%, and the pad volume was redesigned to 30,000 gal of foam. A summary of the calibration analysis can be found in Table 3.

The treatment was pumped and concluded at a maximum bottom-hole proppant concentration of 2.5 PPA, Fig. 11. A total of 25% of the design proppant was pumped at a total injection rate of 40 bbl/min before the pressure started to increase at a steady rate, and it was then decided to transition smoothly to the flush stage, by cutting the proppant and CO_2 rate in gradual steps, while picking up the liquid rate to ensure the bottom-hole injection rate is maintained. The flush step was successfully concluded.

A total of 155 tons of CO_2 was pumped through

Fig. 9 The BHP matching with measured gauge data using the newly calibrated friction numbers.

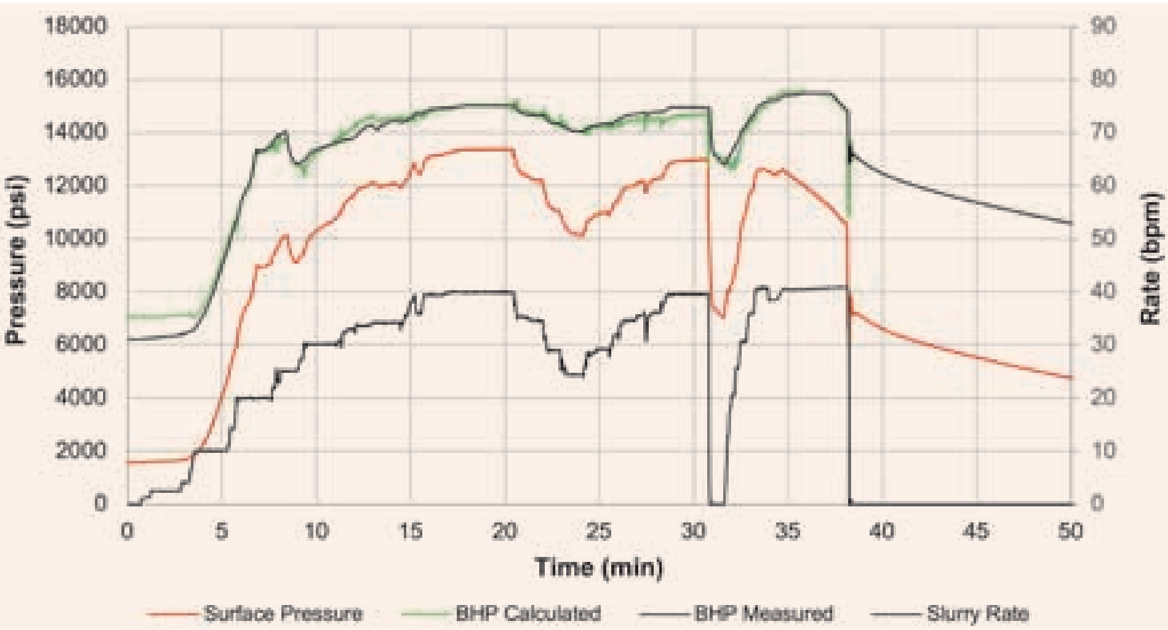

Fig. 10 The pressure comparison of the calibrated friction numbers.

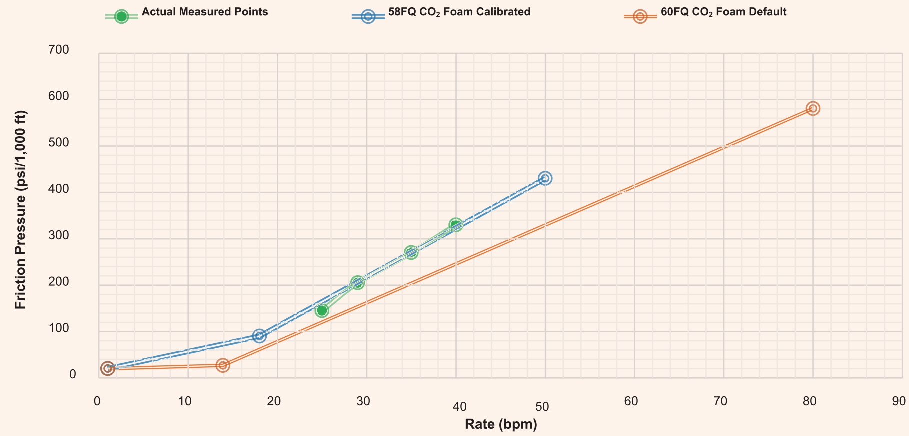

Table 3 Summary for the calibration treatment and redesign.

Calibration Injection and Redesign	
Near Wellbore Pressure Losses (psi)	1,300
End of Job Net Pressure (psi)	3,050
Closure Pressure (psi/ft)	0.67
Fluid Efficiency with Slick Water (%)	9
Fluid Efficiency with Foam (%)	35
Total Proppant Planned (Klbm)	175
Maximum Proppant Concentration (PPA)	3.5
CO_2 Foam Quality (%)	58
Total CO_2 Planned (tons)	300

the treatment while preserving 58% of the constant bottom-hole foam quality. Post-treatment evaluation and further analysis revealed that the reason for pressure increase could be a proppant admittance issue, or alternatively, due to high friction due to CO_2 foam plus an increasing proppant concentration.

End of Well Execution Summary

Fracturing Execution for the Lateral

Table 4 and Figs. 12a, 12b, and 12c provide a comprehensive summary of the seven stages treated along the lateral out of eight planned stages. Stage 6 was skipped due to injectivity limitations. Post-job fracturing pressure match simulations were performed, and the geometry for CO_2 foam fracture was comparable to the other techniques. The longer fracture lengths are governed by lower fracturing fluid viscosity designed for hybrid and foam fracturing treatments.

Fig. 11 The foamed proppant fracturing treatment plot.

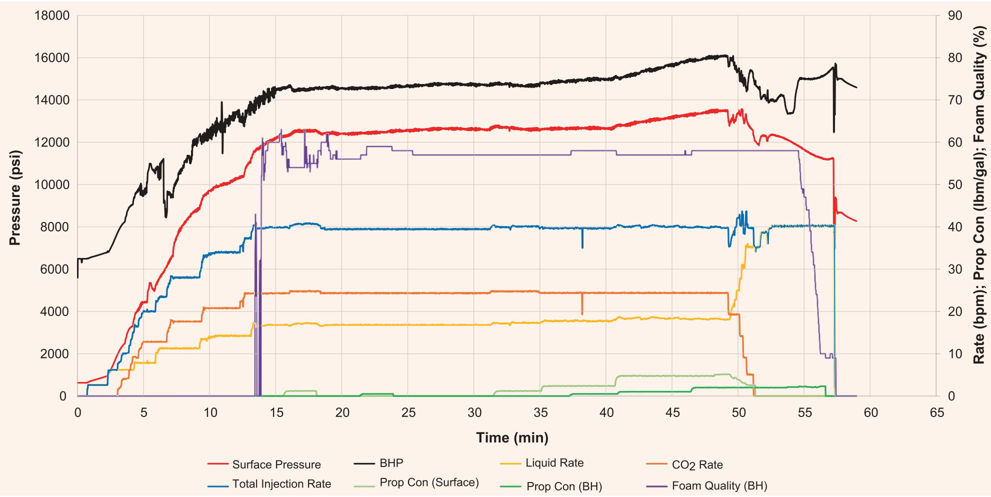

Table 4 *Fracturing technique per stage.*

Stage No.	Fracturing Technique
1	Hybrid treatment with slick water
2	Conventional low guar
3	Conventional low guar
4	Hybrid treatment with slick water
5	Conventional low guar
6	Stage skipped
7	Conventional low guar
8	CO_2 foamed proppant fracturing

Evaluation Workflow

Reduced Freshwater Utilization

Consumption of a large volume of freshwater is a challenge for fracturing applications, especially in arid regions. It also provides an opportunity for improvement. Introducing liquid CO_2 as a significant fraction of the fracturing fluid can alleviate this problem for a high volume of fracturing treatments. This case study shows the actual water savings achieved based on a single stage and the forecast for potential freshwater savings, Fig. 13, if all the stages in the lateral were pumped with 58% CO_2 foam as per the same design that was placed.

Fracturing Fluid Cleanup

The theory of CO_2 enabling efficient fracture cleanup has been well proven in field cases in the past[5]. The reduced interfacial tension between reservoir and

Fig. 12 *Fluid and proppant by stage and average fracturing geometry.*

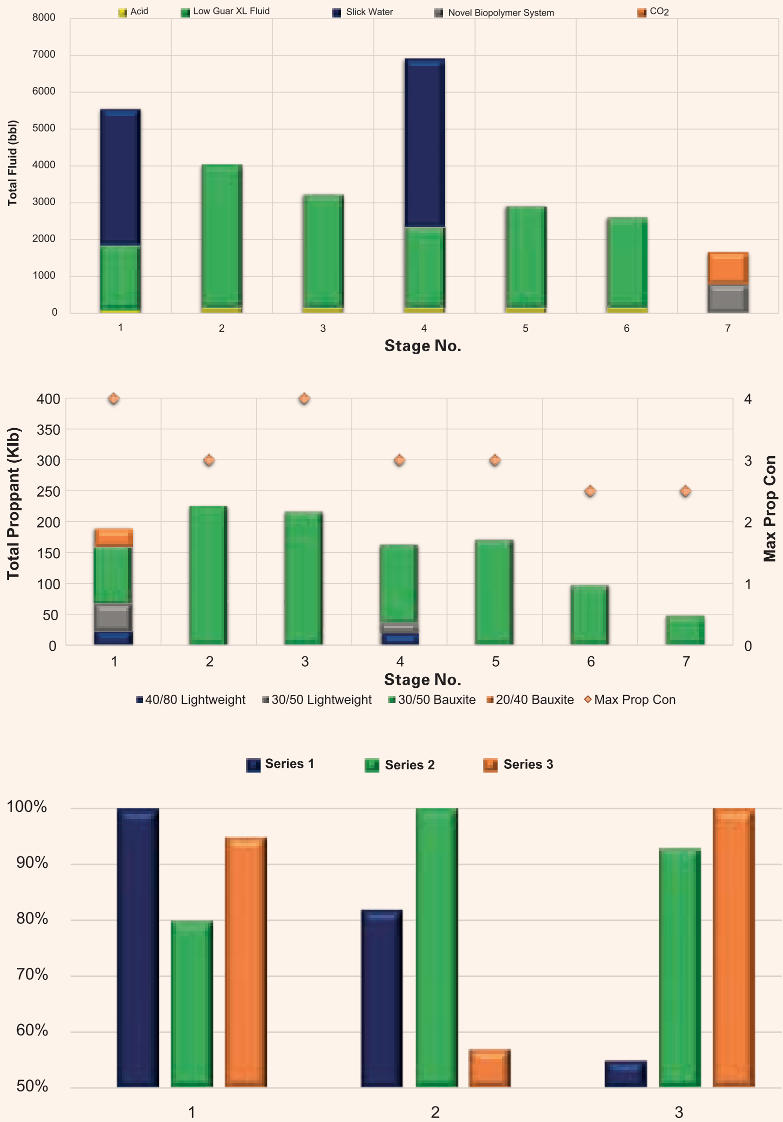

(a) Fluid volume summary per stage.

(b) Proppant mass and proppant concentration summary per stage.

(c) Average fracturing geometry (simulation).

Fig. 13 Water savings potential from CO_2 foam treatments.

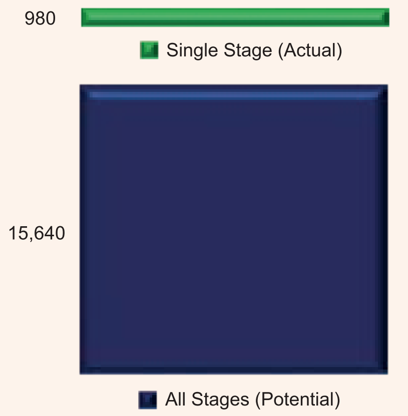

fracturing fluids aids in better recovery, and consequently, reduces the time needed to put the well on production.

The well was flowed back immediately after the last treatment, followed by safe rig-down operations. After the fracturing fluid cleanup criteria were achieved, the plugs were milled, and the flow back operation continued. It should be noted that the plugs used for the completion were drillable fracture plugs (flow through plugs) with an inside diameter of 0.55". But, observing the cleanup trend based on basic sediment and water (BS&W) seen in Fig. 14, before and after plugs were milled, observations and assumptions were made for cleanup and productivity index analysis:

- Because the well was initially put on flow back prior to milling the plugs, one can attribute drawdown and BS&W changes to the last stage, which was CO_2. From Fig. 14, it is clearly seen how efficiently the fracture was cleaned up with the support of foam energy.
- After milling operations were successfully completed, the well continued to recover fracturing fluid accompanied with a slow drop in BS&W. This trend is only possible when minimal drawdown contribution was coming from behind the plugs.

Flow back was continued for ~10 days after the plugs were milled, and it was observed that the cleanup criterion was still not completely achieved based on the increasing BS&W with increasing choke size. Whereas, the cleanup criteria were achieved in 10 hours from the last stage, which is assumed to be the CO_2 foam fracturing flow back. This cleanup time was calculated for each set of data and was normalized per barrel of fluid pumped. For evaluation for the full lateral, the total fluid pumped was considered, and the normalized cleanup time was calculated, Fig. 15. It was observed that the CO_2 treatment stage showed two times improvement in cleanup time.

Post-Fracturing Production: PI Analysis

As detailed in the previous subsection, the assumption that the flow back before milling is from the last stage, i.e., CO_2 foam fracturing treatment, has valid technical justification, and the same reasoning was used for the

Fig. 15 Cleanup time in days per barrel of total fluid (normalized with multipliers).

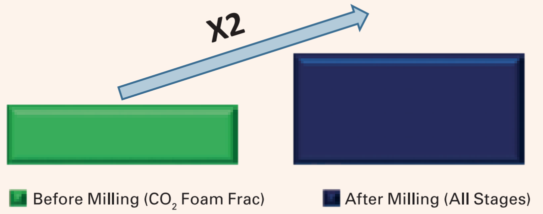

Fig. 14 BS&W and chlorides during post-fracturing flow back at different chokes. The dotted line indicates flow back before plugs were milled and assumed to be flow back from the last stage treated with CO_2 foam; solid lines indicate the flow back after all plugs were milled.

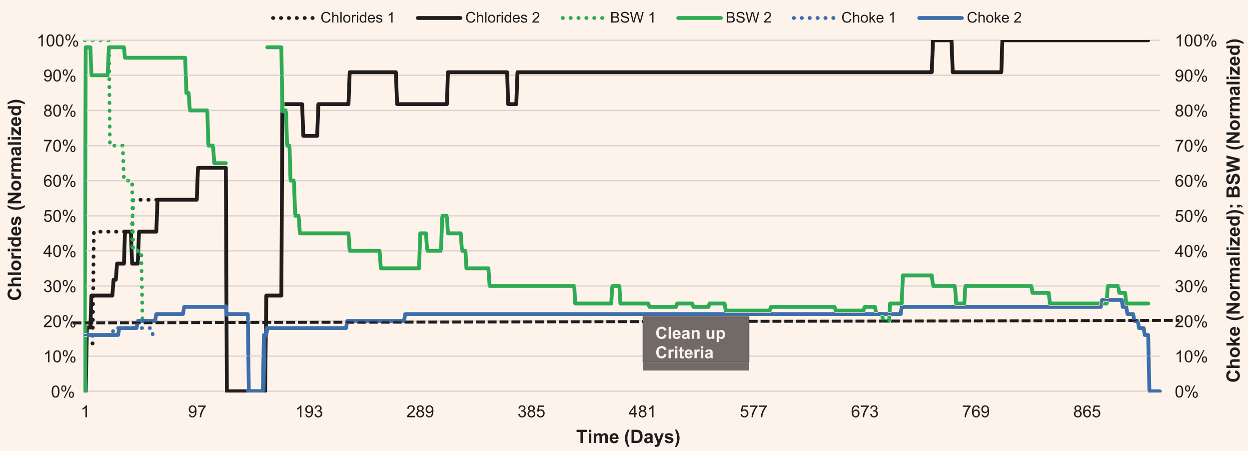

post-fracturing production data sets for evaluating the productivity indices. A time section with stable rates and pressures at the same choke sizes was compared, and it was seen that the PI for all stages of production was only 29% higher than the single stage, Fig. 16.

Furthermore, as part of the evaluation study, the PI was normalized over the proppant mass, porosity, and reservoir fluid mobility — from the vertical pilot hole analyzed from a formation testing tool run during the open hole logging phase correlated to the lateral section — to account for the different proppant pack conductivity and reservoir quality. It was seen that stages 7 and 8 have better reservoir quality, Fig. 17, and are expected to have better production compared to other stages. The CO_2 treatment PI showed to be six times better than all stages when normalized, Fig. 18.

Post-Fracturing Production: Production Log Analysis

A production logging tool (PLT) was run after the milling of the plugs was concluded. The well flowed naturally. The evaluation was done at two choke openings, and the stagewise production contribution is detailed in Table 5. Stages 7 and 8 were seen to be the best producers in the lateral with a total production contribution of 97% to 98%, which can be seen in conjunction with the reservoir quality along the lateral, to complete the evaluation scenario. The same visual representation of the production contribution can be seen in the PLT log, Fig. 19.

The production log also showed that all producing clusters are still flowing a significant amount of water, indicating that the well is still in the cleanup phase from use of the fracturing fluid. It is recommended to

Fig. 16 *PI comparison of all stages.*

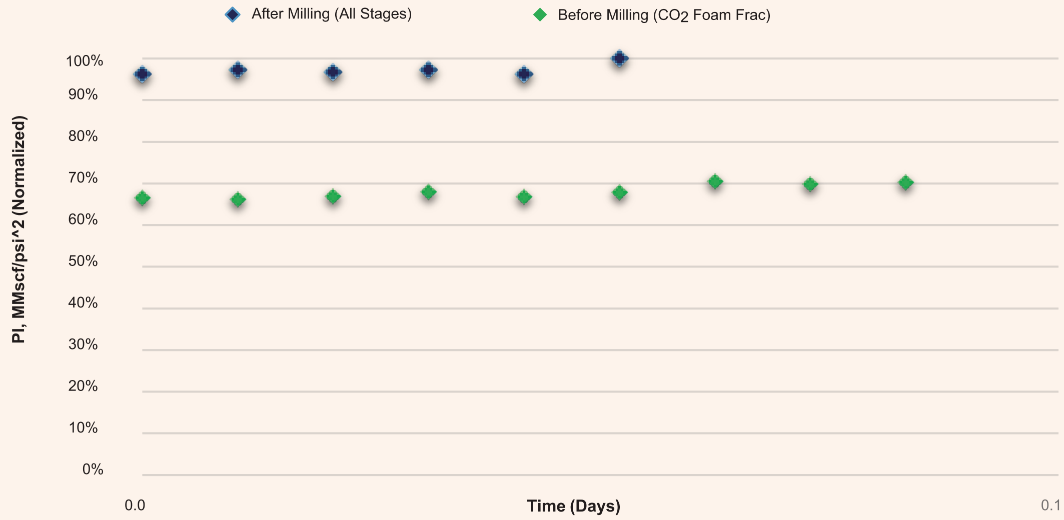

Fig. 17 *PI normalizing parameters — porosity and fluid mobility are given for each stage and averaged; pounds of proppant given is a fraction of the total proppant pumped along the lateral.*

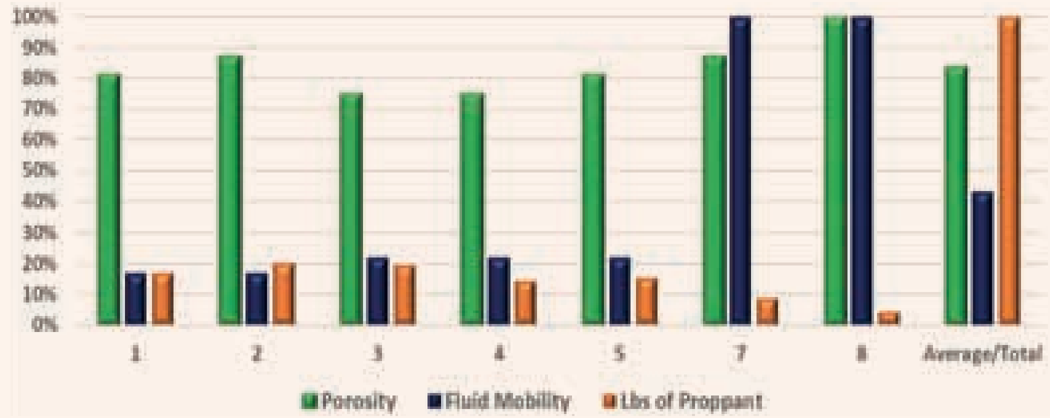

Fig. 18 The CO_2 treatment PI showed to be six times better than all stages when normalized.

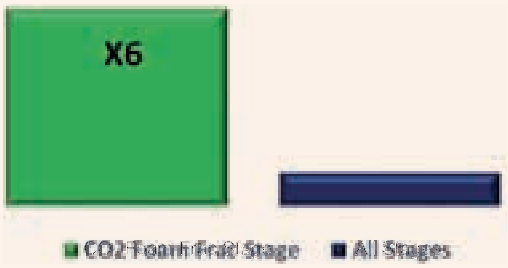

repeat the same production log after the well has been under production for an extended period.

Way Forward

The longest fracture half-lengths were seen to be generated by hybrid and foam fracturing treatments, making these types of fracturing techniques attractive for future tight reservoir candidates. Production logging analysis shows that flow back was left incomplete since all contributing clusters were still producing water. The production log will be repeated after the extended production phase.

In similar completions with multiple clusters per

Table 5 Production contribution from PLT per stage.

Stage #	Production Contribution		Fracturing Technique
	24/64 Choke	34/64 Choke	
8	61%	71%	CO_2 foamed proppant fracturing
7	36%	27%	Conventional low guar
6	0%	0%	Stage skipped
5	3%	2%	Conventional low guar
4	0%	Minor	Hybrid treatment with slick water
3	0%	Minor	Conventional low guar
2	Minor	0%	Conventional low guar
1	Minor	Minor	Hybrid treatment with slick water

Fig. 19 The PLT evaluation.

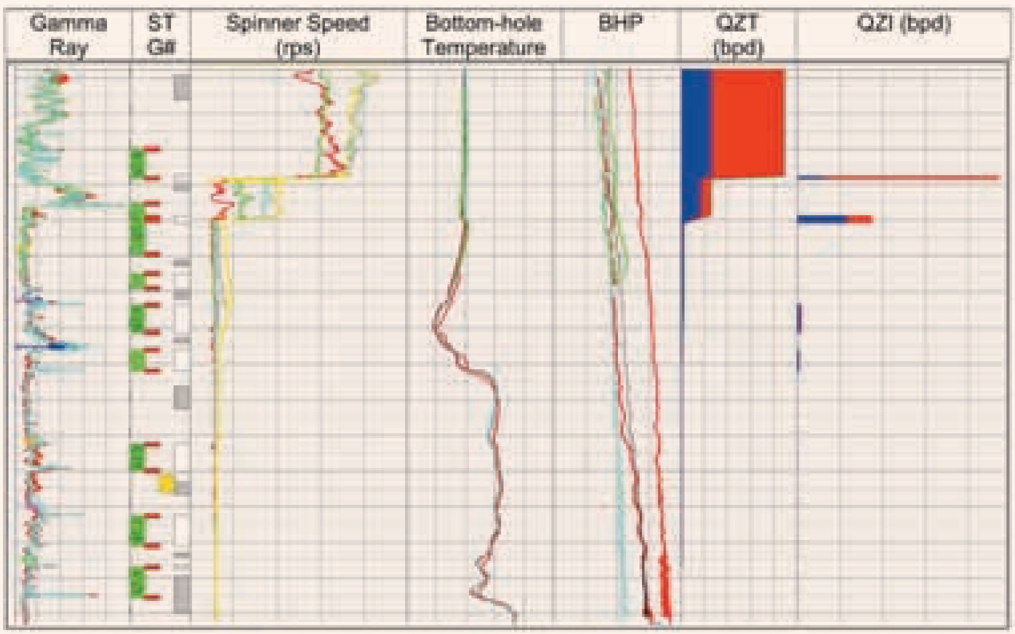

Table 6 The comparison results of Well-A with the offset wells.

	Completion Method	No. of Stages	Fracturing Technology	Normalized Proppant Mass	Normalized Gas Rate	Normalized Flowing Wellhead Pressure
Well-B	Open Hole MSF	5	Conservative polymer load cross-linked	1.00	1.00	1.00
Well-C	Plug-and-Perf	5	Conservative polymer load cross-linked	0.99	0.18	0.19
Well-D	Plug-and-Perf	5	Conservative polymer load cross-linked	0.99	0.00	0.00
Well-A	Plug-and-Perf	7	New approach	1.14	1.51	1.11

stage that need to be treated with a single fracturing operation, particulate diverters may be considered for effective stimulation. Cross-linked fluid for CO_2 foam fracturing can be an alternative option to place a large amount of proppant. Although the success of CO_2 foam fracturing in this case study is evident, it is unclear as to what part of the success could be potentially attributed to the reservoir quality. Production modeling could help further assessment.

To better quantify the impact of CO_2 foam fracturing, more candidates should be selected for CO_2 foam fracturing treatments.

Conclusions

Proppant placement with slick water was proven in a plug-and-perf completion. Also, the applicability of CO_2 foamed fracturing treatment was established with the highest production rates after normalizing, even with the smallest job size placed. Flow back was immediately initiated for a sub-hydrostatic reservoir, which could be due to the added energy from the supercritical CO_2 entering the reservoir. The friction pressure evaluation from the downhole gauge data for CO_2 foams is a critical addition to the database from this case study and can be effectively utilized in future treatments.

The objective of rendering commercially viable wells in the area through a strategic and comprehensive workflow based on the offsets introduced at the beginning of this study (Wells B, C, and D) was effectively completed. Table 6 completes the puzzle by putting together the full comparison of this success story.

Acknowledgments

The authors would like to thank the Saudi Aramco and Schlumberger operational teams who participated in this operation.

This article was prepared for presentation at the SPE Conference at the Oman Petroleum and Energy Show, Muscat, Oman, September 14-16, 2020.

References

1. Cipolla, C.L., Weng, X., Onda, H., Nadaraja, T., et al.: "New Algorithms and Integrated Workflow for Tight Gas and Shale Completions," SPE paper 146872, presented at the SPE Annual Technical Conference and Exhibition, Denver, Colorado, October 3-November 2, 2011.

2. Sharma, M.M., Gadde, P.B., Sullivan, R., Sigal, R., et al.: "Slick Water and Hybrid Fracs in the Bossier: Some Lessons Learnt," SPE paper 89876, presented at the SPE Annual Technical Conference and Exhibition, Houston, Texas, September 26-29, 2004.

3. Tudor, E.H., Nevison, G.W., Allen, S. and Pike, B.: "100% Gelled LPG Fracturing Process: An Alternative to Conventional Water-Based Fracturing Techniques," SPE paper 124495, presented at the SPE Eastern Regional Meeting, Charleston, West Virginia, September 23-25, 2009.

4. Rahim, Z., Al-Kanaan, A.A., Waheed, A., Kayumov, R., et al.: "Foamed Acid Fracturing Enables Efficient Stimulation of Low-Pressure Carbonate Reservoirs," SPE paper 191460, presented at the SPE International Hydraulic Fracturing Technology Conference and Exhibition, Muscat, Oman, October 16-18, 2018.

5. Malik, A.R., Dashash, A.A., Al-Driweesh, S.M., Noaman, Y.M., et al.: "Successful Implementation of CO_2 Energized Acid Fracturing Treatment in Deep, Tight and Sour Carbonate Gas Reservoir in Saudi Arabia that Reduced Freshwater Consumption and Enhanced Well Performance," SPE paper 171916, presented at the Abu Dhabi International Petroleum Exhibition and Conference, Abu Dhabi, UAE, November 10-13, 2014.

About the Authors

Abdulrahman A. Al-Mulhim

B.S. in Petroleum Engineering, University of Leeds

Abdulrahman A. Al-Mulhim is a Gas Production Engineer working in Saudi Aramco's Southern Area Production Engineering Department. He is responsible for designing intervention programs, supervising operations, monitoring wells' performance, and acting as a point of communication between different organizations.

Abdulrahman is the author of several Society of Petroleum (SPE) papers. He also was selected to present a paper at the Abu Dhabi International Expedition and Conference (ADIPEC) in November 2018.

In 2013, Abdulrahman received his B.S. degree in Petroleum Engineering from the University of Leeds, Leeds, U.K.

Saad Hamid

B.S. in Mechanical Engineering, University of Engineering & Technology

Saad Hamid is a Production Engineer working in Saudi Aramco's Southern Area Production Engineering Department. He is involved in production engineering, completions, well integrity, surveillance, and well intervention activities.

Prior to joining Saudi Aramco in 2015, Saad worked for 14 years in various technical roles, including production enhancement, stimulation, completion, coiled tubing, and well intervention with Sanjel and Schlumberger in the Middle East and North America.

He has authored and presented several Society of Petroleum Engineering (SPE) papers at international conferences in Canada, the U.S., and the Middle East.

Saad received his B.S. degree (with honors) in Mechanical Engineering from the University of Engineering & Technology, Lahore, Pakistan.

He is a registered Professional Engineer with the Association of Professional Engineers and Geoscientists of Alberta (APEGA), Canada.

Abdul Muqtadir Khan

M.S. in Petroleum Engineering, University of Texas-Austin

Abdul Muqtadir Khan is currently working as a Lead Technical Engineer for fracturing and stimulation, where he is involved in fracturing projects. Abdul joined Schlumberger in 2013 as Fracturing Field Engineer in South Texas. After two years in that position, he was given the role of a Lead Technical Engineer in Saudi Arabia.

Since 2015, Abdul has been in charge of fracturing and production technical support, providing support for optimization and special projects to Saudi Aramco's Production Engineering Division.

He has 7 years of experience in fracturing treatments in both conventional and unconventional wells.

In 2010, Abdul received his B.S. degree in Petroleum Engineering from Maharashtra Institute of Technology, Pune, India. In 2013, he received his M.S. degree in Petroleum Engineering from the University of Texas at Austin, Austin, TX.

Chan C. Hoong

B.E. in Chemical Engineering, Universiti Teknologi PETRONAS

Chan C. Hoong is currently the Sales and Technical Engineer for Fracturing, Stimulation and Gravel Pack for Schlumberger. He started with Schlumberger in 2010 as a Fracturing and Stimulation Field Engineer based in 'Udhailiyah, Saudi Arabia. In 2013, Chan then became a Fracturing and Stimulation Lead Technical Engineer for Saudi Arabia, providing fracturing and stimulation technical support for Saudi Aramco's Production Engineering Division.

Over the last 10 years, his career experience includes hydraulic fracturing (both conventional and unconventional), matrix stimulation and gravel packing in the Middle East and Asia region consisting of Saudi Arabia, Bahrain, Malaysia, Thailand, Vietnam, Brunei, the Philippines, and Myanmar.

In 2010, Chan received his B.E. degree (with honors) in Chemical Engineering from Universiti Teknologi PETRONAS, Perak, Malaysia.

Application of a Real-Time Mud Density and Rheology Monitoring System to Enhance Drilling in HPHT Gas Wells with MPD Systems

Ebikebena M. Ombe, Odai A. Elyas, Tamer A. Qader, and Mohammed Mehdi

Abstract / The monitoring and management of drilling fluid properties while drilling oil and gas wells is very important, especially when drilling in oil and gas fields where highly pressurized formations with narrow pore pressure and/or fracture gradient windows are encountered. The most critical of these properties include the drilling fluid density or mud weight (MW) and the rheological properties, i.e., plastic viscosity (PV) and yield point (YP).

Changes in these properties are usually the first indication of downhole problems, and therefore, the need to constantly monitor them cannot be overemphasized. While drilling, much effort is put into having a tight control on these drilling fluid properties to avoid even the slightest variations. The conventional approach to monitoring drilling fluid properties in drilling operations involves the drilling fluid engineer carrying out routine tests on mud samples, taken from the active mud system.

These tests include MW checks and funnel viscosity tests to check for any changes in the MW and/or the rheological properties. If any changes or deviations are detected in these tests, then tests that are more detailed are carried out on the mud samples to identify which of the other properties have changed and the possible causes. This is a time-consuming process and by the time the problem is identified, the resulting downhole problems would have deteriorated to cause a major challenge, e.g., stuck pipe, lost circulation, or well control.

This issue requires an automated and continuous system to detect the trending of the drilling fluid density and rheological properties. The density rheology monitoring system (DRMS) is an innovative real-time solution that has been developed to provide real-time values for the MW and rheological properties of the drilling fluid in the active system, thereby allowing for quick detection and an immediate response to any changes in these properties. This is a far more effective approach than the conventional mud checks, since it reduces the lag time between the actual changes in drilling fluid properties and the identification for these changes.

The DRMS consists of the density and rheology unit (DRU) linked to a monitoring system. The DRU measures laboratory grade pressurized density and also takes six-speed viscometer measurements via rapid sampling at the collection point, usually located at the flow line after the shakers and in the active mud tank. The density measurements are taken once every 90 seconds, while the rheology measurements are taken once every 20 minutes.

The monitoring system presents these values digitally and plots the trends graphically so that changes can be identified on the spot. This allows for the early detection and mitigation of the causative downhole problems, as well as proper management of the drilling fluid properties and overall quality.

Introduction

This article discusses drilling operations where the density rheology monitoring system (DRMS) was used for real-time monitoring — of the drilling fluid mud weight (MW) and the rheological properties — while drilling with a managed pressure drilling (MPD) system through high-pressure formations. It will highlight how the DRMS allowed for early detection of the drilling fluid deterioration and prevalent downhole problems, e.g., lost circulation and well control. This application allowed for quick and effective actions to be taken to restore the drilling fluid quality, thereby preventing any downhole problems and allowing for the successful drilling of these high-pressure formations.

This article will also highlight how data from the DRMS can be used for real-time optimization of downhole equivalent circulating density (ECD) while drilling with the MPD system.

Challenge

Measurements of mud density and rheology are much more critical when drilling wells with narrow mud windows such as deep high-pressure, high temperature (HPHT) gas wells and offshore wells. Unfortunately, the conventional approach of monitoring drilling fluid properties results in major risks. This is mainly due to the requirement of maintaining the drilling fluid density and rheology within the very narrow range required to drill the well successfully. As the industry advances, the demand for these difficult wells will increase dramatically, which makes the conventional approach to monitoring the mud properties insufficient, due to the increase in uncertainty between measured drilling fluid properties and actual downhole conditions.

The challenge is to reduce the lag time in between the occurrence of downhole problems and their subsequent detection via the drilling fluid tests and the subsequent corrective measures. The solution to this problem is to enable the early detection of these changes in the fluid system by increasing the testing frequency, thereby providing the ability to identify downhole issues at their inception rather than at the culmination of the problem. This will evidently reduce the occurrence of nonproductive time (NPT) while drilling — caused by downhole problems like stuck pipe and well control incidents — and ultimately help ensure safer drilling operations.

Solution

This issue, and therefore the solution, lends itself to an automated and continuous monitoring system for drilling fluid density and rheological properties. The density rheology monitoring system (DRMS) is a solution that gives real-time values for mud weight (MW) and rheological properties of the drilling fluid in the active system. The system automatically runs frequent tests on the drilling fluid density and rheology. This is a far more effective approach than the conventional manual mud checks, which involve time-consuming tests to identify the changes in drilling fluid properties.

Technology

The DRMS consists of a density and rheology unit (DRU) linked to a monitoring system. It measures laboratory grade pressurized density and also takes six-speed viscometer measurements from which it derives the plastic viscosity (PV) and yield point (YP) values. The measurements are done via rapid sampling at the collection points, usually at the active mud tank or the flow line, Fig. 1.

As mentioned earlier, the density measurements are taken once every 90 seconds, while the rheology measurements are taken once every 20 minutes. The monitoring system presents these values digitally and also plots them graphically so that any changes are not only identified quickly, but also as they occur, rather than at the next mud check. Figure 2 is an example of the rheology, density, and PV/YP measurements plotted against the conventional measurements taken from the same active system.

The system is also designed to allow the simultaneous measurement of the density after each rheology check. This is to allow for effective correlation between the density and rheology measurements.

It should be noted that the DRMS was intended, from its inception, to take measurements at the active fluid tank from which the fluid is pumped to the wellbore. Consequently, for the application discussed in this article, the system was configured to also take measurements from the flow line just before the shakers. This was done to allow for a comparison between drilling fluid properties going into the wellbore and coming out of the wellbore. This would also provide

Fig. 1 *The DRU system layout.*

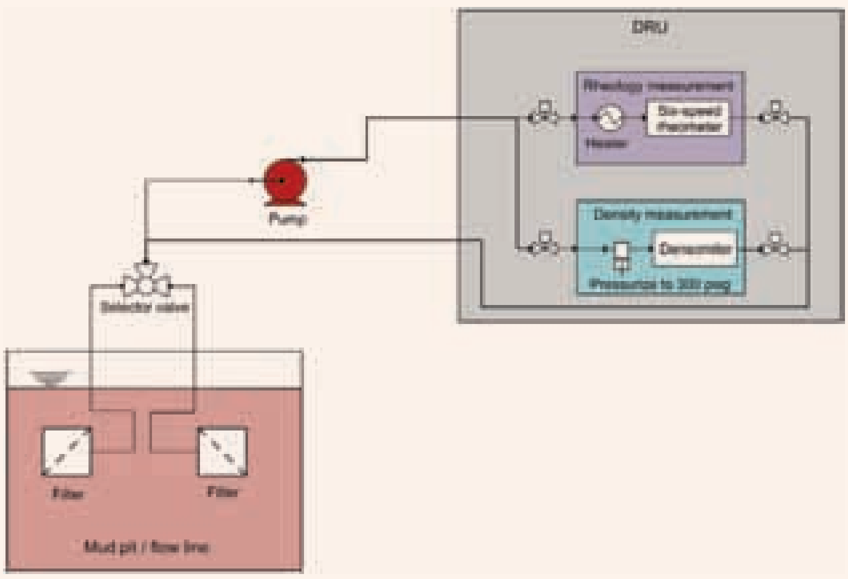

Fig. 2 *The DRU's rheology vs. conventional measurement.*

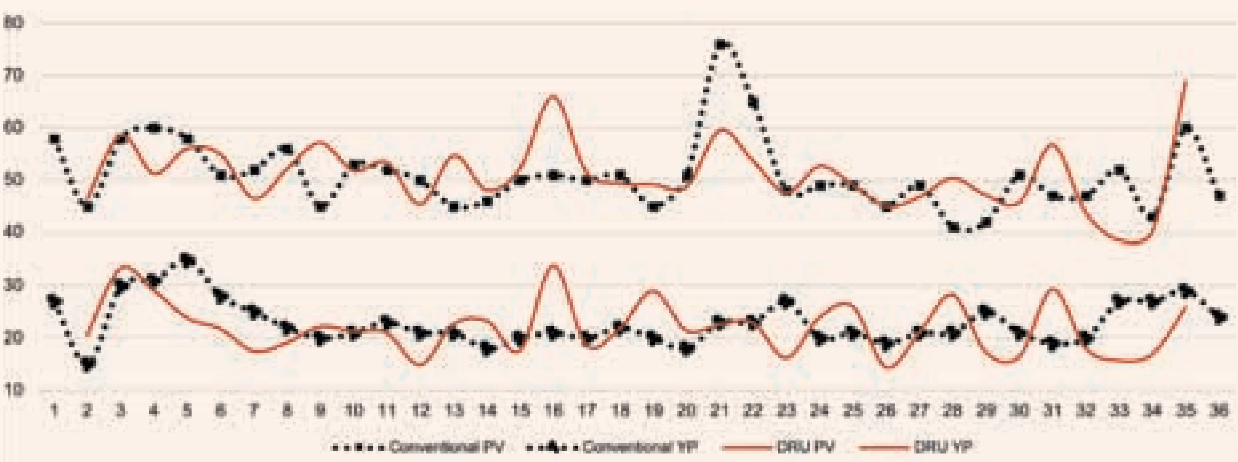

more insight into downhole conditions by showing their effect on the drilling fluid, thereby further enhancing the downhole monitoring and mitigation efforts.

Density Measurements Process

The common measuring device used to measure the drilling fluid's MW at the rig site is the mud balance. The equipment consists of a graduated beam with a weight slider and a bubble level, balanced on a knife edge pivot point. The beam is terminated at one end in a cup to hold a fixed amount of fluid and the other is a lead shot weighted counter-weight. The cup can be either pressurized or non-pressurized. The weight slider is moved along the beam once the cup is filled, and once the bubble indicates the beam is level, then the density is read off the scale on the beam. The balances generally have a working range of 6.5 ppg to 23.0 ppg for the non-pressurized balance and 6.9 ppg to 21.9 ppg for the pressurized balance.

The DRU measures the fluid density with a density sensor using the patented pulse excitation method[1]. This process makes use of a U-shaped tube made of borosilicate glass, or metal, oscillating at its natural frequency. The DRU has sensors that excite and receive signals from the U-tube while a computing system determines its period of oscillation. This oscillation signal is transferred to another computing system that calculates the initial density reading from the U-tube, which serves as a baseline density measurement.

The signals are then amplified by the DRU sensor and sent back to the U-tube to keep it oscillating. When the drilling fluid is introduced to the U-tube, the frequency of the oscillations change. This frequency change is proportional to the change in density of the U-tube, due to the drilling fluid inside it. By measuring this change in frequency and comparing it with the baseline measurements taken earlier, the system derives the density of the drilling fluid.

Once the sample is measured and the system reading is recorded, the density pressure valve is de-energized,

Fig. 3 *The accuracy level of the DRU automated density measurement vs. the conventional measurements.*

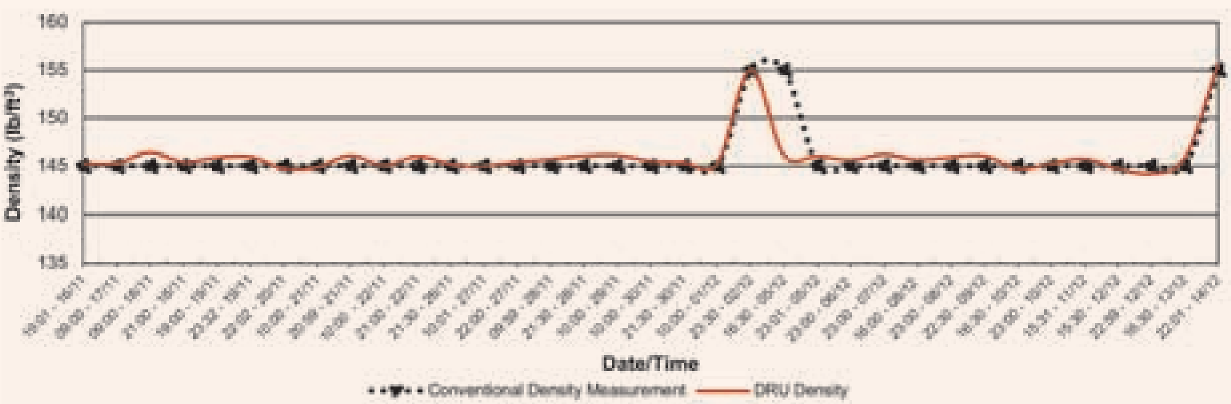

and the system is flushed with nitrogen. To combat any material or particulate settling, the density measurement system is subject to a cleaning cycle that occurs after every 50 density samples measured, which approximates to once per hour of operation. The density loop is back flushed to remove any settled particulates from the U-tube and the inlet manifold.

Figure 3 shows the accuracy level of DRU automated density measurement vs. the conventional measurements. It should be noted is that the entire sampling, measuring, and discharge process is fully automated and does not require any external intervention.

Rheology Measurement Process

At the rig site, there are two traditional methods for measuring the drilling fluids' rheology, which are the Marsh funnel and the direct indicating viscometer. These devices provide the information for deriving and monitoring the fluid's rheological properties.

The traditional Marsh funnel test, which was first proposed by Marsh (1931)[2], is generally a quick, repeatable test taken while drilling to monitor the fluid coming out of the wellbore for significant changes. The time between checks usually varies significantly, depending on the drilling operation. Even if there is a set schedule for measurements, more often than not, there can be significant delays between checks, if the test is even performed at all. These checks are often forestalled by other events on the rig site, especially during critical operations.

The second method would ideally, although not always practicable, use the fluid from the Marsh funnel test to perform a six-speed viscometer measurement with the direct indicating viscometer. This is a routine test, which is performed at least twice a day. Ideally, it should be performed four times during a 24-hour period, but can be performed more frequently if downhole problems are suspected. This timing means that, in general, any changes that are occurring in the drilling fluid may go undetected for long periods of time — between four to 12 hours.

The DRU measures the drilling fluid's rheology by an automated batch analysis every 10 to 60 minutes, depending on the user-defined test temperature and the initial fluid sample temperature. The drilling fluid sample is pumped into the rheology meter — the "rheometer" — within the DRU system, displacing the preceding sample. Once the previous sample is fully displaced, the inlet and outlet valves on the respective DRU flow lines are closed. The sample is then pressurized to approximately 80 psig to 100 psig to break down large air bubbles in the drilling fluid, and ensuring that the rheometer is entirely filled.

Subsequently, the sample is agitated and heated to the desired temperature, typically between 120 °F to 150 °F. The fluid rheology is measured at the rotational shear rates (3, 6, 100, 200, 300, and 600 rev/min) as recommended by the American Petroleum Institute (2009)[3]. Also, the entire sampling, measuring and discharge process is fully automated and does not require any external intervention.

Results of the DRMS Application

As stated earlier, the DRMS, via the monitoring system, presents the MW, PV, and YP values of the drilling fluid digitally and plots the trends graphically. With this graph, the trends of the drilling fluid's density and rheological properties can be monitored, and any anomalies can easily be identified and promptly mitigated unlike the conventional approach of running tests on mud samples in four to six hour intervals. This also helps to minimize any fluctuations in the drilling fluid's

Fig. 4 *The automated fluids density and rheology measurement can be monitored in real-time via software. An example of DRU rheology intervention based on planned fluid properties.*

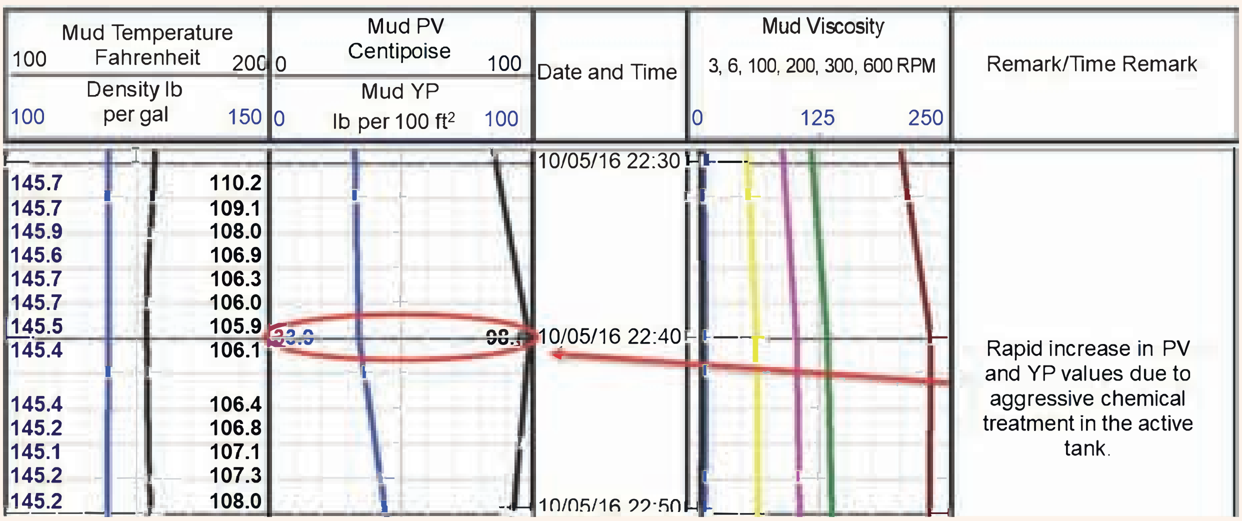

Fig. 5 *The reduction in drilling time and drilling rate after application of the DRMS.*

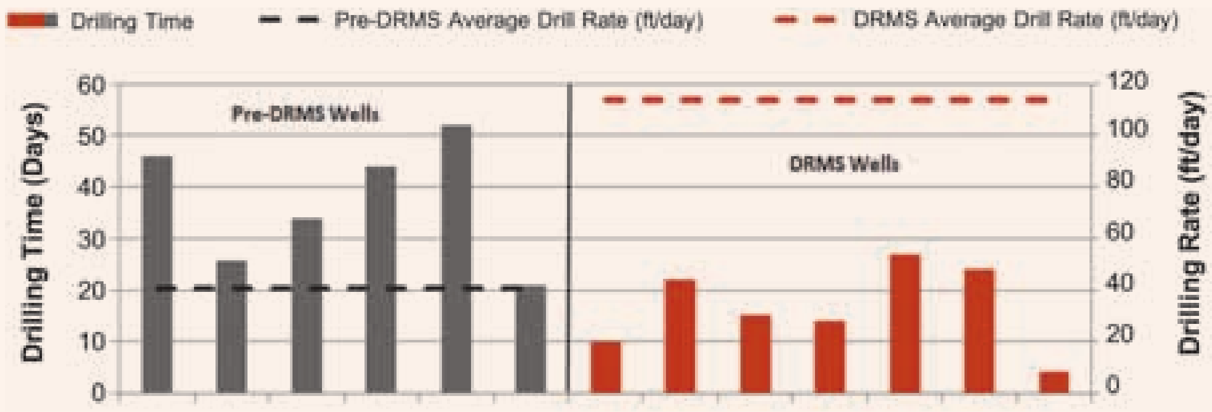

Fig. 6 *The main components of a typical MPD system[4].*

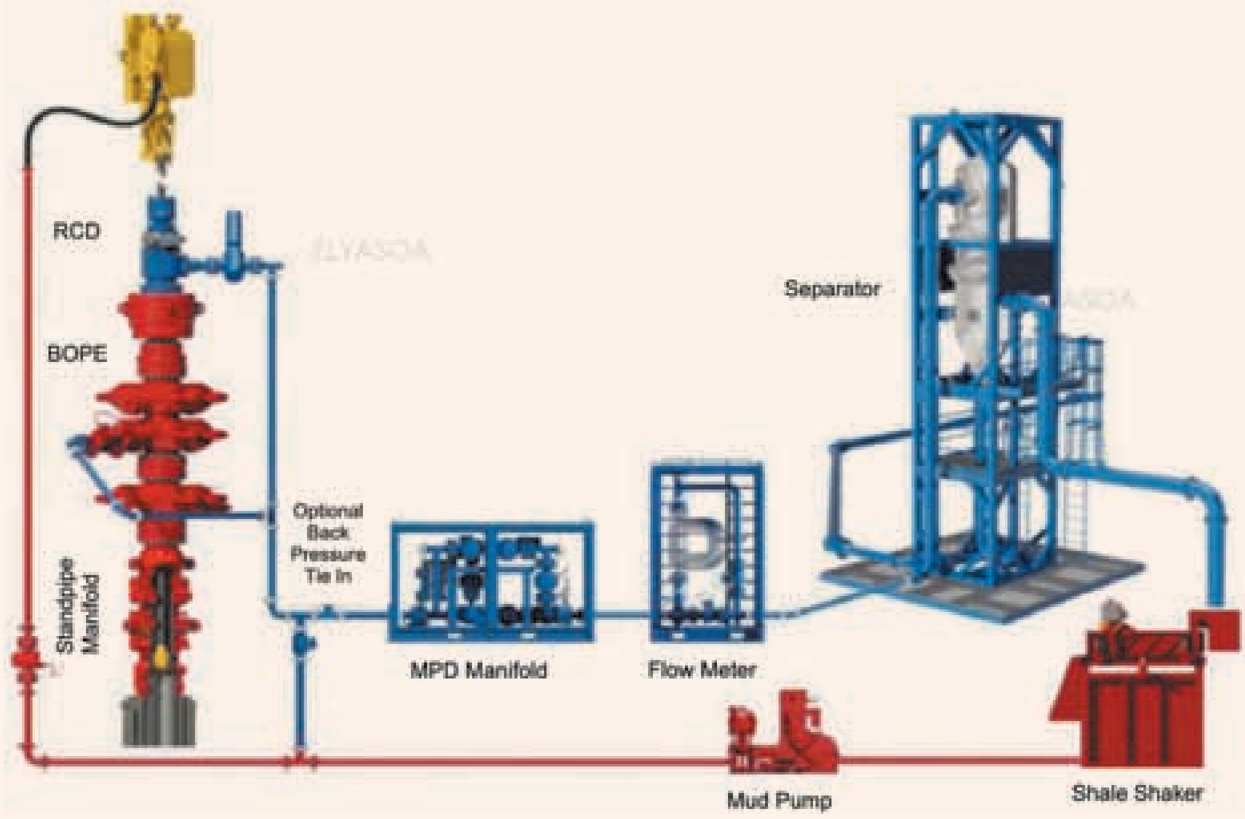

density and rheological properties, thereby enhancing control of fluid properties pumped into the wellbore, and ultimately reducing drilling fluid-related NPT.

Figure 4 illustrates one case in particular of a drilling operation in which the mud properties were negatively impacted by overtreatment of the drilling fluid. Within 20 minutes, the PV and YP values of the drilling fluid increased by 15 cP and 15 lb/100 ft^2, respectively. This could not have been detected by the conventional mud checks, but fortunately the DRMS alerted the drilling fluid engineer to the issue, and the mud was diluted accordingly to bring the rheology back to its desirable values.

The use of the DRMS also contributed to the effective monitoring and maintenance of the drilling fluid, subsequently leading to the reduction of drilling fluid-related

NPT. Ultimately, the application of the DRMS led to the drastic reduction in the time required (drilling days) to drill the wells in that particular field, and a sizable increase in their average drilling rate (ft/day).

Figure 5 is a comparison of drilling time and drilling rate of some other wells in the field before and after the application of the DRMS.

DRMS and Managed Pressure Drilling (MPD) Application

Managed pressure drilling (MPD) is a technique used to drill across formations with a very narrow drilling mud window, i.e., a narrow margin between the pore pressure and fracture gradient. Figure 6 shows the set-up for a typical MPD system. Several components are available in the MPD system, which allows it to operate in various conditions:

- The rotating control device, which allows the rotation of the string while holding pressure.
- The MPD choke valve, which is used to control the surface back pressure.
- The MPD monitoring system, used to provide real-time information about the well's conditions.

The MPD system uses surface back pressure along with a low MW drilling fluid to control the equivalent circulating density (ECD), and thereby maintain the required bottom-hole pressure (BHP) within the drilling mud window while drilling. The MPD system applies the required back pressure automatically via the MPD choke controlled by a hydraulics modeling simulator[5]. The system derives the required surface back pressure and ultimately the required BHP with algorithms based on Eqns. 1 and 2:

$$\textit{Required BHP} = \textit{Hydrostatic Pressure} + \textit{Friction Pressure Loss} + \textit{Surface Back Pressure} \quad (1)$$

The hydrostatic pressure is a function of the drilling fluid's MW and the true vertical depth (TVD) of the well, expressed in field units as follows:

$$\text{Hydrostatic Pressure (psi)} = (MW*TVD)/0.052 \quad (2)$$

where MW = drilling fluid MW (ppg) and TVD = wellbore true vertical depth.

The frictional pressure loss is the pressure lost in the drillstring and annulus due to fluid flow. This pressure loss is directly proportional to the MW, the PV, and the YP as shown in Eqns. 3[6] and 4[7]:

$$\text{Frictional Pressure Loss for Laminar Flow (psi)} = (\{[PV*Q]/[1000*(D_w - D_o)^2]\} + \{YP/[200*(D_w - D_o)]\} + [(PV*Q)/(1500*d^2)] + [YP/(225*d)]\ )*L \quad (3)$$

$$\text{Frictional Pressure Loss for Turbulent Flow (psi)} = 2*f*MW*[Q^2]*[L/(D_w - D_o)] \quad (4)$$

where Q = flow velocity in the well (ft/s), D_w = wellbore diameter (inches), D_o = drillstring outer diameter (inches), d = drillstring inner diameter (inches), L = drillstring length (ft), and f = Fanning Frictional Factor derived from the "Colebrook-White Model," Eqn. 5[7]:

$$1/(\sqrt{f}) = -2\log_{10}[2.51/\{(\{928*MW*Q*(D_w - D_o)\}/[PV+\{5*YP*(D_w - D_o)/Q\}])*\sqrt{f}\}] \quad (5)$$

Conventionally, the MW, PV, and YP values used for the hydraulic simulations are manually input into the MPD hydraulic modeling simulators from the data in the daily mud report. The mud report is a spot check of the fluid system, and it reports the properties at that point in time. The assumption for MPD hydraulics modeling simulators is that the mud is always homogeneous, but this is obviously not always the case. Mud systems are constantly being treated, diluted, or weighted up. Often, from one mud report to the next, the mud properties have changed enough to significantly affect the pressures within the well.

The DRMS can provide more representative values of these mud properties to the MPD hydraulic modeling simulators since it measures these values more frequently, thereby allowing the MPD system to apply more accurate surface back pressure to the well. It should be noted, however, that in MPD operations, the DRMS does not completely eliminate the need for conventional mud checks. The conventional mud checks will still need to be performed to verify the accuracy of the DRMS measurements, and also to provide redundancy measurements in the case of DRMS failures.

Conclusions

The application of the DRMS greatly enhanced the critical drilling operations across the HPHT formation. By providing real-time density and rheology measurements, it helped detect the early onset of downhole problems and allowed for timely intervention. It also helped to better monitor and maintain the drilling fluid properties. The DRMS will also be of great benefit to MPD operations by providing real-time MW and rheological properties for the MPD system to accurately simulate and control the downhole ECD while drilling.

Acknowledgments

This article was presented at the 2020 International Petroleum Technology Conference, Dhahran, Saudi Arabia, January 13-15, 2020.

References

1. Umfer, C.: "Method for Determining a Density Value," European Patent 2952874A1, December 2016.
2. Marsh, H.N.: "Properties and Treatment of Rotary Mud," *Transactions of the AIME*, Vol. 92, Issue 1, December 1931, pp. 234-251.
3. American Petroleum Institute: *Recommended Practice for Field Testing Water-based Drilling Fluids*, API RP 13B-1, 4th edition, American Petroleum Institute, Washington, D.C., March 2009, 104 p.
4. Moid, F., Ghamdi, A.A., Nutaifi, A.M. and Utaibi, A.: "Utilization of Managed Pressure Drilling in Deep High-Pressure High Temperature Gas Wells," SPE paper 194539, presented at the SPE/IADC Managed Pressure Drilling and Underbalanced Operations Conference and Exhibition,

Amsterdam, the Netherlands, April 9-10, 2019.

5. Medley, G.H., Moore, D.D. and Nauduri, A.S.S.: "Simplifying MPD — Lessons Learned," SPE paper 113689, presented at the SPE/IADC Managed Pressure Drilling and Underbalanced Operations Conference and Exhibition, Abu Dhabi, UAE, January 28-29, 2008.
6. Osisanya, S.O. and Harris, O.O.: "Evaluation of Equivalent Circulating Density of Drilling Fluids under High-Pressure/High Temperature Conditions," SPE paper 97018, presented at the SPE Annual Technical Conference and Exhibition, Dallas, Texas, October 9-12, 2005.
7. Shashi Menon, E.: *Transmission Pipeline Calculations and Simulations Manual,* Elsevier Inc., 2014, 612 p.

About the Authors

Ebikebena M. Ombe

M.S. in Offshore and Ocean Technology (Subsea Engineering Option), Cranfield University

Ebikebena M. Ombe is a Drilling Engineer with 15 years of oil and gas drilling industry experience. He works with Saudi Aramco's Gas Drilling Engineering Department, where he is responsible for the design, drilling and completion of gas development wells for Saudi Aramco.

Before joining Saudi Aramco in 2014, Ebikebena worked as a Well Engineer for Shell. While at Shell, he worked with both the front end well design group and the well delivery department, and was involved with the design and construction phases of numerous oil and gas drilling and workover projects. Ebikebena also worked as the regional wells directional survey focal point for Shell's Sub-Saharan Africa drilling operations.

He received his B.S. degree in Metallurgical and Materials Engineering from the Obafemi Awolowo University, Ile-Ife, Nigeria, and his M.S. degree in Offshore and Ocean Technology (Subsea Engineering Option) from Cranfield University, Bedford, U.K.

Odai A. Elyas

B.S. in Petroleum and Natural Gas Engineering, Pennsylvania State University

Odai A. Elyas is a Petroleum Engineer working with the Drilling Technology Team of Saudi Aramco's Exploration and Petroleum Engineering Center – Advanced Research Center (EXPEC ARC). He has worked on several projects in the fields of drilling automation and localization, where he was involved in studying various chemicals used for drilling operations, and analyzing local chemical producers to find suitable products to be deployed in drilling operations.

Odai has also been on several assignments with the Gas Drilling Engineering Department, the Gas Drilling Department and the EXPEC ARC Cementing Services Unit. While on these assignments, he gained extensive experience in drilling high-pressure, high temperature extended reach gas wells, and providing technical support for cementing operations.

Odai received two B.S. degrees, one in Petroleum and Natural Gas Engineering, and the other in Energy Business and Finance, both from Pennsylvania State University, State College, PA. He is looking forward to pursuing his M.S. degree in Petroleum Engineering at the University of Texas at Austin, Austin, TX.

Tamer A. Qader

B.S. in Geology, Benha University

Tamer A. Qader is a Principle Technical Professional working with Halliburton Baroid.

He has more than 15 years of oil and gas experience obtained through a variety of international engineering and project management positions, including drilling fluids, managed pressure drilling, digital solutions, and business development.

Tamer received his B.S. degree in Geology from Benha University, Banha, Egypt.

Mohammed Mehdi

M.S. in Petroleum Geology, University of Peshawar

Mohammed Mehdi is a Petroleum Geologist and Principal Technical Professional working with Halliburton Energy Services.

He has more than 15 years of oil and gas industry experience obtained through a variety of engineering, digital solutions and management positions. Mohammed provides technical support for Halliburton Baroid Separation Solutions Services, especially in the areas of digital solutions, surface data logging, filtration, and drilling waste management services. He has been a digital solutions operations lead in Saudi Arabia for the past four years.

Mohammed received his B.S. degree (honors) in Geology and his M.S. degree in Petroleum Geology, both from the University of Peshawar, Peshawar, Pakistan.

Powering Ahead with Patents

Michael J. Ives

2019 marked another record breaking year in patents awarded to Saudi Aramco and its subsidiaries ARLANXEO and Motiva. At year-end, they had been granted 524 patents from the United States Patent and Trademark Office, compared to 335 granted in 2018.

Across its operations, Saudi Aramco assesses, develops, and incorporates new technology in a manner tailored to company operations to ensure the long-term sustainability of the business, enhance its operational efficiency, increase profitability, and reduce the company's environmental impact.

While the number of patents granted in 2019 is very impressive, the true value lies in the substantial positive impact any one of these innovations could have. Due to the sheer scale of Saudi Aramco's business, a single idea could have positive global ramifications and potentially have an impact measurable in the billions of dollars along with substantial energy savings — benefiting both the company's bottom line and the planet. Even apparently small enhancements in technology and processes can realize significant benefits and value, including maintaining the company's position as a leader in Scope 1 (Direct emissions[1]) upstream carbon intensity, with one of the lowest carbon footprints per unit of hydrocarbons produced.

Saudi Aramco's technology initiatives are grouped into three areas: (1) upstream, (2) downstream, and (3) sustainability.

Upstream technology development is directed primarily to improving methods for discovering new hydrocarbon reserves, improving oil recoveries, increasing productivity, discovering novel catalysts, and reducing hydrocarbon lifting costs.

Downstream technology development is dedicated primarily to maximizing value across the hydrocarbon chain and finding new and improved methods of producing products. For example, Saudi Aramco is developing processes for crude to chemicals, which is looking at the shortest and most optimal pathway to derive chemicals directly through breakthroughs in catalyst and separation devices.

Sustainability technology development is aimed at growing non-fuel applications for crude oil, sustaining low carbon intensity crude oil, driving high-impact low carbon intensity solutions, and advancing sustainable transport, e.g., through company R&D into engines and fuels, which are showing impressive results.

To accelerate innovative breakthroughs, Saudi Aramco manages a global network of research and technology centers to achieve its recovery, discovery, diversification, and sustainability objectives. When this substantial investment in its own R&D is combined with the many partnerships the company has with industry leaders and academic institutions, Saudi Aramco has created an enviable reputation as a business where innovation sits at the very center — clearly illustrated by its impressive patent record in 2019.

1 Direct emissions, which include: (a) fuels combusted in stationary sources on-site, (b) flaring, (c) equipment blowdown, (d) process vents, such as storage tanks and dehydration units, and (e) fugitive emissions from leaking components.

The company and its subsidiaries, ARLANXEO and Motiva, collectively filed 637 U.S. patent applications and received 335 U.S. patents in 2018. In 2019, 1,048 U.S. patent applications were filed and 524 were granted. About 19% of the 2019 granted patents relate to production, 18% drilling, 14% chemicals and refining, and 11% reservoir engineering. With regard to filed patents, about 21% relate to drilling, 16% production, 12% chemicals and refining, and 8% reservoir engineering.

2019 Granted Patents

Loss Circulation Compositions Comprising Portland Cement Clinker and a Suspending Agent Based on a Cross-linked Polysaccharide

Granted Patent: U.S. Patent 10,167,420, Grant Date: January 1, 2019
B. Raghava Reddy

Optimal Well Placement under Constraints

Granted Patent: U.S. Patent 10,167,703, Grant Date: January 1, 2019
Zeid M. Al-Ghareeb

Replacement Tube Plug for Heat Exchanger

Granted Patent: U.S. Patent 10,168,111, Grant Date: January 1, 2019
Dhawi A. Al-Otaibi

Integrated Process for the Production of Benzene and Xylenes from Heavy Aromatics

Granted Patent: U.S. Patent 10,173,950, Grant Date: January 8, 2019
Raed Abudawoud and Zhonglin Zhang

Modified Goswami Cycle-Based Conversion of Gas Processing Plant Waste Heat into Power and Cooling with Flexibility

Granted Patent: U.S. Patent 10,174,640, Grant Date: January 8, 2019
Mahmoud B. Noureldin and Akram H. Kamel

Sequential Fully Implicit Well Model with Tridiagonal Matrix Structure for Reservoir Simulation

Granted Patent: U.S. Patent 10,175,386, Grant Date: January 8, 2019
Ali H. Dogru

Using Radio Waves to Fracture Rocks in a Hydrocarbon Reservoir

Granted Patent: U.S. Patent 10,180,054, Grant Date: January 15, 2019
Jin-Hong Chen, Daniel T. Georgi and Hui-Hai Liu

Measuring Inter-Reservoir Cross Flow Rate through Unintended Leaks in Zonal Isolation Cement Sheaths in Offset Wells

Granted Patent: U.S. Patent 10,180,057, Grant Date: January 15, 2019
Noor M. Anisur Rahman and Hasan A. Nooruddin

Methods of Evaluating Rock Properties while Drilling Using Downhole Acoustic Sensors and a Downhole Broadband Transmitting System

Granted Patent: U.S. Patent 10,180,061, Grant Date: January 15, 2019
Yunlai X. Yang

Reusable Buoyancy Modules for Buoyancy Control of Underwater Vehicles

Granted Patent: U.S. Patent 10,183,400, Grant Date: January 22, 2019
Ali H. Outa, Fadl H. Abdel Latif, Sahejad Patel and Hassane Trigul

Drilling and Operating Sigmoid-Shaped Wells

Granted Patent: U.S. Patent 10,184,297, Grant Date: January 22, 2019
Mohamed N. Noui-Mehidi

Systems, Methods, and Computer Medium to Enhance Hydrocarbon Reservoir Simulation

Granted Patent: U.S. Patent 10,184,320, Grant Date: January 22, 2019
Ali Al-Turki, Majdi Baddourah, M. Ehtesham Hayder and Ahmad Al-Zawawi

Acrylamide-Based Copolymers, Terpolymers, and Use as Hydrate Inhibitors

Granted Patent: U.S. Patent 10,189,986, Grant Date: January 29, 2019
Mohamed S. Elanany, Khalid Majnouni, Rashed Al-Essa, Abdullah R. Al-Malki, Mohammed Al-Daous, Hassan Al-Ajwad, Shadi Adel and Rithauddeen Megat

Nuclear Magnetic Resonance and Saturation Well Logs for Determining Free Water Level and Reservoir Type

Granted Patent: U.S. Patent 10,190,999, Grant Date: January 29, 2019
Gabor Hursan and Shouxiang M. Ma

Accuracy of Water Breakthrough Time Prediction

Granted Patent: U.S. Patent 10,191,182, Grant Date: January 29, 2019
Babatope O. Kayode

Cationic Polymers and Porous Materials

Granted Patent: U.S. Patent 10,196,465, Grant Date: February 5, 2019
Yu Han, Wei Xu, Miao Sun, Qiwei Tian, Xinglong Dong, Zhaohui Liu, Jean-Marie Basset, Youssef Saih and Sohel Shaikh

Cement Compositions Comprising Liquid Elastomers on a Solid Support

Granted Patent: U.S. Patent 10,202,537, Grant Date: February 12, 2019
B. Raghava Reddy

Method to Remove Metals from Petroleum

Granted Patent: U.S. Patent 10,202,552, Grant Date: February 12, 2019
Ki-Hyouk Choi, Emad N. Al-Shafei, Ashok K. Punetha, Joo-Hyeong Lee and Mohammad A. Al-Abdullah

Determination of the Degree of Branching

Granted Patent: U.S. Patent 10,203,319, Grant Date: February 12, 2019
Heike Kloppenburg and Alicia Le-Sattler

Chair Pad System and Associated, Computer Medium and Computer Implemented Methods for Monitoring and Improving Health and Productivity of Employees

Granted Patent: U.S. Patent 10,206,625, Grant Date: February 19, 2019
Samantha J. Horseman

Cracking System Integrating Hydrocracking and Fluidized Catalytic Cracking

Granted Patent: U.S. Patent 10,207,196, Grant Date: February 19, 2019
Musaed M. Al-Thubaiti, Ali M. Al-Somali and Omer R. Koseoglu

Formation Water Salinity from Borehole Measurements

Granted Patent: U.S. Patent 10,208,582, Grant Date: February 19, 2019
Shouxiang M. Ma, Nedhal M. Musharfi, Pablo J. Saldungaray and Harold Pfutzner

Process for Acid Gas Treatment and Power Generation

Granted Patent: U.S. Patent 10,213,730, Grant Date: February 26, 2019
Aadesh Harale, Mourad Younes and Maytham Musawi

Systems and Methods for Producing Propylene

Granted Patent: U.S. Patent 10,214,466, Grant Date: February 26, 2019
Sohel Shaikh, Aqil Jamal and Zhonglin Zhang

Determining Wellbore Leak Crossflow Rate between Formations in an Injection Well

Granted Patent: U.S. Patent 10,215,002, Grant Date: February 26, 2019
Nasser M. Al-Hajri

Gas-Assisted Liquid Fuel Oxygen Reactor

Granted Patent: U.S. Patent 10,215,402, Grant Date: February 26, 2019
Aqil Jamal, Rached Ben-Mansour and Mohamed Habib

Cation Exchange Capacity and Water Saturation from Array Induction Data

Granted Patent: U.S. Patent 10,215,876, Grant Date: February 26, 2019
Shouxiang M. Ma, Ping Zhang and Wael Abdallah

System and Method for Fueling Alternative Fuel Vehicles

Granted Patent: U.S. Patent 10,218,020, Grant Date: February 26, 2019
Aqil Jamal and Thang V. Pham

Integrated Solvent Deasphalting and Steam Pyrolysis System for Direct Processing of a Crude Oil

Granted Patent: U.S. Patent 10,221,365, Grant Date: March 5, 2019
Abdennour Bourane, Raheel Shafi, Essam Sayed, Ibrahim A. Abba and Abdul Rahman Zafer Akhras

Methods for Processing Fumed Metallic Oxides

Granted Patent: U.S. Patent 10,227,237, Grant Date: March 12, 2019
Michele L. Ostraat

Organic Rankine Cycle-Based Conversion of Gas Processing Plant Waste Heat into Power and Cooling

Granted Patent: U.S. Patent 10,227,899, Grant Date: March 12, 2019
Mahmoud B. Noureldin and Akram H. Kamel

System and Method for Infrared Reflection Avoidance

Granted Patent: U.S. Patent 10,228,321, Grant Date: March 12, 2019
Brian J. Parrott

Parallel Solution for Fully Coupled Fully Implicit Wellbore Modeling in Reservoir Simulation

Granted Patent: U.S. Patent 10,229,237, Grant Date: March 12, 2019
Larry S. Fung

Diagnosing Reservoir Health

Granted Patent: U.S. Patent 10,229,360, Grant Date: March 12, 2019
Abdulazeem A. Towailib and Jerry P. Fontanilla

Integrated Hydrocracking and Fluidized Catalytic Cracking System
Granted Patent: U.S. Patent 10,232,285,
Grant Date: March 19, 2019
Musaed M. Al-Thubaiti, Omer R. Koseoglu and Ali M. Al-Somali

Loss Circulation Material for Seepage to Moderate Loss Control
Granted Patent: U.S. Patent 10,233,372,
Grant Date: March 19, 2019
Jothibasu Ramasamy and Md. Amanullah

Loss Circulation Compositions (LCM) Having Portland Cement Clinker
Granted Patent: U.S. Patent 10,233,379,
Grant Date: March 19, 2019
B. Raghava Reddy

Well Treatment Fluid Having an Acidic Nanoparticle-Based Dispersion and a Polyamine
Granted Patent: U.S. Patent 10,233,380,
Grant Date: March 19, 2019
Vikrant B. Wagle, Abdullah S. Al-Yami, Zainab Alsaihati and Abdulaziz Alhelal

Integrated Multistage Solvent Deasphalting and Delayed Coking Process to Produce High Quality Coke
Granted Patent: U.S. Patent 10,233,394,
Grant Date: March 19, 2019
Omer R. Koseoglu

Selective Middle Distillate Hydrotreating Process
Granted Patent: U.S. Patent 10,233,399,
Grant Date: March 19, 2019
Omer R. Koseoglu and Abdulrahman Al-Bassam

Integrated Hydrotreating, Solvent Deasphalting and Steam Pyrolysis System for Direct Processing of a Crude Oil
Granted Patent: U.S. Patent 10,233,400,
Grant Date: March 19, 2019
Abdennour Bourane, Raheel Shafi, Essam Sayed, Ibrahim A. Abba and Abdul Rahman Zafer Akhras

Multilayer Reservoir Well Drainage Region
Granted Patent: U.S. Patent 10,233,749,
Grant Date: March 19, 2019
Noor M. Anisur Rahman and Saud A. Bin Akresh

Integrated Ultrasonic Testing and Cathodic Protection Measurement Probe
Granted Patent: U.S. Patent 10,234,375,
Grant Date: March 19, 2019
Hassane Trigui, Sahejad Patel, Ali Outa, Ayman Amer, Fadl H. Abdel Latif, Ameen Obedan and Hamad Al-Saiari

Emergency Shutdown System for Dynamic and High Integrity Operations
Granted Patent: U.S. Patent 10,234,840,
Grant Date: March 19, 2019
Abdelghani Daraiseh and Patrick S. Flanders

Systems and Methods for Assessing Upstream Oil and Gas Electronic Data Duplication
Granted Patent: U.S. Patent 10,235,080,
Grant Date: March 19, 2019
Sami N. Awfi

Processes for Analysis and Optimization of Multiphase Separators, Particular in Regards to Simulated Gravity Separation of Immiscible Liquid Dispersions
Granted Patent: U.S. Patent 10,238,992,
Grant Date: March 26, 2019
Olanrewaju M. Oshinowo

Magnetic Omni-Wheel with Roller Bracket
Granted Patent: U.S. Patent 10,239,347,
Grant Date: March 26, 2019
Fadl H. Abdel Latif, Ali Outa, Brian J. Parrott, Shigeo Hirose, Michele Guanieri and Paulo Debenest

A Process for Sulfur Recovery from Acid Gas Stream without Catalytic Claus Reactors
Granted Patent: U.S. Patent 10,239,756,
Grant Date: March 26, 2019
Yuguo Wang, Ismail Alami, Rashid M. Othman and Qi Xu

System for Tail Gas Treatment of Sulfur Recovery Units
Granted Patent: U.S. Patent 10,239,763,
Grant Date: March 26, 2019
Mourad Younes, Maytham Musawi and Aadesh Harale

Method of Making Sulfur Extended Asphalt Modified with Crumb Rubber
Granted Patent: U.S. Patent 10,240,040,
Grant Date: March 26, 2019
Mohammed H. Al-Mehthel, Saleh H. Al-Idi, Mohammad Anwar Parvez, Ibnelwaleed A. Hussein and Hamad I. Al-Abdulwahhab

Integrated Process for Activating Hydroprocessing Catalysts with in Situ Produced Sulfides and Disulfides
Granted Patent: U.S. Patent 10,240,096,
Grant Date: March 26, 2019
Omer R. Koseoglu and Robert P. Hodgkins

Process for Combustion of Heavy Oil Residue
Granted Patent: U.S. Patent 10,240,101,
Grant Date: March 26, 2019
Tidjani Niass and Mourad V. Younes

Trimodal Hybrid Loss Prevention Material (LPM) for Preventative and Curative Loss Control
Granted Patent: U.S. Patent 10,240,411,
Grant Date: March 26, 2019
Md. Amanullah

Systems and Methods to Obtain Diagnostic Information Related to a Bidirectional Prover
Granted Patent: U.S. Patent 10,240,967,
Grant Date: March 26, 2019
Chandulal N. Bhatasana

Water Cut Sensor System
Granted Patent: U.S. Patent 10,241,059,
Grant Date: March 26, 2019
Muhammad Arsalan, Muhammad A. Karimi and Atif Shamim

Parallel Solution for Fully Coupled Fully Implicit Wellbore Modeling in Reservoir Simulation
Granted Patent: U.S. Patent 10,242,136,
Grant Date: March 26, 2019
Larry S. Fung

Extended Thermal Stage Sulfur Recovery Process
Granted Patent: U.S. Patent 10,246,329,
Grant Date: April 2, 2019
John P. O'Connell

Loss Circulation Compositions (LCM) Having Portland Cement Clinker
Granted Patent: U.S. Patent 10,246,626,
Grant Date: April 2, 2019
B. Raghava Reddy

Process to Produce Blown Asphalt
Granted Patent: U.S. Patent 10,246,642,
Grant Date: April 2, 2019
Mazin M. Fathi and Ki-Hyouk Choi

Process for Reducing the Total Acid Number in Refinery Feedstocks
Granted Patent: U.S. Patent 10,246,649,
Grant Date: April 2, 2019
Adnan Al-Hajji, Omer R. Koseoglu, Hendrik Muller and Hanadi Al-Jawad

Integrated Solvent Deasphalting, Hydrotreating and Steam Pyrolysis System for Direct Processing of a Crude Oil
Granted Patent: U.S. Patent 10,246,651,
Grant Date: April 2, 2019
Abdennour Bourane, Raheel Shafi, Essam Sayed, Ibrahim A. Abba and Abdul Rahman Zafer Akhras

Drilling Apparatus and Methods for Reducing Circulation Loss
Granted Patent: U.S. Patent 10,246,954,
Grant Date: April 2, 2019
Shaohua Zhou

Electric Submersible Pump Cable Anchored in Coiled Tubing
Granted Patent: U.S. Patent 10,246,960,
Grant Date: April 2, 2019
Randall Shepler and Jinjiang Xiao

Methods and Apparatus for Collecting and Preserving Core Samples from a Reservoir
Granted Patent: U.S. Patent 10,246,962,
Grant Date: April 2, 2019
Anuj Gupta, Daniel T. Georgi and Katherine L. Hull

Electric Submersible Pump with Ultrasound for Solid Buildup Removal
Granted Patent: U.S. Patent 10,246,977,
Grant Date: April 2, 2019
Jinjiang Xiao, Rafael A. Lastra and Randall Shepler

Directional Sensitive Fiber Optic Cable Wellbore System
Granted Patent: U.S. Patent 10,247,838,
Grant Date: April 2, 2019
Frode Hveding

Method for Measuring Formation Water Salinity from within a Borehole
Granted Patent: U.S. Patent 10,247,849,
Grant Date: April 2, 2019
Shouxiang M. Ma, Harold Pfutzner, Ronald E. Plasek, James A. Grau and Raghu Ramamoorthy

Determining Cumulative Water Flow on a Grid-by-Grid Basis in a Geocellular Earth Model
Granted Patent: U.S. Patent 10,248,743,
Grant Date: April 2, 2019
Ahmad Alhuthali and Mohamed Bouaouaja

Activation of Waste Metal Oxide as an Oxygen Carrier for Chemical Looping Combustion Applications
Granted Patent: U.S. Patent 10,252,243,
Grant Date: April 9, 2019
Bandar A. Fadhel, Zaki Yusuf, Ahmad D. Hammad, Ali Hoteit and Tobias Mattisson

High Temperature Layered Mixed Metal Oxide Materials with Enhanced Stability
Granted U.S. Patent 10,252,245,
Grant Date: April 9, 2019
Gasan Alabedi, John Hall, Manohara G. Veerabhadrappa and Hugh C. Greenwell

Catalyst to Attain Low Sulfur Gasoline
Granted Patent: U.S. Patent 10,252,247,
Grant Date: April 9, 2019
Ki-Hyouk Choi, Sameer A. Al-Ghamdi, Ali H. Al-Shareef and Ali H. Al-Hamadah

Auto Thermal Reforming (ATR) Catalytic Structures
Granted Patent: U.S. Patent 10,252,910,
Grant Date: April 9, 2019
Thang V. Pham, Sai P. Katikaneni, Jorge N. Beltramini, Moses O. Adebajo, Joao Carlos Diniz Da Costa and Gao Qing Lu

Auto Thermal Reforming (ATR) Catalytic Systems
Granted Patent: U.S. Patent 10,252,911,
Grant Date: April 9, 2019
Thang V. Pham, Sai P. Katikaneni, Jorge N. Beltramini, Moses O. Adebajo, Joao Carlos Diniz Da Costa and Gao Qing Lu

Process for Xylene Production with Energy Optimization
Granted Patent: U.S. Patent 10,252,958,
Grant Date: April 9, 2019
Qi Xu, Raed Abudawoud, Ahmad A. Jazzar and Zhonglin Zhang

Flash Point Adjustment of Wettability Alteration Chemicals in Hydrocarbon Solvents
Granted Patent: U.S. Patent 10,253,243,
Grant Date: April 9, 2019
Mohammed Ali Ibrahim Sayed and Ghaithan A. Al-Muntasheri

Method for Preventing Formation of Water-Oil Emulsions Using Additives
Granted Patent: U.S. Patent 10,253,245,
Grant Date: April 9, 2019
Remi Mahfouz, Aziz Fihri, Enrico Bovero, Abdullah A. Al-Shahrani, Haitham Aljahani, Abdullah S. Al-Ghamdi and Ihsan Al-Taie

Downhole Heat Orientation and Controlled Fracture Initiation Using Electromagnetic Assisted Ceramic Materials
Granted Patent: U.S. Patent 10,253,608,
Grant Date: April 9, 2019
Sameeh I. Batarseh and Victor Hilab

Downhole Oil/Water Separation System for Improved Injectivity and Reservoir Recovery
Granted Patent: U.S. Patent 10,253,610,
Grant Date: April 9, 2019
Brian A. Roth and Wessam A. Busfar

Determining Rock Properties
Granted Patent: U.S. Patent 10,254,207,
Grant Date: April 9, 2019
Hui-Hai Liu, Bitao Lai, Hui Li and Yanhui Han

Integrated ALMS KPIs with Plant Information System
Granted Patent: U.S. Patent 10,255,797,
Grant Date: April 9, 2019
Anwar R. Al-Odail and Ziyad M. Al-Yahya

Date Seed-Based Multimodal Particulate Admixture for Moderate to Severe Loss Control
Granted Patent: U.S. Patent 10,259,982,
Grant Date: April 16, 2019
Md. Amanullah

Settable, Form Filling Loss Circulation Control Compositions Comprising in Situ Foamed Calcium Aluminate Cement Systems and Method of Use
Granted Patent: U.S. Patent 10,259,985,
Grant Date: April 16, 2019
B. Raghava Reddy

Simultaneous Crude Oil Dehydration, Desalting, Sweetening, and Stabilization
Granted Patent: U.S. Patent 10,260,010,
Grant Date: April 16, 2019
Mohamed Soliman

Fuel Composition for GCI Engines and Method of Production
Granted Patent: U.S. Patent 10,260,015,
Grant Date: April 16, 2019
Gautam T. Kalghatgi, Christopher D. Gosling and Mary Wier

Mitigating Drilling Circulation Loss
Granted Patent: U.S. Patent 10,260,295,
Grant Date: April 16, 2019
Shaohua Zhou

Three-Dimensional Interactive Wellbore Model Simulation System
Granted Patent: U.S. Patent 10,260,318,
Grant Date: April 16, 2019
Imtiaz Ahmed

Downhole Separation Efficiency Technology to Produce Wells through a Dual Completion
Granted Patent: U.S. Patent 10,260,323,
Grant Date: April 16, 2019
Ahmad J. Al-Muraikhi and Ivan T. Cetkovic

Downhole Separation Efficiency Technology to Produce Wells through a Single String
Granted Patent: U.S. Patent 10,260,324,
Grant Date: April 16, 2019
Ahmad J. Al-Muraikhi and Ivan T. Cetkovic

Detecting a Tracer in a Hydrocarbon Reservoir
Granted Patent: U.S. Patent 10,261,216,
Grant Date: April 16, 2019
Shannon L. Eichmann, Sehoon Chang and Wei Wang

ARC Hybrid Particle Mix for Seal and Plug Quality Enhancement
Granted Patent: U.S. Patent 10,266,742,
Grant Date: April 23, 2019
Md. Amanullah, Mohammed K. Arfaj and Turki Alsubaie

Anti-Bit Balling Drilling Fluids and Methods of Making and Use Thereof
Granted Patent: U.S. Patent 10,266,745,
Grant Date: April 23, 2019
Abdullah S. Al-Yami, Ahmed A. Bahamdan, Saleh A. Haidary, Vikrant B. Wagle, Hussain Al-Bahrani, Ali M. Al-Safran, Nasser Al-Hareth and Abdulla H. Awadh

Plugging and Sealing Subterranean Formations
Granted Patent: U.S. Patent 10,266,748,
Grant Date: April 23, 2019
Rajendra A. Kalgaonkar, Vikrant B. Wagle, Abdullah S. Al-Yami and Jin Huang

Polymer Enhanced Surfactant Flooding for Permeable Carbonates
Granted Patent: U.S. Patent 10,266,752,
Grant Date: April 23, 2019
Ming Han, Ali A. Al-Yousif, Alhasan B. Fuseni and Salah H. Al-Saleh

Generating Subterranean Imaging Data Based on Vertical Seismic Profile Data and Ocean Bottom Sensor Data
Granted Patent: U.S. Patent 10,267,937,
Grant Date: April 23, 2019
Leon Liang Zie Hu

3D Blending and Illumination of Seismic Volumes for Automatic Derivation of Discontinuities
Granted Patent: U.S. Patent 10,267,938,
Grant Date: April 23, 2019
Andrew M. Morton and Roger R. Sung

Monitoring Hydrocarbon Reservoirs Using Induced Polarization Effect
Granted Patent: U.S. Patent 10,267,943,
Grant Date: April 23, 2019
Alberto F. Marsala, Michael S. Zhdanov and Vladimir Burtman

Cross-linked Polymeric Blended Membranes for Gas Separation
Granted Patent: U.S. Patent 10,272,394,
Grant Date: April 30, 2019
John Yang and Daniel Harrigan

Mesoporous Zeolites and Methods for the Synthesis Thereof
Granted Patent: U.S. Patent 10,272,418,
Grant Date: April 30, 2019
Tatiana Pilyugina

Underwater Vehicles and Inspection Methods
Granted Patent: U.S. Patent 10,272,980,
Grant Date: April 30, 2019
Fadl H. Abdel Latif, Ali Outa, Sahejad Patel, Ayman Amer and Hassane Trigui

Polysaccharide Coated Nanoparticle Compositions Comprising Ions
Granted Patent: U.S. Patent 10,273,399,
Grant Date: April 30, 2019
Jason Cox, Hooisweng Ow, Howard K. Schmidt and Shannon Eichmann

System and Method for Image Processing and Feature Recognition
Granted Patent: U.S. Patent 10,275,871,
Grant Date: April 30, 2019
Enrico Bovero

Self-Powered Pipeline Hydrate Prevention System
Granted Patent: U.S. Patent 10,277,094,
Grant Date: April 30, 2019
Sameeh I. Batarseh, Nabeel Habib and Talha J. Ahmad

Process for Selective Ethylene Oligomerization with Antifouling Components
Granted Patent: U.S. Patent 10,280,125,
Grant Date: May 7, 2019
Sohel Shaikh, Zhonglin Zhang, Wei Xu, Yohei Kashiwame and Kenji Sogo

Sealing an Undesirable Formation Zone in the Wall of a Wellbore
Granted Patent: U.S. Patent 10,280,705,
Grant Date: May 7, 2019
Alwaleed A. Al-Gouhi and Nabil S. Alkhanaifer

Sampling Techniques to Detect Hydrocarbon Seepage
Granted Patent: U.S. Patent 10,280,747,
Grant Date: May 7, 2019
Mahdi AbuAli, Maher Marhoon and Khaled Arouri

Flow Distribution Device and Method
Granted Patent: U.S. Patent 10,280,772,
Grant Date: May 7, 2019
Farooq N. Al-Jwesm

Apparatus and Method for Oxy-Combustion of Fuels in Internal Combustion Engines
Granted Patent: U.S. Patent 10,280,877,
Grant Date: May 7, 2019
Wajdi Al-Sadat and Esam Hamad

Opto-Mechanical Part for Parabolic Mirror Fine Rotation and On-Axis Linear Positioning
Granted Patent: U.S. Patent 10,281,401,
Grant Date: May 7, 2019
Ezzat M. Hegazi, Vincent Cunningham, Christoph Stamm and Christof Brunner

Nano-Level Evaluation of Kerogen-Rich Reservoir Rock
Granted Patent: U.S. Patent 10,281,413,
Grant Date: May 7, 2019
Katherine L. Hull, Younane N. Abousleiman and Sebastian Csutak

Determining the Deterioration of Oils Using Fluorescence Rise-Time
Granted Patent: U.S. Patent 10,281,448,
Grant Date: May 7, 2019
Ezzat M. Hegazi, Vincent Cunningham and Maha Nour

Method and System for Combined Hydrogen and Electricity Production Using Petroleum Fuels
Granted Patent: U.S. Patent 10,283,795,
Grant Date: May 7, 2019
Aqil Jamal and Thang V. Pham

Method of Reducing Drag in a Conduit
Granted Patent: U.S. Patent 10,287,374,
Grant Date: May 14, 2019
Faisal M. Al-Thenayan, Abdullah R. Al-Malki, Wei Xu, Muhammed Atiqullah, Abdel Salam Al-Sarkhi and Anwar Hossaen

Compositions, Containing Thermoplastics Based on Polyvinyl Chloride and Containing Cross-Linked NBR Microgels Modified with Hydroxyl Groups
Granted Patent: U.S. Patent 10,287,425,
Grant Date: May 14, 2019
Torsten Ziser, Harald Kleinknecht and Lars Wawrzinski

Cement Slurries, Cured Cements and Methods of Making and Use Thereof
Granted Patent: U.S. Patent 10,287,476,
Grant Date: May 14, 2019
Abdullah S. Al-Yami, Hussain Al-Bahrani, Vikrant B. Wagle and Ali Al-Safran

Dispersant in Cement Formulations for Oil and Gas Wells
Granted Patent: U.S. Patent 10,287,477,
Grant Date: May 14, 2019
Abdullah S. Al-Yami, Hussain Al-Bahrani, Vikrant B. Wagle and Ali Al-Safran

Loss Circulation Compositions (LCM) Having Portland Cement Clinker
Granted Patent: U.S. Patent 10,287,479,
Grant Date: May 14, 2019
B. Raghava Reddy

Settable, Form Filling Loss Circulation Control Compositions Comprising in Situ Foamed Non-hydraulic Sorel Cement Systems and Method of Use
Granted Patent: U.S. Patent 10,287,480,
Grant Date: May 14, 2019
B. Raghava Reddy

Settable, Form Filling Loss Circulation Control Compositions Comprising in Situ Foamed Non-hydraulic Sorel Cement Systems and Method of Use
Granted Patent: U.S. Patent 10,287,481,
Grant Date: May 14, 2019
B. Raghava Reddy

Oil Recovery Process Using an Oil Recovery Composition of Aqueous Salt Solution and Dilute Polymer for Carbonate Reservoirs
Granted Patent: U.S. Patent 10,287,485,
Grant Date: May 14, 2019
Subhash C. Ayirala, Abdulkareem M. Sofi and Ali A. Yousef

Oil Recovery Process Using an Oil Recovery Composition of Aqueous Salt Solution and Dilute Polymer for Carbonate Reservoirs
Granted Patent: U.S. Patent 10,287,486,
Grant Date: May 14, 2019
Subhash C. Ayirala, Abdulkareem M. Sofi and Ali A. Yousef

Well Debris Handling System
Granted Patent: U.S. Patent 10,287,853,
Grant Date: May 14, 2019
Chidirim E. Ejim and Jinjiang Xiao

Interrogating Subterranean Hydraulic Fractures Using Magnetoelastic Resonators
Granted Patent: U.S. Patent 10,287,877,
Grant Date: May 14, 2019
Mazen Y. Kanj, Howard K. Schmidt, Yogesh Gianchandani, Scott Green, Kamal Sarabandi, Jun Tang and Jiangfeng Wu

Automatic Pumping Control for Leakoff Tests
Granted Patent: U.S. Patent 10,287,878,
Grant Date: May 14, 2019
Hermann F. Spoerker

Absolute Porosity and Pore Size Determination of Pore Types in Media with Varying Pore Sizes
Granted Patent: U.S. Patent 10,288,571,
Grant Date: May 14, 2019
Hyung T. Kwak, Ali A. Yousif and Salah H. Saleh

Method and Apparatus for Injecting Current over an Electrical Conductor
Granted Patent: U.S. Patent 10,288,663,
Grant Date: May 14, 2019
Saad M. Al-Shammari and Muruganandham Shanmuganathan

Seismic Processing Workflow for Broadband Single-Sensor Single-Source Land Seismic Data
Granted Patent: U.S. Patent 10,288,755,
Grant Date: May 14, 2019
Simon Cordery

Electrical Submersible Pump Monitoring and Failure Prediction
Granted Patent: U.S. Patent 10,288,760,
Grant Date: May 14, 2019
Mohamed N. Noui-Mehidi and Ahmed Y. Bukhamseen

Auto-Generation of Map Landmarks Using Sensor Readable Tags
Granted Patent: U.S. Patent 10,290,137,
Grant Date: May 14, 2019
Hussain M. Al-Nasser and Mahdi Abalharth

Modified Siloxane Composite Membranes for Heavy Hydrocarbon Recovery
Granted Patent: U.S. Patent 10,293,301,
Grant Date: May 21, 2019
John Yang, Veera Venkata R. Tammana, Daniel Harrigan and Milind M. Vaidya

Hydrocracking Catalyst for Hydrocarbon Oil, Method for Producing Hydrocracking Catalyst, and Method for Hydrocracking Hydrocarbon Oil with Hydrocracking Catalyst
Granted Patent: U.S. Patent 10,293,332,
Grant Date: May 21, 2019
Omer R. Koseoglu, Adnan Al-Hajji, Ali Mahmood Al-Somali, Ali H. Al-Abdulal, Mishaal Al-Thukair, Masaru Ushio, Ryuzo Kuroda, Takashi Kameoka, Kouji Nakano and Yuichi Takamori

Systems and Processes for Recovery of Light Alkyl Mono-Aromatic Compounds from Heavy Alkyl Aromatic and Alkyl Bridged Noncondensed Alkyl Aromatic Compounds
Granted Patent: U.S. Patent 10,294,172,
Grant Date: May 21, 2019
Bruce R. Beadle, Vinod Ramaseshan, Rankan S. Bilaus, Omer R. Koseoglu and Robert P. Hodgkins

Integrated System for Quantitative Real-Time Monitoring of Hydrogen-Induced Cracking in Simulated Sour Environment
Granted Patent: U.S. Patent 10,295,508,
Grant Date: May 21, 2019
Abderrazak Traidia, Abdelmounam Sherik and Arnold Lewis

Generating Common Image Gather Using Wave-Field Separation
Granted Patent: U.S. Patent 10,295,685,
Grant Date: May 21, 2019
Dongliang Zhang, Tong Wang Fei and Yi Luo

Quantifying Geologic Growth History of Subsurface Oil Field Structures Based on Structural Growth Indications
Granted Patent: U.S. Patent 10,295,686,
Grant Date: May 21, 2019
Schuman Wu

Parallel Reservoir Simulation with Accelerated Aquifer Calculation
Granted Patent: U.S. Patent 10,296,684,
Grant Date: May 21, 2019
Larry S. Fung and Shouhong Du

Ground Particulate Spent Claus Catalyst Product
Granted Patent: U.S. Patent 10,301,216,
Grant Date: May 28, 2019
Mansour A. Al-Shafei

Catalyst Composition for Making Ultra High Molecular Weight Poly (Alpha-Olefin) Drag Reducing Agents
Granted Patent: U.S. Patent 10,301,410,
Grant Date: May 28, 2019
Faisal M. Al-Thenayan, Abdullah R. Al-Malki, Wei Xu, Anwar Hossaen, Muhammed Atiqullah and Abdel Salam Al-Sarkhi

Polycarbonate Polyol Compositions and Methods
Granted Patent: U.S. Patent 10,301,426,
Grant Date: May 28, 2019
Geoffrey W. Coates, Chris A. Simoneau, Scott D. Allen, Anna E. Cherian, Jay J. Farmer and Alexei A. Gridnev

Invert Emulsion Drilling Fluids
Granted Patent: U.S. Patent 10,301,525,
Grant Date: May 28, 2019
Vikrant B. Wagle and Abdullah S. Al-Yami

Loss Circulation Compositions (LCM) Having Portland Cement Clinker
Granted Patent: U.S. Patent 10,301,529,
Grant Date: May 28, 2019
B. Raghava Reddy

Systems and Methods for the Conversion of Feedstock Hydrocarbons to Petrochemical Products
Granted Patent: U.S. Patent 10,301,556,
Grant Date: May 28, 2019
Sameer A. Al-Ghamdi, Essam Al-Sayed, Ibrahim A. Abba, Abdennour Bourane and Alberto L. Ballesteros

Kalina Cycle-Based Conversion of Gas Processing Plant Waste Heat into Power
Granted Patent: U.S. Patent 10,301,977,
Grant Date: May 28, 2019
Mahmoud B. Noureldin and Akram H. Kamel

Adsorbed Natural Gas Storage Facility
Granted Patent: U.S. Patent 10,302,254,
Grant Date: May 28, 2019
Yuguo Wang, Cemal Ercan, Mohammed G. Hashim, Anwar H. Khawajah and Rashid M. Othman

Distributed Industrial Facility Safety System Modular Remote Sensing Devices
Granted Patent: U.S. Patent 10,303,147,
Grant Date: May 28, 2019
Mohammed Al-Juaid and Mohammed Makhdoum

Front-Heavy Dust Cleaning Vehicle
Granted Patent: U.S. Patent 10,305,420,
Grant Date: May 28, 2019
Brian J. Parrott, Pablo Carrasco Zanini and Ali AlShehri

Chair Pad System and Associated, Computer Medium and Computer Implemented Methods for Monitoring and Improving Health and Productivity of Employees
Granted Patent: U.S. Patent 10,307,104,
Grant Date: June 4, 2019
Samantha J. Horseman

Process for Maximizing Xylenes Production from Heavy Aromatics for Use Therein
Granted Patent: U.S. Patent 10,308,573,
Grant Date: June 4, 2019
Raed Abudawoud, Zhonglin Zhang, Qi Xu and Ahmad A. Jazzar

Aliphatic Polycarbonate Polyol Compositions
Granted Patent: U.S. Patent 10,308,759,
Grant Date: June 4, 2019
Chris A. Simoneau

Methods for Polymer Synthesis
Granted Patent: U.S. Patent 10,308,761,
Grant Date: June 4, 2019
Scott D. Allen, Jeffrey R. Conuel, Chris A. Simoneau and William D. Keefe

Compositions and Methods for Enhanced Fracture Cleanup Using Redox Treatment
Granted Patent: U.S. Patent 10,308,862,
Grant Date: June 4, 2019
Ayman R. Nakhli, Hazim H. Abass and Ahmed S. Otaibi

Polysaccharide Coated Nanoparticle Compositions Comprising Ions
Granted Patent: U.S. Patent 10,308,865,
Grant Date: June 4, 2019
Jason R. Cox, Hooisweng Ow, Howard K. Schmidt and Shannon L. Eichmann

Nonsolvent Asphaltene Removal from Crude Oil Using Solid Heteropoly Compounds
Granted Patent: U.S. Patent 10,308,880,
Grant Date: June 4, 2019
Miao Sun, Faisal M. Melebari and Mohammed Al-Daous

Processing Geophysical Data Using 3D Norm-Zero Optimization for Smoothing Geophysical Inversion Data
Granted Patent: U.S. Patent 10,310,112,
Grant Date: June 4, 2019
Saleh A. Dossary and Jinsong Wang

Electrical Submersible Pump Monitoring and Failure Prediction
Granted Patent: U.S. Patent 10,310,128,
Grant Date: June 4, 2019
Mohamed N. Noui-Mehidi and Ahmed Y. Bukhamseen

Distributed Industrial Facility Safety System
Granted Patent: U.S. Patent 10,311,705,
Grant Date: June 4, 2019
Mohammed Al-Juaid and Mohammed Makhdoum

Catalyst System
Granted Patent: U.S. Patent 10,316,113,
Grant Date: June 11, 2019
Alexandra Berthoud, Gerardus H.J. van Doremaele, Richard T.W. Scott, Francisco Perez and Raffaele Bernardo

Nanosilica Dispersion for Thermally Insulating Packer Fluid
Granted Patent: U.S. Patent 10,316,238,
Grant Date: June 11, 2019
Vikrant B. Wagle, Abdullah S. Al-Yami, Zainab Alsaihati and Abdulaziz Alhelal

Systems and Methods for Stage Cementing
Granted Patent: U.S. Patent 10,316,619,
Grant Date: June 11, 2019
Victor Costa de Oliveira, Rodny B. Masoud, Khaled K. Abouelnaaj and Dean S. Porter

Multilateral Well Drilled with Underbalanced Coiled Tubing and Stimulated with Exothermic Reactants
Granted Patent: U.S. Patent 10,316,637,
Grant Date: June 11, 2019
Abdulrahman Al-Mulhem

Deployment Mechanism for Passive Normalization of a Probe Relative to a Surface
Granted Patent: U.S. Patent 10,317,372,
Grant Date: June 11, 2019
Pablo Carrasco Zanini, Fadl H. Abdel Latif, Sahejad Patel, Shigeo Hirose, Michele Guanieri and Paulo Debenest

Characterizing Lubricant Oil Degradation Using Fluorescence Signals
Granted Patent: U.S. Patent 10,317,388,
Grant Date: June 11, 2019
Ezzat M. Hegazi, Vincent Cunningham and Maha Nour

Method and Device for Measuring Fluid Properties Using an Electromechanical Resonator
Granted Patent: U.S. Patent 10,317,557,
Grant Date: June 11, 2019
Miguel Gonzalez, Max Deffenbaugh, Huseyin Seren and Sebastian Csutak

EMU Impulse Antenna
Granted Patent: U.S. Patent 10,317,558,
Grant Date: June 11, 2019
Howard K. Schmidt, Jesus M. Felix-Servin, Erika S. Ellis, Mazen Y. Kanj and Abdullah Al Shehri

High Temperature, Self-Powered, Miniature Mobile Device
Granted Patent: U.S. Patent 10,320,311,
Grant Date: June 11, 2019
Chinthaka P. Gooneratne, Bodong Li and Shaohua Zhou

Hybrid Particle Mix for Seal and Plug Quality Enhancement
Granted Patent: U.S. Patent 10,323,170,
Grant Date: June 18, 2019
Md. Amanullah, Mohammed K. Arfaj and Turki T. Alsubaie

Loss Circulation Compositions (LCM) Having Portland Cement Clinker
Granted Patent: U.S. Patent 10,323,171,
Grant Date: June 18, 2019
B. Raghava Reddy

Loss Circulation Compositions (LCM) Having Portland Cement Clinker
Granted Patent: U.S. Patent 10,323,172,
Grant Date: June 18, 2019
B. Raghava Reddy

Wellbore Drill Bit Nozzle

Granted Patent: U.S. Patent 10,323,464,
Grant Date: June 18, 2019
Ahmad M. Al-Abduljabbar

Rock Sample Preparation Method by Using Focused Ion Beam for Minimizing Curtain Effect

Granted Patent: U.S. Patent 10,324,049,
Grant Date: June 18, 2019
Dong Kyu Cha, Sultan Enezi, Mohammed Al Otaibi and Ali Abdallah Al-Yousef

Systems and Methods for Real-Time Spectrophotometric Quantification of Crude Oil

Granted Patent: U.S. Patent 10,324,077,
Grant Date: June 18, 2019
Dmitry Kosynkin and Mohammed Al-Askar

Systems, Methods, and Apparatuses for Downhole Lateral Detection Using Electromagnetic Sensors

Granted Patent: U.S. Patent 10,324,221,
Grant Date: June 18, 2019
Muhammad Arsalan, Talha J. Ahmad and Mohamed N. Noui-Mehidi

Metal Organic Framework Absorbent Platforms for Removal of CO_2 and H_2S from Natural Gas

Granted Patent: U.S. Patent 10,328,380,
Grant Date: June 25, 2019
Mohamed Eddaoudi, Amandine Cadiau, Prashant M. Bhatt, Karim Adil and Youssef Belmabkhout

Dual Catalyst Processes and Systems for Propylene Production

Granted Patent: U.S. Patent 10,329,225,
Grant Date: June 25, 2019
Munir D. Khokhar, Faisal H. Alshafei, Noor A. Sulais, Sohel Shaikh and Raed Abudawoud

Hybrid Particle Mix for Seal and Plug Quality Enhancement

Granted Patent: U.S. Patent 10,329,470,
Grant Date: June 25, 2019
Md. Amanullah, Mohammed K. Arfaj and Turki T. Alsubaie

Loss Circulation Compositions (LCM) Having Portland Cement Clinker

Granted Patent: U.S. Patent 10,329,473,
Grant Date: June 25, 2019
B. Raghava Reddy

High Temperature Fracturing Fluids with Nano-Crosslinkers

Granted Patent: U.S. Patent 10,329,475,
Grant Date: June 25, 2019
Ghaithan A. Al-Muntasheri, Feng Liang, Hooisweng Ow, Jason Cox and Martin E. Poitzsch

Dual-Phase Acid-Based Fracturing Composition with Corrosion Inhibitors and Method of Use Thereof

Granted Patent: U.S. Patent 10,329,477,
Grant Date: June 25, 2019
Saleh H. Al-Mutairi, Yaser K. Al-Duailej, Ibrahim S. Al-Yami, Abdullah M. Al-Hajri and Hameed Al-Badairy

Integrated Hydrotreating and Steam Pyrolysis System including Hydrogen Redistribution for Direct Processing of a Crude Oil

Granted Patent: U.S. Patent 10,329,499,
Grant Date: June 25, 2019
Raheel Shafi, Abdennour Bourane, Essam Sayed, Ibrahim A. Abba and Abdul Rahman Zafer Akhras

Entropy-Based Multiphase Flow Detection

Granted Patent: U.S. Patent 10,329,902,
Grant Date: June 25, 2019
Talha J. Ahmad, Michael J. Black, Muhammad Arsalan and Mohamed N. Noui-Mehidi

Utilizing Clean Gas to Reliably Operate Main and Pilot Relief Valve

Granted Patent: U.S. Patent 10,330,210,
Grant Date: June 25, 2019
Mohammed A. Al-Qahtani

Alternating Magnetic Field Flow Meters

Granted Patent: U.S. Patent 10,330,511,
Grant Date: June 25, 2019
Fouad M. Alkhabbaz, Maatoug Al-Maatoug and Luay H. Al-Awami

Determining Structural Tomographic Properties of a Geologic Formation

Granted Patent: U.S. Patent 10,330,526,
Grant Date: June 25, 2019
Howard K. Schmidt, Jesus M. Felix-Servin, Frode Hveding and Daniele Colombo

Electrical Submersible Pump Monitoring and Failure Prediction

Granted Patent: U.S. Patent 10,330,811,
Grant Date: June 25, 2019
Mohamed N. Noui-Mehidi and Ahmed Y. Bukhamseen

EMU Impulse Antenna for Low Frequency Radio Waves Using Giant Dielectric and Ferrite Materials

Granted Patent: U.S. Patent 10,330,815,
Grant Date: June 25, 2019
Erika S. Ellis, Howard K. Schmidt and Jesus M. Felix-Servin

Date Tree Waste-Based Binary Fibrous Mix for Moderate to Severe Loss Control

Granted Patent: U.S. Patent 10,336,930,
Grant Date: July 2, 2019
Md. Amanullah

Systems, Methods, and Apparatuses for Downhole Lateral Detection Using Electromagnetic Sensors

Granted Patent: U.S. Patent 10,337,293,
Grant Date: July 2, 2019
Muhammad Arsalan, Talha J. Ahmad and Mohamed N. Noui-Mehidi

In Situ Replacement of Fluids in a Well Tool

Granted Patent: U.S. Patent 10,337,302,
Grant Date: July 2, 2019
Brian A. Roth, Jinjiang Xiao and Rafael A. Lastra

In Situ Steam Quality Enhancement Using Microwave with Enabler Ceramics for Downhole Applications

Granted Patent: U.S. Patent 10,337,306,
Grant Date: July 2, 2019
Sameeh I. Batarseh

Electrical Submersible Pumping System with Separator

Granted Patent: U.S. Patent 10,337,312,
Grant Date: July 2, 2019
Jinjiang Xiao and Chidirim Enoch Ejim

Estimating Formation Properties Using Saturation Profiles

Granted Patent: U.S. Patent 10,338,014,
Grant Date: July 2, 2019
Ahmad M. Al Harbi, Hyung T. Kwak and Jun Gao

EMU Impulse Antenna with Controlled Directionality and Improved Impedance Matching

Granted Patent: U.S. Patent 10,338,264,
Grant Date: July 2, 2019
Howard K. Schmidt, Jesus M. Felix-Servin and Erika S. Ellis

EMU Impulse Antenna for Low Frequency Radio Waves Using Giant Dielectric and Ferrite Materials

Granted Patent: U.S. Patent 10,338,266,
Grant Date: July 2, 2019
Erika S. Ellis, Howard K. Schmidt and Jesus M. Felix-Servin

High Accuracy Remote Coordinate Machine

Granted Patent: U.S. Patent 10,338,592,
Grant Date: July 2, 2019
Fadl H. Abdel Latif and Pablo Carrasco

Mobile Device Attendance Verification

Granted Patent: U.S. Patent 10,339,733,
Grant Date: July 2, 2019
Raed A. Al-Shaikh, Sadiq S. Mohammed and Muyeed A. Shariff

Underwater Marine Growth Brushing Mechanism with Passive Self-Adjust for Curved Surfaces

Granted Patent: U.S. Patent 10,342,326,
Grant Date: July 9, 2019
Ali Outa, Ayman Amer, Sahejad Patel, Hassane Trigui, Ameen Obedan and Fadl H. Abdel Latif

Systems and Methods for Monitoring and Optimizing Flare Purge Gas with a Wireless Rotameter

Granted Patent: U.S. Patent 10,343,195,
Grant Date: July 9, 2019
Selvam Daniel

Compact Magnetic Crawler Vehicle with Anti-Rocking Supports

Granted Patent: U.S. Patent 10,343,276,
Grant Date: July 9, 2019
Pablo Carrasco, Fadl H. Abdel Latif, Abdullah Arab and Brian J. Parrott

N-hydroxyalkylated Polyamines, Methods of Making N-hydroxyalkylatedpolyamines, and Fluids Containing an N-hydroxyalkylated Polyamine

Granted Patent: U.S. Patent 10,343,976,
Grant Date: July 9, 2019
Matthew Hilfiger and B. Raghava Reddy

Methods and Compositions for in Situ Polymerization Reaction to Improve Shale Inhibition

Granted Patent: U.S. Patent 10,344,198,
Grant Date: July 9, 2019
Abeer M. Al-Olayan

Stabilized Nanoparticle Compositions Comprising Ions
Granted Patent: U.S. Patent 10,344,202, Grant Date: July 9, 2019
Jason R. Cox, Hooisweng Ow and Dmitry Kosynkin

Tank Dewatering Sensing and Valve Control Method and Apparatus
Granted Patent: U.S. Patent 10,344,221, Grant Date: July 9, 2019
Khalid A. Al-Mulhim and Salem M. Al-Qahtani

Integrated Hydrotreating and Steam Pyrolysis System including Residual Bypass for Direct Processing of a Crude Oil
Granted Patent: U.S. Patent 10,344,227, Grant Date: July 9, 2019,
Raheel Shafi, Abdennour Bourane, Esam Sayed, Ibrahim A. Abba and Abdul-Rahman Z. Akhras

Supercritical Water Upgrading Process to Produce High Grade Coke
Granted Patent: U.S. Patent 10,344,228, Grant Date: July 9, 2019
Ki-Hyouk Choi, Mohammed A. Alabdullah, Emad N. Al-Shafei, Massad S. Alanzi, Bandar K. Alotaibi, Bandar H. Alsolami and Ali M. Alsomali

Method of Conversion of a Drilling Mud to a Gel-Based Lost Circulation Material to Combat Lost Circulation during Continuous Drilling
Granted Patent: U.S. Patent 10,344,545, Grant Date: July 9, 2019
Md. Amanullah, Turki T. Alsubaie, Abdulaziz S. Bubshait and Omar A. Fuwaires

Apparatus and Method for Producing Oil and Gas Using Buoyancy Effect
Granted Patent: U.S. Patent 10,344,572, Grant Date: July 9, 2019
Mari H. Alqahtani

Systems and Methods for Transient Pressure Testing of Water Injection Wells to Determine Reservoir Damages
Granted Patent: U.S. Patent 10,344,584, Grant Date: July 9, 2019
Noor M. Anisur Rahman and Saud A. Bin Akresh

Polymeric Tracers
Granted Patent: U.S. Patent 10,344,588, Grant Date: July 9, 2019
Jason R. Cox

Systems, Methods and Apparatuses for Downhole Lateral Detection Using Electromagnetic Sensors
Granted Patent: U.S. Patent 10,344,589, Grant Date: July 9, 2019
Muhammad Arsalan, Talha J. Ahmad and Mohamed N. Noui-Mehidi

Characterization of an Aromaticity Value of Crude Oil by Ultraviolet Visible Spectroscopy
Granted Patent: U.S. Patent 10,345,285, Grant Date: July 9, 2019
Omer R. Koseoglu, Adnan Al-Hajji and Gordon Jamieson

Environment Aware Cross-Layer Communication Protocol in Underground Oil Reservoirs
Granted Patent: U.S. Patent 10,349,249, Grant Date: July 9, 2019
Howard K. Schmidt, Abdallah A. Al-Shehri, Ian F. Akyildiz and Shih-Chun Lin

Dynamic Demulsification System for Use in a Gas-Oil Separation Plant
Granted Patent: U.S. Patent 10,350,515, Grant Date: July 16, 2019
Emad N. Al-Shafei and Rashid Khan

Methods for Synthesizing Hierarchical Zeolites for Catalytic Cracking
Granted Patent: U.S. Patent 10,350,585, Grant Date: July 16, 2019
Mansour Al-Herz, Muased S. Al-Ghrami, Rabindran J. Balasamy, Mohammed A. Siddiqui and Mian R. Saeed

Polymer Compositions and Methods
Granted Patent: U.S. Patent 10,351,654, Grant Date: July 16, 2019
Wayne R. Willkomm and Scott D. Allen

Drilling Fluid Compositions with Enhanced Rheology and Methods of Using Same
Granted Patent: U.S. Patent 10,351,750, Grant Date: July 16, 2019
Hussain Al-Bahrani, Abdullah S. Al-Yami, Ali M. Al-Safran and Abdulaziz Alhelal

Compositions and Methods for Sealing off Flow Channels in Contact with Set Cement
Granted Patent: U.S. Patent 10,351,752, Grant Date: July 16, 2019
B. Raghava Reddy and Matthew Hilfiger

Cement Compositions Comprising Aqueous Latex Containing Dispersed Solid and Liquid Elastomer Phases
Granted Patent: U.S. Patent 10,351,754, Grant Date: July 16, 2019
B. Raghava Reddy

Loss Circulation Material Composition Having Alkaline Nanoparticle-Based Dispersion and Water Insoluble Hydrolysable Polyester
Granted Patent: U.S. Patent 10,351,755, Grant Date: July 16, 2019
Vikrant B. Wagle, Rajendra A. Kalgaonkar, Abdullah S. Al-Yami and Zainab Alsaihati

Treatment of Kerogen in Subterranean Formations
Granted Patent: U.S. Patent 10,351,758, Grant Date: July 16, 2019
Katherine L. Hull, Younane N. Abousleiman, Ghaithan A. Al-Muntasheri and David Jacobi

Interfacial Tension Reduction and Wettability Alteration Using Metal Oxide Nanoparticles to Reduce Condensate Banking
Granted Patent: U.S. Patent 10,351,763, Grant Date: July 16, 2019
Ayman M. Almohsin, Mohammed A. Bataweel and Eyad Alai

Integrated Isomerization and Hydrotreating Apparatus
Granted Patent: U.S. Patent 10,351,785, Grant Date: July 16, 2019
Omer R. Koseoglu

Self-Installing Offshore Platform
Granted Patent: U.S. Patent 10,352,010, Grant Date: July 16, 2019
Rabih A. Khodr

ARC Perm-Squeeze RDF — A Permeable Plug Forming Rapidly Dehydrating Fluid
Granted Patent: U.S. Patent 10,352,116, Grant Date: July 16, 2019
Md. Amanullah

Apparatus and Method for Producing Oil and Gas Using Buoyancy Effect
Granted Patent: U.S. Patent 10,352,135, Grant Date: July 16, 2019
Mari H. Alqahtani

Petrophysically Regularized Time Domain NMR Inversion
Granted Patent: U.S. Patent 10,353,107, Grant Date: July 16, 2019
Ramsin Eyvazzadeh, Edward A. Clerke, Johannes J. Buiting, Paul Smith, Jim Funk, David F. Allen, George Bordakov, Steve F. Crary and Philip Savundararaj

Catalyst for Fluidization Catalytic Cracking and Method for Fluidized Catalytic Cracking
Granted Patent: U.S. Patent 10,357,761, Grant Date: July 23, 2019
Omer R. Koseoglu, Bandar Hussain, Masaru Ushio and Seiji Arakawa

Advanced Heat Integration in Sulfur Recovery Unit — SafarClaus
Granted Patent: U.S. Patent 10,358,349, Grant Date: July 23, 2019
Yazeed S. Al-Shahrani

Swellable Seals for Well Tubing
Granted Patent: U.S. Patent 10,358,888, Grant Date: July 23, 2019
Ahmad M. Al-Abduljabbar and Kamal E. Aghazada

Synthetic Sweet Spots in Tight Formations by Injection of Nano-Encapsulated Reactants
Granted Patent: U.S. Patent 10,358,902, Grant Date: July 23, 2019
Abdulrahman A. Al-Mulhem and Hazim H. Abass

Generating Dynamically Calibrated Geo-Models in Green Fields
Granted Patent: U.S. Patent 10,359,542, Grant Date: July 23, 2019
Babatope Kayode and Faisal Al-Thawad

Methods for Making Catalyst Systems
Granted Patent: U.S. Patent 10,363,547, Grant Date: July 30, 2019
Mohammed Al-Daous

Stage Cementing Tool
Granted Patent: U.S. Patent 10,364,644, Grant Date: July 30, 2019
Shaohua Zhou

Automatic Control of Production and Injection Wells in a Hydrocarbon Field
Granted Patent: U.S. Patent 10,364,655, Grant Date: July 30, 2019
Kalpesh Patel, Rohit Patwardhan, Fouad Saif and Hussain Salloum

Automated Pipeline Pig Handling System
Granted Patent: U.S. Patent 10,364,930, Grant Date: July 30, 2019
Pablo D. Genta

Method for Determining Unconventional Liquid Imbibition in Low Permeability Materials

Granted Patent: U.S. Patent 10,365,200,
Grant Date: July 30, 2019
Hui-Hai Liu, Bitao Lai and JinHong Chen

Giant Dielectric Nanoparticles as High Contrast Agents for Electromagnetic (EM) Fluids Imaging in an Oil Reservoir

Granted Patent: U.S. Patent 10,365,393,
Grant Date: July 30, 2019
Erika S. Ellis, Howard K. Schmidt and Jesus M. Felix-Servin

Directional Sensitive Fiber Optic Cable Wellbore System

Granted Patent: U.S. Patent 10,365,537,
Grant Date: July 30, 2019
Damian P. San Roman Alerigi and Frode Hveding

Calcite Channel Nanofluidics

Granted Patent: U.S. Patent 10,365,564,
Grant Date: July 30, 2019
Dong-Kyu Cha, Mohammed Al-Otaibi and Ali A. Al-Yousef

Harvesting Energy from Fluid Flow

Granted Patent: U.S. Patent 10,367,434,
Grant Date: July 30, 2019
Talha J. Ahmad, Muhammad Arsalan, Michael J. Black and Mohamed N. Noui-Mehidi

Process for Oxidative Desulfurization with Integrated Sulfone Decomposition

Granted Patent: U.S. Patent 10,369,546,
Grant Date: August 6, 2019
Omer R. Koseoglu and Abdennour Bourane

Reusable Buoyancy Modules for Buoyancy Control of Underwater Vehicles

Granted Patent: U.S. Patent 10,369,705,
Grant Date: August 6, 2019
Ali H. Outa, Fadl H. Abdel Latif, Sahejad Patel and Hassane Trigui

Ethylene Copolymerisates Having Improved Low Temperature Properties and Good Oil Resistance, Vulcanizable Mixtures Made Therefrom and Vulcanizates

Granted Patent: U.S. Patent 10,370,472,
Grant Date: August 6, 2019
Susanna Lieber, Olaf Isenberg-Schulz, Ulrich Frenzel and Rainer Kalkofen

Method of Encapsulating Signaling Agents for Use Downhole

Granted Patent: U.S. Patent 10,370,578,
Grant Date: August 6, 2019
Elizabeth Q. Contreras

Methods and Systems for Optimizing Demulsifier and Wash Water Injection Rates in Gas-Oil Separation Plants

Granted Patent: U.S. Patent 10,370,599,
Grant Date: August 6, 2019
Samusideen Salu, Mohamed Soliman and Talal A. Zahrani

Method and Composition for Contemporaneously Dimerizing and Hydrating a Feed Having Butene to Produce a Gasoline Composition

Granted Patent: U.S. Patent 10,370,612,
Grant Date: August 6, 2019
Wei Xu, Thamer A. Mohammad, Aadesh Harale and Kareemuddin M. Shaik

Apparatus and Method to Contain Flange, Pipe and Valve Leaks

Granted Patent: U.S. Patent 10,370,926,
Grant Date: August 6, 2019
Mohammad S. Al-Badran

Well Control Using a Modified Liner Tieback

Granted Patent: U.S. Patent 10,370,943,
Grant Date: August 6, 2019
Mohamed M. El-Nekhily, Nasser M. Al-Hajri, Ibraheem M. Al-Ageel, Ibrahim A. Al-Obaidi and Adib A. Al-Mumen

Determining a Specific Gravity of a Sample

Granted Patent: U.S. Patent 10,371,633,
Grant Date: August 6, 2019
Maha Sayegh, Ezzat M. Hegazi and Vincent B. Cunningham

Blended Land Seismic Data Acquisition Employing Dispersed Source Arrays with Variable Sweep Length

Granted Patent: U.S. Patent 10,371,839,
Grant Date: August 6, 2019
Constantinos X. Tsingas

Maintaining a Solar Power Module

Granted Patent: U.S. Patent 10,374,546,
Grant Date: August 6, 2019
James C. Hassell and Luiz Do Val

Development of Anti-Bit Balling Fluids

Granted Patent: U.S. Patent 10,377,939,
Grant Date: August 13, 2019
Abdullah S. Al-Yami, Ahmed A. Bahamdan, Saleh A. Haidary, Vikrant B. Wagle, Hussain Al-Bahrani, Ali M. Al-Safran, Nasser Al-Hareth and Abdulla H. Awadh

Cement Having Cross-Linked Polymers

Granted Patent: U.S. Patent 10,377,940,
Grant Date: August 13, 2019
Elizabeth Q. Contreras

Vibration-Induced Installation of Wellbore Casing

Granted Patent: U.S. Patent 10,378,298,
Grant Date: August 13, 2019
Victor Costa De Oliveira, Dean S. Porter and Khaled K. Abouelnaaj

Permeable Lost Circulation Drilling Liner

Granted Patent: U.S. Patent 10,378,307,
Grant Date: August 13, 2019
John T. Allen and Brett Bouldin

Prevention of Gas Accumulation above ESP Intake with Inverted Shroud

Granted Patent: U.S. Patent 10,378,322,
Grant Date: August 13, 2019
Chidirim E. Ejim, Rafael A. Lastra and Jinjiang Xiao

Method and Apparatus for Controlling Wellbore Operations

Granted Patent: U.S. Patent 10,378,339,
Grant Date: August 13, 2019
Ossama Sehsah, Victor Costa De Oliveira and Mario Rivas

Entropy-Based Multiphase Flow Detection

Granted Patent: U.S. Patent 10,378,343,
Grant Date: August 13, 2019
Talha J. Ahmad, Michael J. Black, Muhammad Arsalan and Mohamed N. Noui-Mehidi

Nitrogen Enriched Air Supply for Gasoline Compression Ignition Combustion

Granted Patent: U.S. Patent 10,378,427,
Grant Date: August 13, 2019
Jaeheon Sim, Junseok Chang and Seung-Hak Choi

Heat Exchanger Configuration for Adsorption-Based Onboard Octane On-Demand and Cetane On-Demand

Granted Patent: U.S. Patent 10,378,462,
Grant Date: August 13, 2019
Eman Tora, Amer A. Amer, Junseok Chang and Esam Z. Hamad

Nano-Level Evaluation of Kerogen-Rich Reservoir Rock

Granted Patent: U.S. Patent 10,379,068,
Grant Date: August 13, 2019
Katherine L. Hull, Younane N. Abousleiman and Sebastian Csutak

Magnetic Induction-Based Localization for Wireless Sensor Networks in Underground Oil Reservoirs

Granted Patent: U.S. Patent 10,379,248,
Grant Date: August 13, 2019
Howard K. Schmidt, Ian F. Akyildiz, Shih-Chun Lin and Abdullah A. Shehri

Systems and Methods for Accurate Measurement of Gas from Wet Gas Wells

Granted Patent: U.S. Patent 10,384,161,
Grant Date: August 20, 2019
Abdulmohsen S. Al-Kuait and Muhammad Arsalan

Supercritical Reactor Systems and Processes for Petroleum Upgrading

Granted Patent: U.S. Patent 10,384,179,
Grant Date: August 20, 2019
Ki-Hyouk Choi, Abdullah T. Alabdulhadi and Mohammed A. Alabdullah

Additives for Gas Phase Oxidative Desulfurization Catalysts

Granted Patent: U.S. Patent 10,384,197,
Grant Date: August 20, 2019
Omer R. Koseoglu, Yaming Jin, Zinfer Ismagilov, Svetlana Yashnik, Mikhail Kerzhentsev and Valentin Parmon

1,3-Butadiene Synthesis

Granted Patent: U.S. Patent 10,384,987,
Grant Date: August 20, 2019
Claus Dreisbach, Stefan Schlenk, Martina Hoffmann, Christoph Larcher and Thomas Foellinger

Novel Anti-Agglomerants for the Rubber Industry

Granted Patent: U.S. Patent 10,385,200,
Grant Date: August 20, 2019
David Thompson and Clinton Lund

Ecofriendly Emulsifier Synthesis from Esterified Waste Vegetable Oil for Wellbore Drilling Fluids

Granted Patent: U.S. Patent 10,385,254,
Grant Date: August 20, 2019
Jothibasu Ramasamy and Md. Amanullah

Settable, Form Filling Loss Circulation Control Compositions Comprising in Situ Foamed non-Hydraulic Sorel Cement Systems and Method of Use

Granted Patent: U.S. Patent 10,385,255,
Grant Date: August 20, 2019
B. Raghava Reddy

Delayed Coking Plant Combined Heating and Power Generation

Granted Patent: U.S. Patent 10,385,275,
Grant Date: August 20, 2019
Mahmoud B. Noureldin and Hani M. Al-Saed

Electrode Material for Electrolytic Hydrogen Generation

Granted Patent: U.S. Patent 10,385,462,
Grant Date: August 20, 2019
Belabbes Merzougui, Bukola S. Abidemi, Mohammad Qamar, Adeola A. Akinpelu and Mohamed N. Noui-Mehidi

Downhole Chemical Injection Method and System for Use in ESP Applications

Granted Patent: U.S. Patent 10,385,664,
Grant Date: August 20, 2019
Jinjiang Xiao and Hattan Banjar

Downhole Wellbore High Power Laser Heating and Fracturing Stimulation and Methods

Granted Patent: U.S. Patent 10,385,668,
Grant Date: August 20, 2019
Sameeh I. Batarseh

Inverted Y-Tool for Downhole Gas Separation

Granted Patent: U.S. Patent 10,385,672,
Grant Date: August 20, 2019
Amr M. Zahran

Fluid Driven Commingling System for Oil and Gas Applications

Granted Patent: U.S. Patent 10,385,673,
Grant Date: August 20, 2019
Jinjiang Xiao, Rafael A. Lastra and Shoubo Wang

Self-Contained, Fully Mechanical, 1 Out of 2 Flow Line Protection System

Granted Patent: U.S. Patent 10,386,005,
Grant Date: August 20, 2019
Patrick S. Flanders, Austin Brell and Michael A. Picou

Systems and Methods for Determining Water Cut of a Fluid Mixture

Granted Patent: U.S. Patent 10,386,312,
Grant Date: August 20, 2019
Muhammad A. Karimi, Atif Shamim and Muhammad Arsalan

Automated Near Surface Analysis by Surface Consistent Refraction Methods

Granted Patent: U.S. Patent 10,386,519,
Grant Date: August 20, 2019
Daniele Colombo and Federico Miorelli

Systems and Methods for Securely Transferring Selective Data Sets between Terminals

Granted Patent: U.S. Patent 10,389,685,
Grant Date: August 20, 2019
Fouad Al-Khabbaz, Hussain Al-Zahir, Maatoug Al-Maatoug and Zakarya Abu-Al-Saud

Methods of Producing Hierarchical Beta Zeolites with Tunable Mesoporosity through Pore Directing Agent Assisted Base Leaching

Granted Patent: U.S. Patent 10,391,480,
Grant Date: August 27, 2019
Sergio Fernandez and Ke Zhang

Wirelessly Controlled Subsystems for Underwater Remotely Operated Vehicles

Granted Patent: U.S. Patent 10,392,086,
Grant Date: August 27, 2019
Hassane Trigui, Sahejad Patel, Ali Outa, Ayman Amer, Fadl H. Abdel Latif and Ameen Obedan

Date Tree Trunk-Based Fibrous Loss Circulation Materials

Granted Patent: U.S. Patent 10,392,549,
Grant Date: August 27, 2019
Md. Amanullah and Jothibasu Ramasamy

Spacer Fluid Compositions, Methods, and Systems for Aqueous-Based Drilling Mud Removal

Granted Patent: U.S. Patent 10,392,550,
Grant Date: August 27, 2019
Abdullah S. Al-Yami, Hussain Al-Bahrani and Vikrant B. Wagle

Polycarbonate Block Copolymers

Granted Patent: U.S. Patent 10,392,556,
Grant Date: August 27, 2019
David M. Hatfield, John W. Stevens, Scott D. Allen, John M. Salladay and Chris A. Simoneau

Removing Submerged Piles of Offshore Production Platforms

Granted Patent: U.S. Patent 10,392,769,
Grant Date: August 27, 2019
Prakasha Kuppalli

Measuring Inter-Reservoir Cross Flow Rate between Adjacent Reservoir Layers from Transient Pressure Tests

Granted Patent: U.S. Patent 10,392,922,
Grant Date: August 27, 2019
Noor M. Anisur Rahman and Hasan A. Nooruddin

Mapping Fracture Length Using Downhole Ground Penetrating Radar

Granted Patent: U.S. Patent 10,392,929,
Grant Date: August 27, 2019
Jesus M. Felix-Servin, Erika S. Ellis, Ersan Turkoglu and Howard K. Schmidt

Predicting Water Holdup Measurement Accuracy of Multiphase Production Logging Tools

Granted Patent: U.S. Patent 10,393,916,
Grant Date: August 27, 2019
Shouxiang M. Ma, Dmitry Eskin, Wael Abdallah and Shawn D. Taylor

Wellbore Non-Retrieval Sensing System

Granted Patent: U.S. Patent 10,394,193,
Grant Date: August 27, 2019
Bodong Li, Chinthaka P. Gooneratne and Shaohua Zhou

Mobile Device Attendance Verification with Personal Identifier

Granted Patent: U.S. Patent 10,395,449,
Grant Date: August 27, 2019
Raed A. Al-Shaikh, Sadiq M. Sait and Muyeed A. Shariff

Mobile Device Attendance Verification with Location Data

Granted Patent: U.S. Patent 10,395,450,
Grant Date: August 27, 2019
Raed A. Al-Shaikh, Sadiq M. Sait and Muyeed A. Shariff

Mobile Device Attendance Verification with International Mobile Equipment Identity

Granted Patent: U.S. Patent 10,395,451,
Grant Date: August 27, 2019
Raed A. Al-Shaikh, Sadiq M. Sait and Muyeed A. Shariff

Maintaining a Solar Power Module

Granted Patent: U.S. Patent 10,396,708,
Grant Date: August 27, 2019
James C. Hassell and Luiz Do Val

Settable, Form-Filling Loss Circulation Control Compositions Comprising in Situ Foamed Calcium Aluminate Cement Systems and Method of Use

Granted Patent: U.S. Patent 10,400,154,
Grant Date: September 3, 2019
B. Raghava Reddy

Densifying Carbon Dioxide with a Dispersion of Carbon Dioxide-Philic Water Capsules

Granted Patent: U.S. Patent 10,400,158,
Grant Date: September 3, 2019
Fawaz Al-Otaibi, Sunil L. Kokal, Howard K. Schmidt and Yun Chang

Characterization of Crude Oil and its Fractions by Thermogravimetric Analysismers

Granted Patent: U.S. Patent 10,401,344,
Grant Date: September 3, 2019
Omer R. Koseoglu, Adnan Al-Hajji and Amer A. Al-Tuwailibu

Integrated Process for Activating Hydroprocessing Catalysts with in Situ Produced Sulfides and Disulfides

Granted Patent: U.S. Patent 10,400,183,
Grant Date: September 3, 2019
Omer R. Koseoglu and Robert P. Hodgkins

Downhole in Situ Heat Generation to Remove Filter Cake

Granted Patent: U.S. Patent 10,400,527,
Grant Date: September 3, 2019
Pubudu Gamage and Matthew Hilfiger

Systems and Methods for Acoustic Testing of Laminated Rock to Determine Total Organic Carbon Content

Granted Patent: U.S. Patent 10,400,591,
Grant Date: September 3, 2019
Adel A. Al-Qahtani

Drilling and Operating Sigmoid-Shaped Wells

Granted Patent: U.S. Patent 10,400,514,
Grant Date: September 3, 2019
Mohamed N. Noui-Mehidi

Apparatus and Method for Smart Material Analysis

Granted Patent: U.S. Patent 10,400,515,
Grant Date: September 3, 2019
Enrico Bovero

Methods and Systems for Determining Gas Permeability of a Subsurface Formation

Granted Patent: U.S. Patent 10,401,274,
Grant Date: September 3, 2019
Hui-Hai Liu, Bitao Lai, Jilin Jay Zhang, Daniel T. Georgi and Xinwo Huang

Microwave Horn Antennas-Based Transducer System for CUI Inspection without Removing the Insulation
Granted Patent: U.S. Patent 10,401,278,
Grant Date: September 3, 2019
Ali Shehri and Ayman Amer

Hybrid Electric and Magnetic Surface to Borehole and Borehole to Surface Method
Granted Patent: U.S. Patent 10,401,528,
Grant Date: September 3, 2019
Gary W. McNeice, Daniele Colombo, Jiuping Chen, Nestor Cuevas, Michael Wilt and Ping Zhang

Polymeric Tracers
Granted Patent: U.S. Patent 10,400,154,
Grant Date: September 10, 2019
Jason R. Cox

Zeolites, the Production Thereof, and their Uses for Upgrading Heavy Oils
Granted Patent: U.S. Patent 10,407,311,
Grant Date: September 10, 2019
Essam Al-Sayed, Lianhui Ding, Kareemuddin M. Shaik, Abdennour Bourane and Manal A. Eid

Process for Ethylene Oligomerization to Produce Alpha-Olefins
Granted Patent: U.S. Patent 10,407,358,
Grant Date: September 10, 2019
Wei Xu, Kareemuddin M. Shaik, Zhonglin Zhang, Rodrigo S. Rivera, Sohel Shaikh and Hussain Yami

Steam-less Process for Converting Butenes to 1,3-Butadiene
Granted Patent: U.S. Patent 10,407,363,
Grant Date: September 10, 2019
Miao Sun, Mark P. Kaminsky, Faisal H. Alshafei, Munir D. Khokhar, Zhonglin Zhang and Sohel Shaikh

Sulfur Extended Asphalt Modified with Crumb Rubber for Paving and Roofing
Granted Patent: U.S. Patent 10,407,557,
Grant Date: September 10, 2019
Mohammed H. Al-Mehthel, Mohammad Anwar Parvez, Ibnelwaleed A. Hussein, Hamad I. Al-Abdulwahhab and Saleh H. Al-Idi

High Temperature Viscoelastic Surfactant (VES) Fluids Comprising Nanoparticle Viscosity Modifiers
Granted Patent: U.S. Patent 10,407,606,
Grant Date: September 10, 2019
Leiming Li, Sehmus Ozden, Ghaithan A. Al-Muntasheri, Feng Lian and B. Raghava Reddy

Chemical Plugs for Preventing Wellbore Treatment Fluid Losses
Granted Patent: U.S. Patent 10,407,609,
Grant Date: September 10, 2019
Rajendra A. Kalgaonkar, Vikrant B. Wagle, Abdullah S. Al-Yami and Ayman Almohsin

Process and System for Conversion of Crude Oil to Petrochemicals and Fuel Products Integrating Solvent Deasphalting of Vacuum Residue
Granted Patent: U.S. Patent 10,407,630,
Grant Date: September 10, 2019
Bader Bahammam, Naif Al Osaimi, Sami Barnawi and Mohammad S. Al-Ghamdi

Wellbore Parted Casing Access Tool
Granted Patent: U.S. Patent 10,408,013,
Grant Date: September 10, 2019
Adib A. Al-Mumen, Ibrahim A. Al-Obaidi, Nelson O. Pinero Zambrano and Abdullah E. Al-Noaimi

Gas Cap Low Permeability Reservoir with Fish Bone as Gas Expansion Conduit
Granted Patent: U.S. Patent 10,408,032
Grant Date: September 10, 2019
Ahmad J. Al-Muraikhi, Yanhui A. Wang and Ivan G. Ramirez

Polymeric Tracers
Granted Patent: U.S. Patent 10,408,045,
Grant Date: September 10, 2019
Jason R. Cox

Solvent-Based Adsorbent Regeneration for Onboard Octane on Demand and Cetane on Demand
Granted Patent: U.S. Patent 10,408,139,
Grant Date: September 10, 2019
Esam Z. Hamad, Eman Tora, Amer A. Amer and Junseok Chang

Directional Sensitive Fiber Optic Cable Wellbore System
Granted Patent: U.S. Patent 10,409,018,
Grant Date: September 10, 2019
Frode Hveding

Catalyst Systems Useful in Dehydrogenation Reactions
Granted Patent: U.S. Patent 10,413,887,
Grant Date: September 17, 2019
Mohammed Al-Daous

Stabilized Rubbers
Granted Patent: U.S. Patent 10,414,901,
Grant Date: September 17, 2019
Sven Brandau, Andreas Kaiser, Bjorn Loges, Robert Staeber, Alan Bewsher and Paul Smith

Date Tree Waste-Based Binary Fibrous Mix for Moderate to Severe Loss Control
Granted Patent: U.S. Patent 10,414,965,
Grant Date: September 17, 2019
Md. Amanullah

Loss Circulation Compositions (LCM) Having Portland Cement Clinker
Granted Patent: U.S. Patent 10,414,967,
Grant Date: September 17, 2019
B. Raghava Reddy

Settable, Form Filling Loss Circulation Control Compositions Comprising in Situ Foamed Calcium Aluminate Cement
Granted Patent: U.S. Patent 10,414,968,
Grant Date: September 17, 2019
B. Raghava Reddy

Thixotropic Cement Slurry and Placement Method to Cure Lost Circulation
Granted Patent: U.S. Patent 10,415,330,
Grant Date: September 17, 2019
Joseph M. Shine Jr.

Core Catcher for Unconsolidated Sediment Samples
Granted Patent: U.S. Patent 10,415,337,
Grant Date: September 17, 2019
Nikolaos Michael and Peng Lu

Downhole High Power Laser Scanner Tool and Methods
Granted Patent: U.S. Patent 10,415,338,
Grant Date: September 17, 2019
Sameeh I. Batarseh

Conditioning a Subterranean Formation
Granted Patent: U.S. Patent 10,415,358,
Grant Date: September 17, 2019
Jilin J. Zhang, Feng Liang, Leiming Li and Bitao Lai

Separating Gas and Liquid in a Wellbore
Granted Patent: U.S. Patent 10,415,361,
Grant Date: September 17, 2019
Amr Zahran

Measuring Rock Wettability
Granted Patent: U.S. Patent 10,416,063,
Grant Date: September 17, 2019
Jun Gao, Hyung T. Kwak and Ahmad Al Harbi

Methods and Systems for Determining Gas Permeability of a Subsurface Formation
Granted Patent: U.S. Patent 10,416,064,
Grant Date: September 17, 2019
Huangye Chen, Hui-Hai Liu and Jilin J. Zhang

EMU Impulse Antenna with Controlled Directionality and Improved Impedance Matching
Granted Patent: U.S. Patent 10,416,335,
Grant Date: September 17, 2019
Howard K. Schmidt, Jesus M. Felix-Servin and Erika S. Ellis

Synthesis of Ordered Microporous Activated Carbons by Chemical Vapor Deposition
Granted Patent: U.S. Patent 10,421,058,
Grant Date: September 24, 2019
Yuguo Wang, Cemal Ercan, Rashid Othman, Minkee Choi and Seokin Choi

Methanol Terminated Polymers Containing Ether
Granted Patent: U.S. Patent 10,421,825,
Grant Date: September 24, 2019
Norbert Steinhauser

Reversible Aminal Gel Compositions, Methods, and Use
Granted Patent: U.S. Patent 10,421,891,
Grant Date: September 24, 2019
Peter J. Boul, B. Raghava Reddy, Matthew Hilfiger and Carl J. Thaemlitz

Hydrocarbon Recovery Using Complex Water and Carbon Dioxide Emulsions
Granted Patent: U.S. Patent 10,421,895,
Grant Date: September 24, 2019
Fawaz M. Alotaibi and Sunil L. Kokal

Targeting Enhanced Production through Deep Carbonate Stimulation: Stabilized Acid Emulions Containing Insoluble Solid Materials with Desired Wetting Properties
Granted Patent: U.S. Patent 10,421,898,
Grant Date: September 24, 2019
Amy Cairns, Ghaithan A. Al-Muntasheri, Mohammed Sayed, Liling Fu, Genggeng Qi and Emmanuel P. Giannelis

Hydrogen Production from an Integrated Electrolysis Cell and Hydrocarbon Gasification Reactor
Granted Patent: U.S. Patent 10,422,046,
Grant Date: September 24, 2019
Omer R. Koseoglu and Jean-Pierre Ballaguet

Method of Conversion of a Drilling Mud to a Gel-Based Lost Circulation Material to Combat Lost Circulation during Continuous Drilling
Granted Patent: U.S. Patent 10,422,194,
Grant Date: September 24, 2019
Md. Amanullah, Turki T. Alsubaie, Abdulaziz S. Bubshait and Omar A. Fuwaires

Magnetic Proppants for Enhanced Fracturing
Granted Patent: U.S. Patent 10,422,209,
Grant Date: September 24, 2019
Sameeh I. Batarseh

Adsorbent Circulation for Onboard Octane on Demand and Cetane on Demand
Granted Patent: U.S. Patent 10,422,288,
Grant Date: September 24, 2019
Esam Z. Hamad, Eman Tora, Amer A. Amer and Junseok Chang

Flow Regime Identification of Multiphase Flows by Face Recognition Bayesian Classification
Granted Patent: U.S. Patent 10,422,673,
Grant Date: September 24, 2019
Michael J. Black, Talha J. Ahmad and Mohamed N. Noui-Mehidi

Method for Nonlinear High Salinity Water Cut Measurements
Granted Patent: U.S. Patent 10,422,762,
Grant Date: September 24, 2019
Michael J. Black and Mohamed N. Noui-Mehidi

Data Processing System for Quantifying Geologic Growth History of Subsurface Oil Field Structures Based on Structural Growth Indications
Granted Patent: U.S. Patent 10,422,904,
Grant Date: September 24, 2019
Schuman Wu

Quantifying Geologic Growth History of Subsurface Oil Field Structures Based on Structural Growth Indications with Instructions from Data Storage Device
Granted Patent: U.S. Patent 10,422,905,
Grant Date: September 24, 2019
Schuman Wu

Methods and Systems for Determining Bulk Density, Porosity, and Pore Size Distribution of Subsurface Formations
Granted Patent: U.S. Patent 10,422,916,
Grant Date: September 24, 2019
Jilin J. Zhang, Jin-Hong Chen and Stacey M. Althaus

Nanocomposite Electrode Materials for Use in High Temperature and High-Pressure Rechargeable Batteries
Granted Patent: U.S. Patent 10,424,782,
Grant Date: September 24, 2019
Muhammad Arsalan, Edreese Alsharaeh, Yasmin Mussa and Faheem Ahmed

Methods for Synthesizing Hierarchical Zeolites for Catalytic Cracking
Granted Patent: U.S. Patent 10,427,142,
Grant Date: October 1, 2019
Mansour Al-Herz, Muased S. Al-Ghrami, Rabindran J. Balasamy, Mohammed A. Siddiqui and Mian R. Saeed

High Strength Polyurethane Foam Compositions and Methods
Granted Patent: U.S. Patent 10,428,173,
Grant Date: October 1, 2019
Scott D. Allen, Aisa Sendijarevic and Vahid Sendijarevic

Collecting Drilling Microchips
Granted Patent: U.S. Patent 10,428,606,
Grant Date: October 1, 2019
Mohammad S. Al-Badran and Bodong Li

Reverse Circulation Well Tool
Granted Patent: U.S. Patent 10,428,607,
Grant Date: October 1, 2019
Shaohua Zhou

Apparatus and Method for in Situ Stabilization of Unconsolidated Sediment in Core Samples
Granted Patent: U.S. Patent 10,428,611,
Grant Date: October 1, 2019
Nikolaos A. Michael, Maher I. Marhoon and Peng Lu

System and Method for Removing Sand from a Wellbore
Granted Patent: U.S. Patent 10,428,635,
Grant Date: October 1, 2019
Muhammad Ayub and Nabeel S. Habib

Dynamic Multi-Legs Ejector for Use in Emergency Flare Gas Recovery System
Granted Patent: U.S. Patent 10,429,067,
Grant Date: October 1, 2019
Samusideen Salu, Mohamed Soliman and Nisar Ansari

Recovery and Re-Use of Waste Energy in Industrial Facilities
Granted Patent: U.S. Patent 10,429,135,
Grant Date: October 1, 2019
Mahmoud B. Noureldin and Hani M. Al-Saed

Small Flow Capacity Displacement Prover for Proving Flow Meter with Large Flow Capacity
Granted Patent: U.S. Patent 10,429,230,
Grant Date: October 1, 2019
Chandulal N. Bhatasana

Photoacoustic Gas Detection
Granted Patent: U.S. Patent 10,429,350,
Grant Date: October 1, 2019
Weichang Li, Sebastian Csutak, Angelo Sampedro and Gregory D. Ham

Smart Water Flooding Processes for Increasing Hydrocarbon Recovery
Granted Patent: U.S. Patent 10,429,372,
Grant Date: October 1, 2019
Ali Alyousef and Subhash Ayirala

Electrical Submersible Pump Monitoring and Failure Prediction
Granted Patent: U.S. Patent 10,429,533,
Grant Date: October 1, 2019
Mohamed N. Noui-Mehidi and Ahmed Y. Bukhamseen

Method of Encapsulating Signaling Agents for Use Downhole
Granted Patent: U.S. Patent 10,435,613,
Grant Date: October 8, 2019
Elizabeth Q. Contreras

Methods and Compositions for in Situ Polymerization Reaction to Improve Shale Inhibition
Granted Patent: U.S. Patent 10,435,614,
Grant Date: October 8, 2019
Abeer M. Al-Olayan

Methods and Compositions for in Situ Polymerization Reaction to Improve Shale Inhibition
Granted Patent: U.S. Patent 10,435,615,
Grant Date: October 8, 2019
Abeer M. Al-Olayan

Treatment of Kerogen in Subterranean Formations
Granted Patent: U.S. Patent 10,435,617,
Grant Date: October 8, 2019
Katherine L. Hull, Younane N. Abousleiman, Ghaithan A. Al-Muntasheri and David Jacobi

Estimating Measures of Formation Flow Capacity and Phase Mobility from Pressure Transient Data under Segregated Oil and Water Flow Conditions
Granted Patent: U.S. Patent 10,435,996,
Grant Date: October 8, 2019
Hasan A. Nooruddin and Noor M. Anisur Rahman

Multilateral Well Drilled with Underbalanced Coiled Tubing and Stimulated with Exothermic Reactants
Granted Patent: U.S. Patent 10,436,006,
Grant Date: October 8, 2019
Abdulrahman Al-Mulhem

Systems and Methods for Wirelessly Monitoring Well Conditions
Granted Patent: U.S. Patent 10,436,022,
Grant Date: October 8, 2019
Chinthaka P. Gooneratne, Bodong Li and Shaohua Zhou

Detecting Subteranean Structures
Granted Patent: U.S. Patent 10,436,024,
Grant Date: October 8, 2019
Andrey Bakulin, Pavel Golikov and Ilya Silvestrov

Natural Gas Liquid Fractionation Plant Waste Heat Conversion to Potable Water Using Modified Multi-Effect Distillation System
Granted Patent: U.S. Patent 10,436,077,
Grant Date: October 8, 2019
Mahmoud B. Noureldin and Akram H. Kamel

Adsorption-Based Fuel Systems for Onboard Cetane on Demand and Octane on Demand
Granted Patent: U.S. Patent 10,436,126,
Grant Date: October 8, 2019
Esam Z. Hamad, Amer A. Amer, Eman Tora and Junseok Chang

Systems for Recovery and Re-Use of Waste Energy in Hydrocracking-Based Configuration for Integrated Crude Oil Refining and Aromatics Complex
Granted Patent: U.S. Patent 10,436,517,
Grant Date: October 8, 2019
Mahmoud B. Noureldin and Hani M. Al-Saed

Fluorophore Enhanced Multidimensional Photonic Sensors
Granted Patent: U.S. Patent 10,436,655,
Grant Date: October 8, 2019
Enrico Bovero, Gasan Alabedi and Abdullah A. Al-Shahrani

Methods and Systems for Determining Gas Permeability of a Subsurface Formation
Granted Patent: U.S. Patent 10,436,696,
Grant Date: October 8, 2019
Hui-Hai Liu, Bitao Lai, Jilin J. Zhang, Daniel T. Georgi and Xinwo Huang

Apparatus and Method for the Nondestructive Measurement of Hydrogen Diffusivity
Granted Patent: U.S. Patent 10,436,741,
Grant Date: October 8, 2019
Mohamed S.K. Ur Rahman, Abderrazak Traidia and Abdullah Enezi

Ruthenium- or Osmium-Based Complex Catalysts
Granted Patent: U.S. Patent 10,441,948,
Grant Date: October 15, 2019
Zhenli Wei

Process for Xylene Production with Energy Optimization
Granted Patent: U.S. Patent 10,442,742,
Grant Date: October 15, 2019
Qi Xu, Raed Abudawoud, Ahmad A. Jazzar and Zhonglin Zhang

Synthesis of Substituted Salicylaldehyde Derivatives
Granted Patent: U.S. Patent 10,442,816,
Grant Date: October 15, 2019
Jay J. Farmer and Gabriel E. Job

Compositions and Methods for Enhanced Fracture Cleanup Using Redox Treatment
Granted Patent: U.S. Patent 10,442,977,
Grant Date: October 15, 2019
Ayman R. Nakhli, Hazim H. Abass and Ahmed S. Otaibi

Compositions and Methods for Enhanced Fracture Cleanup Using Redox Treatment
Granted Patent: U.S. Patent 10,442,978,
Grant Date: October 15, 2019
Ayman R. Nakhli, Hazim H. Abass and Ahmed S. Otaibi

Mitigation of Condensate Banking Using Surface Modification
Granted Patent: U.S. Patent 10,442,983,
Grant Date: October 15, 2019
Hooisweng Ow, Feng Liang, Mohammed Sayed and Jason R. Cox

Using Radio Waves to Fracture Rocks in a Hydrocarbon Reservoir
Granted Patent: U.S. Patent 10,443,367,
Grant Date: October 15, 2019
Jin-Hong Chen, Daniel T. Georgi, Davis L. Arthur and Hui-Hai Liu

Natural Gas Liquid Fractionation Plant Cooling Capacity and Potable Water Generation Using Integrated Vapor Compression-Ejector Cycle and Modified Multi-Effect Distillation System
Granted Patent: U.S. Patent 10,443,453,
Grant Date: October 15, 2019
Mahmoud B. Noureldin and Akram H. Kamel

System and Method for Encoding Pipeline Welds
Granted Patent: U.S. Patent 10,443,787,
Grant Date: October 15, 2019
Enrico Bovero, Gasan Alabedi, Ali F. Al Qabani and Majed F. Al Rajeh

Systems for Recovery and Re-Use of Waste Energy in Crude Oil Refining and Aromatics Complex
Granted Patent: U.S. Patent 10,443,946,
Grant Date: October 15, 2019
Mahmoud B. Noureldin and Hani M. Al-Saed

Determining Structural Tomographic Properties of a Geologic Formation
Granted Patent: U.S. Patent 10,444,065,
Grant Date: October 15, 2019
Howard K. Schmidt, Jesus M. Felix-Servin, Frode Hveding and Daniele Colombo

Systems and Methods for Constructing and Testing Composite Photonic Structures
Granted Patent: U.S. Patent 10,444,163,
Grant Date: October 15, 2019
Abdullah A. Al-Shahrani, Abdullah S. Al-Ghamdi and Enrico Bovero

Absolute Porosity and Pore Size Determination of Pore Types in Media with Varying Pore Sizes
Granted Patent: U.S. Patent 10,444,171,
Grant Date: October 15, 2019
Hyung T. Kwak, Ali A. Yousif and Salah H. Saleh

Multiple Function Dual Core Flooding Apparatus and Methods
Granted Patent: U.S. Patent 10,444,218,
Grant Date: October 15, 2019
Xianmin Zhou, Fawaz Al-Otaibi, Ahmed A. Eidan, Sunil L. Kokal and Almohannad A. Alhashboul

Automated Solar Panel Cleaning
Granted Patent: U.S. Patent 10,447,199,
Grant Date: October 15, 2019
Ahmad M. Naffa'a and Saeed Aljabri

Fluorinated Polyimide-Based Epoxy Materials
Granted Patent: U.S. Patent 10,450,406,
Grant Date: October 22, 2019
Gasan Alabedi, Aziz Fihri, Ihsan Al-Taie, Haleema A. Alamri and Abdullah A. Al-Shahrani

Nanosilica Dispersion Well Treatment Fluid
Granted Patent: U.S. Patent 10,450,492,
Grant Date: October 22, 2019
Vikrant B. Wagle and Abdullah S. Al-Yami

Settable, Form Filling Loss Circulation Control Compositions Comprising in Situ Foamed Calcium Aluminate Cement Systems and Methods of Using Them
Granted Patent: U.S. Patent 10,450,495,
Grant Date: October 22, 2019
B. Raghava Reddy

Loss Circulation Compositions (LCM) Having Portland Cement Clinker
Granted Patent: U.S. Patent 10,450,496,
Grant Date: October 22, 2019
B. Raghava Reddy

Loss Circulation Compositions (LCM) Having Portland Cement Clinker
Granted Patent: U.S. Patent 10,450,497,
Grant Date: October 22, 2019
B. Raghava Reddy

Compositions and Methods for Enhanced Fracture Cleanup Using Redox Treatment
Granted Patent: U.S. Patent 10,450,499,
Grant Date: October 22, 2019
Ayman R. Nakhli, Hazim H. Abass and Ahmed S. Otaibi

Rapidly Cooling a Geologic Formation in Which a Wellbore is Formed
Granted Patent: U.S. Patent 10,450,839,
Grant Date: October 22, 2019
Aslan Bulekbay, Abdulkareem Harbi and Abdullah Khamees

Magnetic Crawler Vehicle with Passive Rear-Facing Apparatus
Granted Patent: U.S. Patent 10,451,222,
Grant Date: October 22, 2019
Pablo Carrasco, Fadl H. Abdel Latif, Ali Outa and Brian J. Parrott

Natural Gas Liquid Fractionation Plant Waste Heat Conversion to Power Using Kalina Cycle
Granted Patent: U.S. Patent 10,451,359,
Grant Date: October 22, 2019
Mahmoud B. Noureldin and Akram H. Kamel

Nuclear Magnetic Resonance Gas Isotherm Technique to Evaluate Reservoir Rock Wettability
Granted Patent: U.S. Patent 10,451,530,
Grant Date: October 22, 2019
Hyung T. Kwak and Ahmad M. Al Harbi

Measuring the Wettability of Porous Media Based on the Temperature Sensitivity of Nuclear Magnetic Resonance Relaxation Time
Granted Patent: U.S. Patent 10,451,571,
Grant Date: October 22, 2019
Hyung T. Kwak and Ahmad M. Al Harbi

Nano-Indentation Test to Determine Mechanical Properties of Reservoir Rock
Granted Patent: U.S. Patent 10,451,601,
Grant Date: October 22, 2019
Yanhui Han, Younane N. Abousleiman, Katherine L. Hull and Ghaithan A. Al-Muntasheri

Optical Master Unit Alarm Collector and Translator
Granted Patent: U.S. Patent 10,453,330,
Grant Date: October 22, 2019
Badie A. Guwaisem and Hassan Al-Helal

Thermal Control System
Granted Patent: U.S. Patent 10,455,730,
Grant Date: October 22, 2019
Mohamed Y. Haj-Maharsi and Yasser Al-Howeish

Coordinated Water Environment Mobile Robots
Granted Patent: U.S. Patent 10,456,924,
Grant Date: October 29, 2019
Ali Outa, Fadl H. Abdel Latif, Hassane Trigui and Sahejad Patel

Date Palm Seed-Based Lost Circulation Material (LCM)
Granted Patent: U.S. Patent 10,457,846,
Grant Date: October 29, 2019
Md. Amanullah

Invert Emulsion Drilling Fluids with Fatty Acid and Fatty Amine Rheology Modifiers
Granted Patent: U.S. Patent 10,457,847, Grant Date: October 29, 2019
Vikrant B. Wagle and Abdullah S. Al-Yami

Reduced Corrosion Iron Sulfide Scale Removing Fluids
Granted Patent: U.S. Patent 10,457,850, Grant Date: October 29, 2019
Hejian Sun, Leiming Li and Feng Liang

Polymer Flooding Processes for Viscous Oil Recovery in Carbonate Reservoirs
Granted Patent: U.S. Patent 10,457,851, Grant Date: October 29, 2019
Subhash C. Ayirala, Abdulkareem M. Sofi, Ali A. Yousef and Jinxun Wang

Methods and Materials for Treating Subterranean Formations Using a Three-Phase Emulsion-Based Fracturing Fluid
Granted Patent: U.S. Patent 10,457,856, Grant Date: October 29, 2019
Rajendra A. Kalgaonkar

Double Emulsified Acids and Methods for Producing and Using the Same
Granted Patent: U.S. Patent 10,457,858, Grant Date: October 29, 2019
Mohammed H. Al-Khaldi and Tariq A. Al-Mubarak

Sealing an Undesirable Formation Zone in the Wall of a Wellbore
Granted Patent: U.S. Patent 10,458,199, Grant Date: October 29, 2019
Alwaleed A. Al-Gouhi and Nabil S. Alkhanaifer

Choke System for Wellhead Assembly Having a Turbine Generator
Granted Patent: U.S. Patent 10,458,206, Grant Date: October 29, 2019
Faisal M. Al-Dossary and Mohammed S. Al-Zahrani

System and Method for Acoustic Container Volume Calibration
Granted Patent: U.S. Patent 10,458,831, Grant Date: October 29, 2019
Ihsan Al-Taie, Vincent B. Cunningham, Ayman Amer and Ali Outa

Integrated System for Quantitative Real-Time Monitoring of Hydrogen-Induced Cracking in Simulated Sour Environment
Granted Patent: U.S. Patent 10,458,960, Grant Date: October 29, 2019
Abderrazak Traidia, Abdelmounam Sherik and Arnold Lewis

Methods and Systems for Estimating Sizes and Effects of Wellbore Obstructions in Water Injection Wells
Granted Patent: U.S. Patent 10,459,118, Grant Date: October 29, 2019
Mohammed D. Al-Ajmi and Sami Alnuaim

Process for Maximizing Production of Xylenes from Heavy Reformate without Purge
Granted Patent: U.S. Patent 10,464,868, Grant Date: November 5, 2019
Qi Xu and Raed Abudawoud

Salen Complexes with Dianionic Counterions
Granted Patent: U.S. Patent 10,464,960, Grant Date: November 5, 2019
Anna E. Cherian, Gabriel E. Job and Jay J. Farmer

Methods and Materials for Treating Subterranean Formations Using a Three-Phase Emulsion-Based Fracturing Fluid
Granted Patent: U.S. Patent 10,465,109, Grant Date: November 5, 2019
Rajendra A. Kalgaonkar

Subsurface Safety Valve for Cable Deployed Electrical Submersible Pump
Granted Patent: U.S. Patent 10,465,477, Grant Date: November 5, 2019
Mohannad Abdelaziz, Brian A. Roth and Jinjiang Xiao

Gravel Packing System and Method
Granted Patent: U.S. Patent 10,465,484, Grant Date: November 5, 2019
Robert J. Turner and Brian A. Roth

Measuring a Water Cut of Hydrocarbon Fluid in a Production Pipe
Granted Patent: U.S. Patent 10,466,182, Grant Date: November 5, 2019
Jose Oliverio Alvarez

Silicone Rubber Foam Brush
Granted Patent: U.S. Patent 10,469,026, Grant Date: November 5, 2019
Pablo Carrasco Zanini, Brian J. Parrott and Ali AlShehri

Maintaining a Solar Power Module
Granted Patent: U.S. Patent 10,469,027, Grant Date: November 5, 2019
James C. Hassell and Luiz Do Val

Metal Complex Comprising Amidine and Substituted Cyclopentadienyl Ligands
Granted Patent: U.S. Patent 10,472,431, Grant Date: November 12, 2019
Peter Karbaum, Richard T.W. Scott and John van De Moosdijk

Delayed Polymer Gelation Using Low Total Dissolved Solids Brine
Granted Patent: U.S. Patent 10,472,553, Grant Date: November 12, 2019
Amar J. Alshehri and Jinxun Wang

Polymer Enhanced Surfactant Flooding for Permeable Carbonates
Granted Patent: U.S. Patent 10,472,558, Grant Date: November 12, 2019
Ming Han, Ali A. Al-Yousif, Alhasan B. Fuseni and Salah H. Al-Saleh

Process and System for Conversion of Crude Oil to Petrochemicals and Fuel Products Integrating Delayed Coking of Vacuum Residue
Granted Patent: U.S. Patent 10,472,574, Grant Date: November 12, 2019
Bader Bahammam, Naif Al Osaimi, Sami Barnawi and Mohammad S. Al-Ghamdi

Methods and Systems for Optimizing Demulsifier and Wash Water Injection Rates in Gas-Oil Separation Plants
Granted Patent: U.S. Patent 10,472,576, Grant Date: November 12, 2019
Samusideen Salu, Mohamed Soliman and Talal A. Zahrani

Production of Upgraded Petroleum by Supercritical Water
Granted Patent: U.S. Patent 10,472,578, Grant Date: November 12, 2019
Ki-Hyouk Choi, Joo-Hyeong Lee, Mohammad S. Garhoush and Ali H. Alshareef

Process and System for Conversion of Crude Oil to Petrochemicals and Fuel Products Integrating Vacuum Gas Oil Hydrocracking and Steam Cracking
Granted Patent: U.S. Patent 10,472,579, Grant Date: November 12, 2019
Bader Bahammam, Naif Al Osaimi, Sami Barnawi and Mohammad S. Al-Ghamdi

Process and System for Conversion of Crude Oil to Petrochemicals and Fuel Products Integrating Steam Cracking and Conversion of Naphtha into Chemical-Rich Reformate
Granted Patent: U.S. Patent 10,472,580, Grant Date: November 12, 2019
Bader Bahammam, Naif Al Osaimi, Sami Barnawi and Mohammad S. Al-Ghamdi

Removing Submerged Piles of Offshore Production Platforms
Granted Patent: U.S. Patent 10,472,791, Grant Date: November 12, 2019
Prakasha Kuppalli

Entropy-Based Multiphase Flow Detection
Granted Patent: U.S. Patent 10,472,957, Grant Date: November 12, 2019
Talha J. Ahmad, Michael J. Black, Muhammad Arsalan and Mohamed N. Noui-Mehidi

Determining Spotting Fluid Properties
Granted Patent: U.S. Patent 10,472,958, Grant Date: November 12, 2019
Md. Amanullah and Turki T. Alsubaie

Method and Device for Testing a Material Sample in a Standard Test for in-Plane Fracture Toughness Evaluation
Granted Patent: U.S. Patent 10,473,569, Grant Date: November 12, 2019
Abderrazak Traidia, Mustapha Jouiad and Elias Chatzidouros

Apparatus, System and Method for Inspecting Composite Structures Using Quantitative Infrared Thermography
Granted Patent: U.S. Patent 10,473,603, Grant Date: November 12, 2019
Ayman Amer, Thibault Villette, Abderrazak Traidia and Fadl H. Abdel Latif

Slug Flow Monitoring and Gas Measurement
Granted Patent: U.S. Patent 10,473,623, Grant Date: November 12, 2019
Talha J. Ahmad, Michael J. Black and Mohamed N. Noui-Mehidi

Gravity Modeling a Rifted Continental Margin
Granted Patent: U.S. Patent 10,474,767, Grant Date: November 12, 2019
Ahmed Salem

Computer Vision System and Method for Tank Calibration Using Optical Reference Line Method
Granted Patent: U.S. Patent 10,475,203, Grant Date: November 12, 2019
Ali Outa, Brian J. Parrott and Fadl H. Abdel Latif

Systems, Computer Medium and Methods for Management Training Systems
Granted Patent: U.S. Patent 10,475,351,
Grant Date: November 12, 2019
Samantha J. Horseman and Brent Mattson

IPV4 Addressing Schema Design Methodology Using a Visual Interactive Tool
Granted Patent: U.S. Patent 10,476,837,
Grant Date: November 12, 2019
Atif Z. Khan

Interface and Authorization for Cross-Network Communications
Granted Patent: U.S. Patent 10,477,362,
Grant Date: November 12, 2019
Hussain A. Al-Nasser, Hanan Al-Ali, Murtada Al-Qushairi, Zahrah Al-Mousa and Mohammad Al-Munea

Systems and Methods Comprising Smart Sample Catcher for Drilling Operations
Granted Patent: U.S. Patent 10,478,754,
Grant Date: November 19, 2019
Ossama Sehsah, Victor Costa de Oliveira and Mario Rivas

Enriched Acid Gas for Sulfur Recovery
Granted Patent: U.S. Patent 10,479,685,
Grant Date: November 19, 2019
Nasser A. Al-Qahtani

Two Component Lost Circulation Pill for Seepage to Moderate Loss Control
Granted Patent: U.S. Patent 10,479,918,
Grant Date: November 19, 2019
Jothibasu Ramasamy and Md. Amanullah

Date Tree Trunk and Rachis-Based Superfine Fibrous Materials for Seepage Loss Control
Granted Patent: U.S. Patent 10,479,920,
Grant Date: November 19, 2019
Md. Amanullah and Jothibasu Ramasamy

Enhancement of Claus Tail Gas Treatment by Sulfur Dioxide-Selective Membrane Technology and Sulfur Dioxide-Selective Absorption Technology
Granted Patent: U.S. Patent 10,479,684,
Grant Date: November 19, 2019
Md. Amanullah and Jothibasu Ramasamy

Cement Having Cross-Linked Polymers
Granted Patent: U.S. Patent 10,479,921,
Grant Date: November 19, 2019
Md. Amanullah and Jothibasu Ramasamy

Treatment of Kerogen in Subterranean Formations
Granted Patent: U.S. Patent 10,479,927,
Grant Date: November 19, 2019
Katherine L. Hull, Younane N. Abousleiman, Ghaithan Al-Muntasheri and David Jacobi

Water Treatment Schemes for Injection Water Flooding Recovery Processes in Carbonate Reservoirs
Granted Patent: U.S. Patent 10,479,928,
Grant Date: November 19, 2019
Subhash Ayirala and Ali Yousef

Mat for Wellhead Cellar
Granted Patent: U.S. Patent 10,480,271,
Grant Date: November 19, 2019
Mohammad S. Al-Badran

Nanoparticle-Based Shear Thickening Materials
Granted Patent: U.S. Patent 10,480,281,
Grant Date: November 19, 2019
Md. Amanullah and Jothibasu Ramasamy

Downhole Chemical Injection Method and System for Use in ESP Applications
Granted Patent: U.S. Patent 10,480,299,
Grant Date: November 19, 2019
Jinjiang Xiao and Hattan Banjar

Electrical Submersible Pump Flow Meter
Granted Patent: U.S. Patent 10,480,312,
Grant Date: November 19, 2019
Md. Amanullah and Jothibasu Ramasamy

Organic Rankine Cycle-Based Conversion of Gas Processing Plant Waste Heat into Power and Cooling
Granted Patent: U.S. Patent 10,480,352,
Grant Date: November 19, 2019
Mahmoud B. Noureldin and Akram H. Kamel

Natural Gas Liquid Fractionation Plant Waste Heat Conversion to Simultaneous Power and Potable Water Using Kalina Cycle and Modified Multi-Effect Distillation System
Granted Patent: U.S. Patent 10,480,354,
Grant Date: November 19, 2019
Mahmoud B. Noureldin and Akram H. Kamel

Natural Gas Liquid Fractionation Plant Waste Heat Conversion to Simultaneous Power, Cooling and Potable Water Using Modified Goswami Cycle and New Modified Multi-Effect Distillation System
Granted Patent: U.S. Patent 10,480,355,
Grant Date: November 19, 2019
Mahmoud B. Noureldin and Akram H. Kamel

Recovery and Re-Use of Waste Energy in Industrial Facilities
Granted Patent: U.S. Patent 10,480,864,
Grant Date: November 19, 2019
Mahmoud B. Noureldin and Hani M. Al-Saed

Acoustic Calibration Array for Tanks and Vessels
Granted Patent: U.S. Patent 10,480,982,
Grant Date: November 19, 2019
Brian J. Parrott and Fadl H. Abdel Latif

Underwater Vehicles with Integrated Surface Cleaning and Inspection
Granted Patent: U.S. Patent 10,481,134,
Grant Date: November 19, 2019
Ayman Amer and Fadl H. Abdel Latif

Surface Consistent Statics Solution and Amplification Correction
Granted Patent: U.S. Patent 10,481,287,
Grant Date: November 19, 2019
Mamadou S. Diallo

Statistical Methods for Assessing Downhole Casing Integrity and Predicting Casing Leaks
Granted Patent: U.S. Patent 10,481,292,
Grant Date: November 19, 2019
Abdulrahman T. Mishkhes, Mohammed D. Al-Ajmi and Mubarak Al-Shammari

Statistical Methods for Assessing Downhole Casing Integrity and Predicting Casing Leaks
Granted Patent: U.S. Patent 10,481,293,
Grant Date: November 19, 2019
Abdulrahman T. Mishkhes, Mohammed D. Al-Ajmi and Mubarak Al-Shammari

High Accuracy Remote Coordinate Machine
Granted Patent: U.S. Patent 10,481,604,
Grant Date: November 19, 2019
Fadl H. Abdel Latif and Pablo Carrasco

Mechanical Energy Storage in Flow Batteries to Enhance Energy Storage
Granted Patent: U.S. Patent 10,483,567,
Grant Date: November 19, 2019
Ahmad D. Hammad, Stamatios Souentie and Issam T. Amr

Date Tree Spikelet-Based Additive for Mechanical Reinforcement of Weak and Unstable Lost Circulation Material (LCM) Seals/Plugs
Granted Patent: U.S. Patent 10,487,253,
Grant Date: November 26, 2019
Md. Amanullah

Enhanced Filtration Control Packages, Wellbore Servicing Fluids Utilizing the Same, and Methods of Maintaining the Structure of a Wellbore
Granted Patent: U.S. Patent 10,487,254,
Grant Date: November 26, 2019
Abdullah S. Al-Yami, Vikrant B. Wagle, Hussain Al-Bahrani, Ali M. Al-Safran and Nasser Al-Hareth

Polysaccharide Coated Nanoparticle Compositions Comprising Ions
Granted Patent: U.S. Patent 10,487,259,
Grant Date: November 26, 2019
Jason R. Cox, Hooisweng Ow, Howard K. Schmidt and Shannon L. Eichmann

Hydrocarbon Recovery Using Complex Water and Carbon Dioxide Emulsions
Granted Patent: U.S. Patent 10,487,260,
Grant Date: November 26, 2019
Fawaz M. Alotaibi and Sunil L. Kokal

Process and System for Conversion of Crude Oil to Petrochemicals and Fuel Products Integrating Vacuum Residue Conditioning and Base Oil Production
Granted Patent: U.S. Patent 10,487,275,
Grant Date: November 26, 2019
Bader Bahammam, Naif Al Osaimi, Sami Barnawi and Mohammad S. Al-Ghamdi

Process and System for Conversion of Crude Oil to Petrochemicals and Fuel Products Integrating Vacuum Residue Hydroprocessing
Granted Patent: U.S. Patent 10,487,276,
Grant Date: November 26, 2019
Bader Bahammam, Naif Al Osaimi, Sami Barnawi and Mohammad S. Al-Ghamdi

Drilling and Operating Sigmoid-Shaped Wells
Granted Patent: U.S. Patent 10,487,585,
Grant Date: November 26, 2019
Mohamed N. Noui-Mehidi

Vibration-Induced Installation of Wellbore Casing

Granted Patent: U.S. Patent 10,487,604,
Grant Date: November 26, 2019
Victor Costa de Oliveira, Dean S. Porter and Khaled K. Abouelnaaj

Entropy-Based Multiphase Flow Detection

Granted Patent: U.S. Patent 10,487,648,
Grant Date: November 26, 2019
Talha J. Ahmad, Michael J. Black, Muhammad Arsalan and Mohamed N. Noui-Mehidi

Natural Gas Liquid Fractionation Plant Waste Heat Conversion to Cooling Capacity Using Kalina Cycle

Granted Patent: U.S. Patent 10,487,699,
Grant Date: November 26, 2019
Mahmoud B. Noureldin and Akram H. Kamel

High Spatial Resolution Nuclear Magnetic Resonance Logging

Granted Patent: U.S. Patent 10,488,352,
Grant Date: November 26, 2019
Jin-Hong Chen, Stacey M. Althaus, Yang Zhao and Mohammad Delshad

Copolymer Rubber Containing Nitrile Groups

Granted Patent: U.S. Patent 10,494,467,
Grant Date: December 3, 2019
Werner Obrecht, Hiyam Salem, Susanna Lieber, Irene Moll and Andreas Kaiser

ARC Fiber Trio-Date Tree Waste-Based Trinary Fibrous Mix for Moderate to Severe Loss Control

Granted Patent: U.S. Patent 10,494,558,
Grant Date: December 3, 2019
Md. Amanullah

Cement Slurries, Cured Cement and Methods of Making and Use Thereof

Granted Patent: U.S. Patent 10,494,559,
Grant Date: December 3, 2019
Abdullah S. Al-Yami, Hussain Al-Bahrani, Vikrant B. Wagle and Ali Al-Safran

Development of Anti-Bit Balling Fluids

Granted Patent: U.S. Patent 10,494,560,
Grant Date: December 3, 2019
Abdullah S. Al-Yami, Abdulaziz A. Bahamdan, Saleh A. Haidary, Vikrant B. Wagle, Hussain Al-Bahrani, Ali M. Al-Safran, Nasser Al-Hareth and Abdulla H. Awadh

Loss Circulation Compositions (LCM) Having Portland Cement Clinker

Granted Patent: U.S. Patent 10,494,561,
Grant Date: December 3, 2019
B. Raghava Reddy

Enhanced Oil Recovery by in Situ Steam Generation

Granted Patent: U.S. Patent 10,494,566,
Grant Date: December 3, 2019
Ayman R. Al-Nakhli and Michael J. Black

Systems and Methods for Cracking Hydrocarbon Streams such as Crude Oils Utilizing Catalysts, which Include Zeolite Mixtures

Granted Patent: U.S. Patent 10,494,574,
Grant Date: December 3, 2019
Muased S. Al-Ghrami, Aaron Akah and Anas Aqeeli

Refinery pre-Heat Train Systems and Methods

Granted Patent: U.S. Patent 10,494,576,
Grant Date: December 3, 2019
Mahmoud B. Noureldin and Zeeshan Farooq

Integrated Residuum Hydrocracking and Hydrofinishing

Granted Patent: U.S. Patent 10,494,578,
Grant Date: December 3, 2019
Vinod Ramaseshan, Yufeng He, Hiren Shethna and Mohammed Wohaibi

Used Automobile Tires as Loss Circulation Material

Granted Patent: U.S. Patent 10,494,884,
Grant Date: December 3, 2019
Md. Amanullah and Mohammed K. Arfaj

Sealing an Undesirable Formation Zone in the Wall of a Wellbore

Granted Patent: U.S. Patent 10,494,894,
Grant Date: December 3, 2019
Alwaleed A. Al-Gouhi and Nabil S. Alkhanaifer

Natural Gas Liquid Fractionation Plant Waste Heat Conversion to Simultaneous Power and Cooling Capacities Using Integrated Organic-Based Compressor-Ejector-Expander Triple Cycles System

Granted Patent: U.S. Patent 10,494,958,
Grant Date: December 3, 2019
Mahmoud B. Noureldin and Akram H. Kamel

Determining Permeability of Porous Media Based on Nuclear Magnetic Resonance Measurement

Granted Patent: U.S. Patent 10,495,589,
Grant Date: December 3, 2019
Hyung T. Kwak

Catalyst Compositions and their Use for Hydrogenation of Nitrile Rubber

Granted Patent: U.S. Patent 10,500,578,
Grant Date: December 10, 2019
Werner Obrecht, Sarah David, Qingchun Liu and Zhenli Wei

Process and System for the Production of Paraxylene and Benzene from Streams Rich in C6 to C12+ Aromatics

Granted Patent: U.S. Patent 10,501,389,
Grant Date: December 10, 2019
Qi Xu, Raed H. Abudawoud and Zhonglin Zhang

Iron Sulfide Dissolver

Granted Patent: U.S. Patent 10,501,679,
Grant Date: December 10, 2019
Harry D. Oduro and Mohammed Khaldi

Treating Seawater for Hydrocarbon Production

Granted Patent: U.S. Patent 10,501,680,
Grant Date: December 10, 2019
Feng Liang, Leiming Li, Hejian Sun and Mohammed A. Bataweel

Polysaccharide Coated Nanoparticle Compositions Comprising Ions

Granted Patent: U.S. Patent 10,501,682,
Grant Date: December 10, 2019
Jason R. Cox, Hooisweng Ow, Howard K. Schmidt and Shannon L. Eichmann

Encapsulation and Controlled Delivery of Strong Mineral Acids

Granted Patent: U.S. Patent 10,501,687,
Grant Date: December 10, 2019
Ghaithan Al-Muntasheri, Ginger D. Rothrock, Leah M. Johnson and Sarah Shepherd

Drilling and Operating Sigmoid-Shaped Wells

Granted Patent: U.S. Patent 10,501,993,
Grant Date: December 10, 2019
Mohamed N. Noui-Mehidi

Smart Selective Drilling Fluid System

Granted Patent: U.S. Patent 10,502,009,
Grant Date: December 10, 2019
Ossama Sehsah

New Systems for Recovery and Re-Use of Waste Energy in Crude Oil Refining Facility and Aromatics Complex through Simultaneous Intra-Plant Integration and Plants' Thermal Coupling

Granted Patent: U.S. Patent 10,502,494,
Grant Date: December 10, 2019
Mahmoud B. Noureldin and Hani M. Al-Saed

Systems for Recovery and Re-Use of Waste Energy in Crude Oil Refining Facility and Aromatics Complex

Granted Patent: U.S. Patent 10,502,495,
Grant Date: December 10, 2019
Mahmoud B. Noureldin and Hani M. Al-Saed

Point-of-Sale Octane/Cetane-on-Demand Systems for Automotive Engines

Granted Patent: U.S. Patent 10,508,017,
Grant Date: December 17, 2019
Esam Z. Hamad, Amer A. Amer, Husain A. Baaqel and Ahmad O. Al-Khowaiter

Enhancement of Claus Tail Gas Treatment by Sulfur Dioxide Selective Membrane Technology

Granted Patent: U.S. Patent 10,508,033,
Grant Date: December 17, 2019
Milind M. Vaidya, Iran D. Charry-Prada, Sebastien A. Duval and Jean Pierre Ballaguet

Extended Thermal Stage Sulfur Recovery Process

Granted Patent: U.S. Patent 10,508,034,
Grant Date: December 17, 2019
John P. O'Connell

Methods and Systems of Upgrading Heavy Aromatics Stream to Petrochemical Feedstock

Granted Patent: U.S. Patent 10,508,066
Grant Date: December 17, 2019
Omer R. Koseoglu and Robert Hodgkins

Catalyst Compositions and their Use for Hydrogenation of Nitrile Rubber

Granted Patent: U.S. Patent 10,508,156,
Grant Date: December 17, 2019
Werner Obrecht, Sarah David, Qingchun Liu and Zhenli Wei

Nanosilica Dispersion Lost Circulation Material (LCM)

Granted Patent: U.S. Patent 10,508,226,
Grant Date: December 17, 2019
Nasser Al-Hareth, Abdullah S. Al-Yami and Vikrant B. Wagle

Controlled Release of Surfactants for Enhanced Oil Recovery
Granted Patent: U.S. Patent 10,508,227,
Grant Date: December 17, 2019
Yun Chang and Mazen Y. Kanj

High Temperature Fracturing Fluids with Nano-Crosslinkers
Granted Patent: U.S. Patent 10,508,230,
Grant Date: December 17, 2019
Ghaithan A. Al-Muntasheri, Feng Liang, Hooisweng Ow, Jason Cox and Martin E. Poitzsch

Integrated Thermal Processing for Mesophase Pitch Production, Asphaltene Removal, and Crude Oil and Residue Upgrading
Granted Patent: U.S. Patent 10,508,240,
Grant Date: December 17, 2019
Remi Mahfouz, Wei Xu, Faisal M. Melebari and Mohammed Al-Daous

Integrated Process for in Situ Organic Peroxide Production and Oxidative Heteroatom Conversion
Granted Patent: U.S. Patent 10,508,246,
Grant Date: December 17, 2019
Omer R. Koseoglu and Abdennour Bourane

Removing Scale from a Wellbore
Granted Patent: U.S. Patent 10,508,517,
Grant Date: December 17, 2019
Aslan Bulekbay, Sultan Attiah, Talal Al-Mutairi and Abdulrahman Al-Sousy

Iterative Method for Estimating Productivity Index (PI) Values in Maximum Reservoir Contact (MRC) Multilateral Completions
Granted Patent: U.S. Patent 10,508,521,
Grant Date: December 17, 2019
Ahmad T. Shammari, Hassan A. Hussain, Obiomalotaoso L. Isichei and Bayan A. Momtan

Logging Fracture Toughness Using Drill Cuttings
Granted Patent: U.S. Patent 10,508,539,
Grant Date: December 17, 2019
Mohammad H. Haque, Yanhui Han, Younane N. Abousleiman and Katherine L. Hull

Strain Energy-Based Method and Apparatus to Determine the Coefficient of Resilience of Lost Circulation Materials
Granted Patent: U.S. Patent 10,508,978,
Grant Date: December 17, 2019
Md. Amanullah, Mohammed K. Arfaj and Turki T. Alsubaie

Flaky Date Fruit Cap for Moderate to Severe Loss Control
Granted Patent: U.S. Patent 10,513,647,
Grant Date: December 24, 2019
Md. Amanullah

Techniques to Manage Mud Properties
Granted Patent: U.S. Patent 10,513,648,
Grant Date: December 24, 2019
Md. Amanullah

Addition of Monovalent Salts for Improved Viscosity of Polymer Solutions Used in Oil Recovery Applications
Granted Patent: U.S. Patent 10,513,652,
Grant Date: December 24, 2019
Saleh F. Hassan and Abdulkareem M. Al-Sofi

Gas-Oil Separation Plant Systems and Methods for Rag Layer Treatment
Granted Patent: U.S. Patent 10,513,663,
Grant Date: December 24, 2019
Mohamed Soliman, Khalid Alanizi, Samusideen Salu and Talal Al-Zahrani

Integrated Aromatic Separation Process with Selective Hydrocracking and Steam Pyrolysis Processes
Granted Patent: U.S. Patent 10,513,664,
Grant Date: December 24, 2019
Omer R. Koseoglu

Vanadium Corrosion Inhibitors in Gas Turbine Applications
Granted Patent: U.S. Patent 10,513,665,
Grant Date: December 24, 2019
Ki-Hyouk Choi

Wellbore Cement Having Spent Polymer Capsule Shells
Granted Patent: U.S. Patent 10,513,905,
Grant Date: December 24, 2019
Elizabeth Q. Contreras

Controlling High-Pressure Production Trap Separation Efficiency
Granted Patent: U.S. Patent 10,513,913,
Grant Date: December 24, 2019
Miguel Lopez, Ramsey White, Pradeepkumar K. Krishnankutty and Rohit Patwardhan

Consolidated Material to Equalize Fluid Flow into a Wellbore
Granted Patent: U.S. Patent 10,513,915,
Grant Date: December 24, 2019
Abdulrahman A. Al-Mulhem

Pyrophoric Liquid Ignition System for Pilot Burners and Flare Tips
Granted Patent: U.S. Patent 10,514,166,
Grant Date: December 24, 2019
Mohamed Soliman and Ali Al-Abbas

Methods for Dehydrogenating Reactant Hydrocarbons
Granted Patent: U.S. Patent 10,518,249,
Grant Date: December 31, 2019
Mohammed Al-Daous

Flaky Date Fruit Cap for Moderate to Severe Loss Control
Granted Patent: U.S. Patent 10,519,357,
Grant Date: December 31, 2019
Md. Amanullah

Capsule Design for the Capture of Reagents
Granted Patent: U.S. Patent 10,519,359,
Grant Date: December 31, 2019
Elizabeth Q. Contreras

Treatment of Sulfide Scales
Granted Patent: U.S. Patent 10,519,406,
Grant Date: December 31, 2019
Katherine L. Hull and Brent Cooper

Systems and Methods for Operating Hydrocarbon Wells to Inhibit Breakthrough Based on Reservoir Saturation
Granted Patent: U.S. Patent 10,519,768,
Grant Date: December 31, 2019
Suleiman Altaheini

Nano-Indentation Tests to Characterize Hydraulic Fractures
Granted Patent: U.S. Patent 10,520,407,
Grant Date: December 31, 2019
Katherine L. Hull and Younane N. Abousleiman

Have an article you would like to publish? Here are our guidelines.

These guidelines are designed to simplify and help standardize submissions. They need not be followed rigorously. If you have any questions, please call us.

Length

Average of 2,500-4,000 words, plus illustrations/photos and captions. Maximum length should be 5,000 words. Articles in excess will be shortened.

What to send

Send text in Microsoft Word format via email plus one hard copy. Send illustrations/photos and captions separately but concurrently, both as email and as hard-copy (see file format section for more information).

Procedure

Notification of acceptance is usually within three weeks after the submission deadline. The article will be edited for style and clarity and returned to the author for review. All articles are subject to the company's normal review. No paper can be published without a signature at the manager level or above.

Format

No single article need include all of the following parts. The type of article and subject covered will determine which parts to include.

Working Title
Lorem Ipsum here.

Abstract
Usually 150-300 words to summarize the main points.

Introduction
Different from the abstract in that it sets the stage for the content of the article, rather than telling the reader what it is about.

Main body
May incorporate subtitles, artwork, photos, etc.

Conclusion/Summary
Assessment of results or restatement of points in introduction.

Endnotes/References/Bibliography
Use only when essential. Use author/date citation method in the main body. Numbered footnotes or endnotes will be converted. Include complete publication information. Standard is *The Associated Press Stylebook*, 52^{nd} ed. and *Wesbter's New World College Dictionary*, 5^{th} ed.

Acknowledgments
Use to thank those who helped make the article possible.

Illustration/Tables/Photos and explanatory text

Submit these separately. Do not place in text. Positioning in the text may be indicated with placeholders. Initial submission may include copies of originals; however, publication will require the originals. When possible, submit both electronic versions and printouts. Color is preferable.

File Format

Illustration files with .EPS extensions work best. Other acceptable extensions are .TIFF/.JPEG/.PICT.

Permission(s) to reprint, if appropriate

Previously published articles are acceptable but can be published only with written permission from the copyright holder.

Author(s)/Contibutor(s)

Please include a brief biographical statement.

Submission/Acceptance Procedures

Papers are submitted on a competitive basis and are evaluated by an editorial review board comprised of various department managers and subject matter experts. Following initial selection, authors whose papers have been accepted for publication will be notified by email.

Papers submitted for a particular issue but not accepted for that issue may be carried forward as submissions for subsequent issues, unless the author specifically requests in writing that there be no further consideration.

Submit articles to:

Editor
The Saudi Aramco Journal of Technology
C-3D, Room AN-1080
North Admin Building #175
Dhahran 31311, Saudi Arabia
Tel: +966-013-876-0498
Email: *william.bradshaw.1@aramco.com.sa*

Submission deadlines

Issue	Paper submission deadline	Release date
Winter 2020	August 13, 2020	December 31, 2020
Spring 2021	November 16, 2020	March 31, 2021
Summer 2021	February 9, 2021	June 30, 2021
Fall 2021	May 11, 2021	September 30, 2021

There is more.

Stuck Pipe Early Warning System Utilizing Moving Window Machine Learning Approach

Omogbolahan S. Ahmed, Beshir M. Aman, Majed A. Zahrani, and Folorunsho I. Ajikobi

Abstract / As stuck pipes continue to be a major contributor to nonproductive time (NPT) in drilling operations for oil and gas, efforts to mitigate this incident cannot be over emphasized. A machine learning approach is presented in this article to identify warning signals and provide early indications for an impending stuck pipe possibility during drilling activities, so as to take proactive measures to mitigate its occurrence.

Clay Typing from Downhole Array Electromagnetic Measurements

Dr. Ping Zhang, Dr. Wael Abdallah, Dr. Shouxiang M. Ma, and Dr. Chengbing Liu

Abstract / The amount and type of clays in reservoirs have a significant impact on formation evaluation and reservoir performance studies. Currently, clay typing requires either reservoir cores for laboratory analysis or advanced logs such as elemental spectral mineralogy (ESM) logs, both are available in only a small fraction of wells drilled. In this study, we will explore a possibility of using commonly measured logs to estimate clay volumes. Specifically, the logs used for the study are formation resistivity (RT), total formation porosity (PHIT), and gamma ray (GR).

Using "Digital Twin" of Coriolis Meters for Multiphase Flow Measurement

Dr. Sakethraman Mahalingam and Dr. Muhammad Arsalan

Abstract / Multiphase flow meters are often built based on one or many single-phase flow metering technologies. Following the trend, Coriolis meters are being increasingly used in upstream applications in conjunction with an independent water cut meter to measure multiphase flow. Coriolis meters are well-known for fiscal metering applications as they offer unparalleled accuracy without having to input detailed information on the fluid being metered. They offer two distinct measurements: (1) density, and (2) mass flow rate, which is often not possible with other metering technologies.

A New Robust Drilling Rate Model

Mohammed M. Al-Rubaii, Dr. Rahul N. Gajbhiye, Dr. Abdullah S. Al-Yami, and Dr. Raed A. Alouhali

Abstract / The drilling rate remains a major challenge when it comes to planning and drilling workover and development wells. The main mission of a drilling engineer is to design a well, optimizing time, cost, economics, and safety. An analysis of previously drilled wells operations' records is required to perform optimization techniques to reduce the drilling cost of new wells. Among the many potential optimizations, the rate of penetration (ROP) has the most obvious impact on the cost-effectiveness of drilling a well, but to ensure the optimized ROP, it must be engineered.

To read these articles and others, go to *www.saudiaramco.com/jot*

أرامكو السعودية
saudi aramco

Aramco
Journal
of Technology

Liked this issue? Sign up. It's free.

To begin receiving the *Aramco Journal of Technology* please complete this form, scan and send by email to ***william.bradshaw.1@aramco.com.***

Got questions?

Just give us a call at +966-013-876-0498 and we'll be happy to help!

Scan the QR code to go straight to your email and attach the form!

Subscription Form

Name	
Title	
Organization	
Address	
City	
State/Province	
Postal code	
Country	
Email address	
Number of copies	

Saudi Arabian Oil Company (Saudi Aramco), is a company formed by Royal Decree No. M/8 dated 04/04/1409H, and is a joint stock company, with certificate of registration number 2052101150 having its principal office at P.O. Box 5000, Dhahran, Postal Code 31311, Kingdom of Saudi Arabia, and a fully paid capital of SAR 60,000,000,000.

www.saudiaramco.com/jot